NASA TECHNICAL
MEMORANDUM

NASA TM X-64598

AN EVALUATION OF EARTH RESOURCES OBSERVATION OPPORTUNITIES FROM AN ORBITING SATELLITE

By E. H. Bauer and B. S. Perrine
Aero-Astrodynamics Laboratory

May 19, 1971

NASA

George C. Marshall Space Flight Center
Marshall Space Flight Center, Alabama

1. Report No.	2. Government Accession No.	3. Recipient's Catalog No.
NASA TM X-64598		

4. Title and Subtitle	5. Report Date
AN EVALUATION OF EARTH RESOURCES OBSERVATION OPPORTUNITIES FROM AN ORBITING SATELLITE	May 19, 1971
	6. Performing Organization Code

7. Author(s)	8. Performing Organization Report No.
E. H. Bauer and B. S. Perrine	
	10. Work Unit No.

9. Performing Organization Name and Address	11. Contract or Grant No.
George C. Marshall Space Flight Center Marshall Space Flight Center, Alabama 35812	
	13. Type of Report and Period Covered TECHNICAL MEMORANDUM

12. Sponsoring Agency Name and Address	14. Sponsoring Agency Code
NASA Washington, D.C. 20546	

15. Supplementary Notes

16. Abstract

The National Aeronautics and Space Administration is currently engaged in integrating, on the Skylab Workshop, an Earth Resources Experiment Package (EREP) which will be exercised by each of three separate flight crews in the 1973 time frame. Other continuously manned missions which include an EREP are in the planning phase. For effective mission planning, a knowledge of the opportunities for experiment performance and of the interdependence of experiment requirements and systems constraints is mandatory. This report discusses the development and application of a new mission analysis simulation technique designed to evaluate and optimize these opportunities. Factors influencing available opportunities, such as orbital parameters, solar lighting at the target, system limitations, etc., are incorporated in the simulation and analyzed to determine their effects. The USA is considered the prime target with either USA coverage time or the number of passes over the USA used as a payoff function. Optimization for various mission parameters, such as orbital inclination, launch time, and launch date, are included. The 50° inclined circular orbit at 435 km altitude is analyzed in depth. USA coverage time and number of passes for missions in this orbit, such as Skylab and possibly the Shuttle sortie missions, are provided.

17. Key Words (Suggested by Author(s))	18. Distribution Statement
Earth Resources Experiment Package, Observation Opportunities, Mission Analysis Simulation Technique, Lighting Constraint, Orbit Selection Criteria, Beta Induced Variation, Sun Incidence Angle, Regression Cycle, Skylab, Shuttle	Unclassified-Unlimited E. D. Geissler Director, Aero-Astrodynamics Laboratory

19. Security Classif. (of this report)	20. Security Classif. (of this page)	21. No. of Pages	22. Price*
UNCLASSIFIED	UNCLASSIFIED	89	$3.00

*For sale by the Clearinghouse for Federal Scientific and Technical Information
Springfield, Virginia 22151

TABLE OF CONTENTS

LIST OF ILLUSTRATIONS

LIST OF ILLUSTRATIONS (Continued)

LIST OF ILLUSTRATIONS (Continued)

LIST OF ILLUSTRATIONS (Continued)

LIST OF SYMBOLS

Symbol	Definition
A	observation area on map in Ω_e, θ coordinates
CSM	Command and Service Module
EREP	Earth Resources Experiment Package
I, i	inclination of the satellite orbit
lat	geocentric latitude of a point on the earth
$\hat{N}$	unit vector normal to the satellite orbit plane
n	number of passes across A
OA	orbital assembly
P	pass
$\hat{S}$	unit vector in the direction of the sun
SL-1	unmanned Saturn Workshop (SWS), first launch in Skylab mission
SL-2	first manned Skylab mission, up to 28 days duration, of CSM docked with SL-1 SWS
SL-3, SL-4	manned CSM/SL-1 SWS Skylab missions, up to 56 days duration each
SWS	Saturn Workshop
T_N	nodical period of the satellite
t_i	duration of an individual pass over A
t_o	average observation time of A per day
$\hat{V}$	unit vector in direction $\hat{S} \times \hat{N}$
W	width of a rectangular area, A, in Ω_e,θ coordinate
X	angle between the ascending node and the meridian of the sub-satellite point
X-IOP/Z	solar inertial attitude
Z-LV(E)	earth pointing attitude

DEFINITION OF SYMBOLS (Continued)

Symbol	Definition
β	angle between $\hat{S}$ and the projection of $\hat{S}$ onto the orbit plane (positive when the angle between $\hat{S}$ and $\hat{N} < 90°$)
β_c	beta angle constraint
$\lvert\beta\rvert$	absolute value of β
δ	declination of the sun
θ	argument of latitude of a sub-satellite point
θ_1	θ for ascending pass
θ_2	θ for descending pass
θ_{LL}	minimum value of θ for which the elevation angle constraint is satisfued
θ_{UL}	maximum value of θ for which the elevation angle constraint is satisfied
θ_{ON}	value of θ when the satellite passes orbital noon
$\Delta\theta$	height of a rectangular area, A in Ω_e,θ coordinates
$\Delta\theta_c$	range of θ from θ_{LL} to θ_{ON} or from θ_{ON} to θ_{UL}
Ω_e	angle from the Greenwich meridian to an ascending node of the satellite ground track
Ω_{e1}	Ω_e for a satellite ground track making an ascending pass over a point in the observation area
Ω_{e2}	Ω_e for a satellite ground track making a descending pass over a point in the observation area
Ω_S	angle between the ascending node of the orbit and the meridian of the sun
$\dot{\Omega}$	regression rate of the line of nodes of the satellite orbit
$\Delta\Omega_e$	angle between two adjacent satellite ground tracks measured along the equator

DEFINITION OF SYMBOLS (Continued)

Symbol	Definition
ω_e	rotation rate of the earth
ω_o	orbital rotation rate of the satellite

AN EVALUATION OF EARTH RESOURCES OBSERVATION OPPORTUNITIES FROM AN ORBITING SATELLITE

SUMMARY

The National Aeronautics and Space Administration is currently engaged in integrating, on the Skylab Workshop, an Earth Resources Experiment Package (EREP) which will be exercised by each of three separate flight crews in the 1973 time frame. Other continuously manned missions which include an EREP are in the planning phase. For effective mission planning, a knowledge of the opportunities for experiment performance and of the interdependence of experiment requirements and systems constraints is mandatory. This report discusses the development and application of a new mission analysis simulation technique designed to evaluate and/or optimize these opportunities. Factors influencing available opportunities, such as orbital parameters, solar lighting at the target, system limitations, etc., are incorporated in the simulation and analyzed to determine their effect. The USA is considered the prime target with either USA coverage time or number of passes over the USA used as a payoff function. Optimization for various mission parameters, such as orbital inclination, launch time, and launch date, are included. The 50° inclined circular orbit at 435 km altitude is analyzed in depth. USA coverage time and number of passes for missions in this orbit, such as the Skylab and possibly the Shuttle sortie missions, are provided.

Typical results show that when constraints, for example, target lighting, are imposed, a sensitivity to sun declination is evidenced as a function of the target latitude, with the higher latitudes experiencing higher sensitivity. (This sensitivity can be considered seasonal, and therefore preference is seen for summer missions over winter missions for viewing of northern latitude targets.) Launch time of day is shown to be a major factor for short duration missions, i.e., 28 days, but lessens in importance when the mission length approaches or becomes an integral multiple of an orbital regression cycle ($\approx$ 60 days). Figures are included to determine USA coverage time and number of passes for any mission from the 50°-inclined, 435 km circular orbit of the Skylab mission.

I. INTRODUCTION

The current NASA plan is to integrate earth-viewing experiments on board future manned earth orbital missions, e.g., Skylab and Space Station. The Earth Resources Experiment Package (EREP) for Skylab includes several sensors selected for gathering data in earth-oriented areas such as agriculture, forestry, oceanography, geology, geography, and ecology. Data from these sensors will be an aid toward the goals of responsible management of earth resources and the human environment, weather prediction and modification, and definition of earth geometry and surface characteristics. A knowledge of the earth-oriented data gathering opportunities available during any mission is necessary for effective mission and flight planning. However, these opportunities are functions of many factors, such as trajectory parameters, experiment and system limitations, target location and size, cloud cover, and crew time availabilities.

This report discusses the development and the results of using a tool for optimizing or evaluating a number of these factors as they apply to earth resources experimentation. Section II discusses the development of the simulation, and Section III the application. The effects of inclination, launch date, launch time, and various constraints upon the availability of earth resources related observation opportunities are evaluated. The analysis does not incorporate the effect of cloud cover on the earth resources opportunities. A treatment of this particular area is covered in references 1 and 2.

Although any mission can be simulated, the Skylab program is used as a specific example. This program has been established as a series of three long-duration, manned missions in near-earth orbit. The first mission (called Mission SL-1/SL-2) will begin with the launch into orbit of an unmanned laboratory, SL-1 SWS. This SWS laboratory consists of an S-IVB stage shell (empty LOX and LH_2 tanks and thrust structure without engine) which will be outfitted for manned habitation. Attached to this shell are an Airlock Module, Multiple Docking Adapter, Apollo Telescope Mount, and Instrument Unit. This assembly will contain facilities for conducting medical, solar astronomy, earth resources, and other technical experiments. A second launch will transport a three-man crew to rendezvous with the SWS. The crew will dock their Command Service Module (CSM) to the SWS and will proceed to inhabit and operate the orbital assembly (SWS plus CSM) for approximately one month. To conclude the mission, the crew will prepare the SWS for orbital storage and will return to earth via the CSM. A second crew will man the orbital assembly for up to two months on each of two revisit missions (Missions SL-3 and SL-4).

The Earth Resources Experiment Package (EREP) to be used throughout this program is composed of a number of earth-oriented experiments including a Multispectral Photographic Facility, Infrared Spectrometer, a 10-Band Multispectral Scanner, a Microwave Radiometer Scatterometer, and an L-Band Radiometer. These experiments are fully discussed in reference 3. The EREP will be hard-mounted in the Multiple Docking Adapter (MDA) of the orbiting assembly, thus requiring the entire cluster to maneuver from the prime mission attitude (solar inertial) to a local horizontal attitude for earth viewing. These attitudes are sketched in Figure 13. The attitude requirement, because of subsystem considerations, limits the earth resources data-taking opportunities in terms of frequency, length, and time of performance in the mission. Thus, all of the daylight USA opportunities which are available are not usable in a practical sense. The total number of daylight USA opportunities and the penalty incurred through adding attitude-dependent constraints are provided.

II. SIMULATION DEVELOPMENT

In this section, a method for determining the amount of potential experimentation time spent by a satellite over any geographical area on the earth is developed. This time will be called the observation time. Since this calculation will involve a number of independent variables, each of which can have a range of values, the method should be as analytical as possible. The approach taken is to remap the points in the geographical area of interest into a form which makes the area of the new map directly proportional to the observation time. Geometrical constraints on the times when successful earth observations can be made are then placed upon the map. In general, these are functions of time. The area on this map not excluded by the constraints (and thus available for observation) is then determined and related to the observation time.

To make this mapping, two angles, defined by figure 1, relate a point on the earth to a satellite in orbit. A satellite which passes over point A must have traveled through one of two central angles since passing the equator, θ_1 or θ_2. The angles between the prime meridian and the point where the satellite crossed the equator are Ω_{e1} and Ω_{e2}. In Appendix A it is shown that the θ's and Ω_e's are related to the latitude and longitude of the point by the following equations:

$$\theta_1 = \sin^{-1} \frac{\sin \text{lat}}{\sin i} \qquad (1)$$

$$\Omega_{e1} = \text{longitude} + \tan^{-1}(\cos i \tan \theta_1) - \frac{\omega_e + \dot{\Omega}}{\omega_o} \theta_1 \qquad (2)$$

$$\theta_2 = \pi - \theta_1 \qquad (3)$$

$$\Omega_{e2} = \text{longitude} + \tan^{-1}(\cos i \tan \theta_2) - \frac{\omega_e + \dot{\Omega}}{\omega_o} \theta_2. \qquad (4)$$

It should be noted from equation (1) that the magnitude of the latitude must be less than the inclination in order to maintain sin lat/sin i less than one. Using equations (1) through (4), any point on the earth, with a latitude between -i and +i, can be mapped into two points in (Ω_e,θ) space, one point corresponding to an ascending pass (Ω_{e1},θ_1), the other corresponding to a descending pass (Ω_{e2},θ_2). Figure 2 shows how the continental United States would map into this space. The portion of the map at the lower left is created by the ascending passes, while the portion in the upper right is created by descending passes. Satellite ground tracks on this map will be straight vertical lines separated by the amount the earth rotates plus the amount the orbital line of nodes regresses during one orbital (nodical) period. This separation is denoted by equation (5).

$$\Delta\Omega_e = (\omega_e + \dot{\Omega})T_N = \frac{\omega_e + \dot{\Omega}}{\omega_o} 2\pi. \qquad (5)$$

The ground tracks are traced out by the satellite one at a time starting at the bottom of figure 2 and moving toward the top. The first track to be traced is the one on the extreme left. The next track is just to the right of it, and so on until the last track on the extreme right is traced. These tracks will be repeated each day in this fashion (not necessarily having the same set of Ω_e's every day, however). An area on the new map can be shown to be proportional to the observation time in the following manner. Take some convenient rectangular area as shown in figure 3. The time which the satellite will spend over this area will be the number of ground tracks, n, across the area multiplied by the amount of time spent by each ground track, t_i.

$$t_i = \Delta\theta/\omega_o. \qquad (6)$$

$$n = W/\Delta\Omega_e.$$

Thus, the observation time over the area is represented by

$$t_o = \frac{\Delta\theta W}{\omega_o \Delta\Omega_e} .$$

Substituting for $\Delta\Omega_e$ from equation (5) and recognizing $\Delta\theta W$ as the area, A,

$$t_o = \frac{A}{2\pi(\omega_e + \dot{\Omega})} . \qquad (7)$$

Each time the earth makes one revolution, there will be n ground tracks across A, and each day an additional t_o will be accumulated. Thus, t_o is the observation time per day. The area need not be rectangular. An irregular area can be thought of as being the sum of many small rectangular pieces similar to the differential elements of the calculus. Rigorously, t_o should be called the average observation time per day, because, for t_o to be the true observation time, n in equation (6) should be an integer; i.e., the width of a rectangular area, A, should contain exactly an integral number of $\Delta\Omega_e$'s. If this is not true, and say that the width of the area was between $n\Delta\Omega_e$ and $(n+1)\Delta\Omega_e$, then sometimes there would be n ground tracks across A, and sometimes n+1, depending upon the positioning of the grid of ground tracks relative to A. Over a long period of time, however, the number of ground tracks will tend to average to a value of $W/\Delta\Omega_e$. Thus, the average observation time is being calculated.

In actual practice, the total area on the map may not be available for useful observation because of various constraints placed on the experiment or satellite systems. The following is an example from the Skylab program of the type of constraint which exists for earth resources experiments. To obtain successful photographs of the ground, the sun must have a sun elevation angle greater than some constraining value. Sun elevation angle is defined in figure 4 as the angle between the solar vector and the local horizontal. It can be seen that it is the complement of the sun incidence angle also shown in the figure. For the subsequent derivations, it is more convenient to express the constraint in terms of the sun incidence angle. Figure 5 shows that the sun incidence angle at the sub-satellite point on the earth is equal to the angle between the satellite position vector and the earth-sun line (neglecting the slight error due to the oblateness of the earth). Figure 6 shows that there is a certain segment of the orbit within which the sun incidence angle is less than the constraint. This

segment is defined by an upper and lower limit of θ, θ_{UL}, and θ_{LL} which lies on either side of orbital noon as shown in the figure. The values for the constraints on θ depends upon the position of the solar vector relative to the orbit which in turn is determined by the declination of the sun, δ, and the angle between the meridian of the sun and the ascending node of the orbit Ω_S. The equations for θ_{LL} and θ_{UL} are derived in Appendix B. During the time it takes for the ground track pattern to be formed across the map shown in figure 2, the values of δ and Ω_S will remain relatively constant. Thus θ_{LL} and θ_{UL} will not change appreciably during this time and, as shown in figure 7, these constraints are placed on the map as horizontal lines at $\theta = \theta_{LL}$ and $\theta = \theta_{UL}$. The area of the United States remaining between these two lines is then proportional to the available observation time which satisfies the sun elevation angle constraint. Since δ and Ω_S are functions of time, θ_{LL} and θ_{UL} and the observation time are implicit functions of time due to their dependence upon δ and Ω_S. In the simulation the values of δ, Ω_S, θ_{LL}, θ_{UL} and the observation time are updated daily.

Also shown in figure 6 is an angle, designated β, which is the angle between the earth-sun line and the projection of the earth-sun line on the orbit plane (orbital noon). For the Skylab program there will be a constraint placed on this β angle in that no observations can be made when its magnitude exceeds some value determined by such restrictions as thermal environment and power requirements from solar arrays.

In order to demonstrate how the above parameters change with time, consider the following example. The earth resources satellite is launched (in a northeasterly direction) into a 50° inclination, 435 km (235 n.mi.) circular orbit on June 1 at 5:30 p.m. EST. Experiment and satellite systems constraints dictate that measurements cannot be made unless the sun elevation angle is greater than 30° and β lies within the range from -30° to +30°. Figure 8 shows the time history of β, Ω_S, and δ and the resulting values of θ_{LL} and θ_{UL}. Now consider how the changing values of θ_{UL} and θ_{LL} affect the available observation time over the continental United States by referring to figures 7 and 8. Initially, θ_{UL} is below the United States, and thus, no observation time is available. But as θ_{UL} begins to increase above 33°, observation time becomes available for the ascending passes. Eventually the descending passes also become available and θ_{LL} begins to eliminate a portion of the ascending passes. Finally, θ_{UL} is completely above the portion of the map corresponding to descending passes, and the increasing θ_{LL} causes the observation time to continue to decrease. Figure 9 shows a plot of the history of this observation time. The vertical lines at June 5 and July 14 indicate the period of days during which the β angle does not exceed a constraint of ±30°. What has been shown is called one observation time, or coverage cycle. This cycle will be repeated each time Ω_S goes from 0 to 360°. Each cycle will appear somewhat different because of the changing solar declination.

Similarly, referring to figures 2 and 7, the behavior of the individual orbit passes during an observation time cycle can be described. Initially when θ_{UL} is below the lower boundary of the United States (figure 7), even though the satellite is creating ground tracks across the map (figure 2), the lighting constraint will not be satisfied. As θ_{UL} proceeds to increase and fall across the ascending portion of the United States map, the first ascending pass or two (the ones which occur on the extreme left of figure 2) have acceptable lighting. As θ_{UL} continues to increase, eventually some of the descending passes become acceptable (those crossing the descending portion of the map.) As θ_{LL} moves up figure 7, it will first eliminate the first ascending passes of each day. After θ_{LL} has increased to 80°, only the descending passes are acceptable. Eventually θ_{LL} will increase so that there will no longer be any acceptable passes until the next observation cycle.

The above calculations have been included in a small computer program which was used in the analysis of the effects of inclination, launch date, launch time, and various constraints upon the availability of earth resources opportunities. This analysis is presented in the following section.

III. ANALYSIS

In this section factors which influence available earth resources opportunities, such as solar lighting at the target, system limitations, and orbital parameters are analyzed. The USA is considered the prime target (although other representative targets are included). Optimization of USA coverage over various mission parameters such as orbital inclination, launch time, and launch date is performed. USA coverage time and number of passes for missions (such as Skylab and possibly the Shuttle sortie missions) in the reference 50° inclined circular orbit at 435 km (235 n.mi.) altitude are provided.

A. Influence of Lighting Constraint

The average time that a satellite in a 50° inclination, 435 km orbit, spends over the USA each day is a constant $\approx$ 38 minutes. From figure 2, it can be seen that this time is spread over $\approx$ 6 passes per day. Each pass on this special map is separated in time by the orbital period ($\approx$ 93 minutes) and by $\Delta\Omega_e$ in ground trace. The passes begin at the left of the map and step across to the right, normally resulting in three ascending passes followed by three descending passes per day. All, some, or none of the six passes each day will occur over the USA in the daylight. A constraint imposed in this analysis is that the USA

target be adequately illuminated, although it is realized that data-taking during some dark portions of an orbit is desirable for any comprehensive earth resources mission. In this study, a lighting constraint is imposed through a requirement that the solar elevation angle at the spacecraft subpoint, or target, be greater than a specified angle. This angle, called the sun elevation angle, was defined in figure 4. This constraint defines the degree of illumination required at the target for acceptable observation.

Figures 7 and 8 can be used to verify that imposing a sun elevation angle constraint of $\geq 30°$ at the target limits not only the amount of observation time but also the coverage to a maximum of ≈ 44 days out of the 60-day cycle. A sun elevation angle constraint greater than 30° decreases further the number of acceptable days of coverage per cycle.

The average number of passes per day (n) associated with a lighting-constrained coverage cycle can be estimated by dividing the extent of the longitude range of the map which lies within the theta bounds by the delta longitude transgressed in one orbit, $n = W/T_N(\omega_e + \dot{\Omega})$. For example, in figure 7, "W" would be from 112° to 237° for a total longitude range of 125°. Because the theta upper and lower limits which determine W vary daily, the number of acceptable passes per day is not a constant.

Figure 10 represents a typical daylight coverage time history for the USA. The average time per day for the 50° inclined orbit is plotted versus date. USA coverage can be seen to occur in 60-day cycles with greater total time per cycle in the summer months than in the winter. This effect is due to the changing declination of the sun plus the existence of a lighting constraint. Less daylight coverage time is provided in the winter when the sun is well below the equator. (The winter position of the sun maximizes daylight coverage for targets in the lower hemisphere such as Australia, but minimizes USA daylight coverage.) As was shown in figure 6, the lighting constraint imposed is not simply an angular function about the noon meridian, such as requiring a USA pass to occur when the sun is within 60° of the meridian of the target ($\approx$ 8:00 a.m. to 4:00 p.m.). It is imposed as a function of the angle between the sun vector and target, which, in this case, must be less than 60° and thus would also be a function of the declination of the sun and the latitude of the target. Near a summer solstice, when the sun is at a +23° latitude, for a target at 48°N latitude at local noon, the rays of the sun would be falling on the target surface making a 25° angle with the vertical (sun elevation angle of 65°). This angle is well within the lighting constraint. However, near a winter solstice, when the sun is at -23° latitude, the rays of the sun would be falling on the same target surface making a 71° angle with the vertical (sun elevation angle of 19°), and would thus be outside the lighting constraint. For this reason, breaks occur in the coverage time within a

cycle during the winter because no segment of the orbital plane lies within a 60° cone about the earth-sun vector.

Figure 11 gives the effect of the lighting constraint on the envelope of the coverage cycle peaks (each 60-day coverage cycle would fall under these envelopes). This figure shows the relative penalty due to the lighting constraint during the winter months. During the winter, the sun elevation angle, for the USA as a target, is generally less than 30°, which results in poor winter coverage. Coverage at elevation angles above 60° is possible only during the months when the sun is in the upper hemisphere.

It is generally desirable that the target have a sun elevation angle greater than 30°. However, in the winter (when the sun is in the lower hemisphere), the upper latitudes of the USA are not very well illuminated. Therefore, a relaxation of the constraint is necessary. The target lighting constraint desired for at least one of the EREP experiments (S190 - Multispectral Photographic Facility) requires that the solar elevation angle at the target be ≧ 30° in the summer hemisphere and ≧ 20° in the winter hemisphere. To provide a smooth constraint relaxation and to prevent a discontinuity at the constraint relaxation time, the sun elevation angle constraint was relaxed for winter viewing (of a target in the northern hemisphere) through the following procedure:

Sun Declination	Sun Elevation Angle Constraint
All positive declinations	≧ 30°
From 0 to -10°	Linear interpolation from ≧ 30° to ≧ 20°
Less than -10°	≧ 20°

For a southern hemisphere target, the lighting constraint would be mirrored; i.e., the lighting relaxation to ≧ 20° would begin at a sun declination of +10°. Hereafter, the above procedure is used as the sun elevation constraint; it is identified as "sun elevation ≧ 30°/20°." The term "daylight" in this report (as in daylight coverage) implies satisfaction of the lighting constraint.

Figure 12 presents a daily USA coverage history using the 30°/20° lighting constraint philosophy. Launch is assumed to be 9:30 a.m. EST, November 9, into a 50° inclined circular orbit at 435 km (235 n.mi.) altitude. This particular launch time and date were at one time considered for the Skylab mission. In this mission, the EREP will be hard-mounted in the MDA portion of the orbiting assembly, requiring the entire cluster to be maneuvered to, and maintained in, the necessary

Z-local vertical (Z-LV(E)) attitude (figure 13) required for earth viewing. This attitude requirement limits the earth resources data-taking opportunities in terms of frequency, length, and time of performance during the mission. Thus, all of the time shown in figure 12 is not, in a practical sense, usable. However, it does represent the totality of opportunities available from which selections can be made. The penalty incurred as a consequence of adding the attitude-dependent constraints will be discussed later.

A lighting constraint is active in another area, namely, adequate lighting for the recovery of the manned command module. Overlaid on the abscissa of figure 12 are the acceptable daylight recovery windows. Acceptable spacecraft recovery lighting is defined as recovery no earlier than two hours before sunrise and no later than two hours before sunset at the prime recovery latitude (32°N). Days when this lighting is satisfied for orbits ascending from south to north into the recovery area are identified by the horizontal bar above the axis. Descending orbit recovery windows are located below the axis. These recovery windows are functions of launch date and time in the same way as USA daylight viewing opportunities; i.e., the recovery windows are correlated to the USA daylight coverage cycles. Regardless of the launch time and date of the experiment package carrier, recovery windows for both the ascending and descending orbits occur during the middle of a coverage cycle. The opening of the ascending recovery window begins almost simultaneously with the beginning of a coverage cycle, and the descending orbit recovery window closes $\approx$ 8 days beyond its associated coverage cycle. Thus, it can be seen that on any day in which daylight USA coverage is possible, the lighting constraints for recovery on that day are simultaneously satisfied. Lowering the recovery latitude to $\approx 20°$ increases the recovery window length by $\approx$ 2 days on each end, or four days, and decreases the overlap period in the middle of the cycle by $\approx$ 3 days. Since daylight USA coverage implies recovery opportunities, the recovery windows are not shown in subsequent figures.

B. Influence of Launch Time

Launch time of the orbiting workshop, laboratory, or space station affects the point in a coverage cycle where the mission begins. Figure 12 represents a 9:30 a.m. launch on November 9. Launching at times earlier in the day shifts the coverage cycles to the left with respect to the days-from-launch scale. Launches later in the day shift the coverage cycles to the right. For example, a 5:00 p.m. EST northeasterly launch from the Cape places day 1 near the beginning of a coverage cycle and a midnight launch places day 1 at the end of a cycle where at least 14 days must pass before daylight USA coverage is again established. A two-hour change in launch time is equivalent to a coverage cycle shift

of ≈ 5 days. A 24-hour change likewise equates into a 60-day (or entire cycle) shift which places the day 1 position back in the same relative position. However, when the cycle is shifted, its maximum and its shape change correspondingly to fall within the dashed envelope shown in figures 10, 11, and 12. These envelopes are a function of the lighting constraint only. The launch time effect is shown in figure 14 for a representative summer coverage cycle. Day 1 can be seen to fall farther into the daylight coverage cycle as launch time becomes earlier, starting at ≈ 5:00 p.m. The launch time of ≈ 2 p.m. EST places day 1 shortly after the beginning of a daylight coverage cycle. An ≈ 8:00 a.m. EST launch places day 1 in the middle of the cycle where in the summer all the USA passes, both ascending and descending, are in the daylight. A 2:00 a.m. EST launch begins the mission near the end of the period of daily daylight opportunities. Coverage cycles repeat every 60 days, although the cycle size and duration varies with season. Regardless of season, however, an 8:00 a.m. launch always places day 1 at the center of a coverage cycle.

C. Influence of a Beta Angle Constraint

Overlaid on figure 10 are those intervals when $|\beta|$ exceeds 30° and 50°. The stippled areas represent days when $|\beta|$ is greater than 30°. These days in the stippled areas are not available as EREP earth viewing opportunities if the maneuver to Z-LV(E) is constrained to times when β lies between ±30°. Likewise, days when $|\beta|$ is greater than 50° are represented by the solid strips within the stippled area. These areas are extended below the date scale to include days when no coverage time is available. During the summer months, the β constraint effect on USA coverage is negligible, but in the remainder of the year (for a 30° beta constraint), the contrary is true. Relaxing the β constraint to 50° almost eliminates β as a constraining factor on USA daylight coverage time. Relaxing the lighting constraint increases the average time per day during the winter cycles; whereas, relaxing the β constraint increases the number of days available for earth resources experiment operation. It will be shown that in the fall and spring, relaxation of the beta constraint (from 30°) produces significant improvement in coverage time.

Each individual coverage cycle can be integrated to obtain total average USA daylight coverage time per cycle. Since, at most, 44 days of each 60-day cycle contain daylight USA coverage time, a cycle can represent missions with durations as short as 44 days or as long as 60 days.

Figure 15 presents the beta-induced variation in daylight USA coverage time, per regression cycle, that can be obtained in a 44- to 60-day mission throughout the year. A regression cycle is defined as the time necessary for the ascending node of the orbital plane to regress 360° relative to the earth-sun line; it is synonymous with coverage or observation cycle. The launch time used for the observation cycles which make up figure 15 is 6:00 p.m. EST which places day 1 near the beginning of a cycle of daylight opportunities over the USA. USA coverage time on days when the β angle is greater in magnitude than the constrained value is excluded; thus, the β penalty can be seen, particularly during early spring and fall missions. Winter missions also are penalized through a β constraint, but coverage time then is already severely penalized (up to 64 percent) by the lighting constraint.

The beta-induced variation in the total number of acceptable daylight passes over the USA is given in figure 16. The same factors which restrict daylight coverage time over the USA also determine the number of daylight passes over the USA. The time and number-of-passes curves are thus very similar.

D. Total USA Coverage for any Mission Length from a 50° Inclination, 435 km Circular Orbit

The total daylight coverage time and total number of candidate passes for any mission from this reference orbit can be roughly estimated by using figures 15 and 16. The values (as a function of the β constraint) which are shown above any specific date on these figures represent USA coverage time or passes that can be obtained from a 44- to 60-day mission launched at $\approx$ 6:00 p.m. on that date. (A regression cycle is 60 days in length, but with the 6:00 p.m. launch, the last 16 days produce no daylight USA coverage.) Knowing launch date and mission length, one can use the values as plotted on the curves (or a percentage of them). For example, estimations for a 60-day mission can be read directly off the curve above the appropriate launch date. Estimation of a 120-day mission would contain the sum from two 60-day coverage cycles, the first value read above the initial launch date, and the second value for the succeeding cycle read above the date 60 days later. For longer missions, this procedure continues, summing each 60 days, as long as the mission length is an even multiple of the regression cycle. For missions less than 44 days, or for the remainder of missions not an integral multiple of the 60-day regression cycle (i.e., the last 30 days in 150-day mission), some percentage of the values from the curves would be necessary.

These estimations from figures 15 and 16 are rough, since different launch times and non-integral multiples of the regression cycle introduce errors, particularly with the combination of shorter missions (or remainders)

and early morning launch times. For example, a 30-day mission launched at 6:00 p.m. EST produces ≈ 65 percent of the total coverage cycle values of figures 15 and 16 because almost all of the 30 days produce daylight coverage. However, the same mission launched at 2:00 a.m. EST would produce only ≈ 35 percent of the coverage cycle values because it would begin near the end of the cycle and at least 16 days of the mission would acquire no daylight coverage.

For better estimates, the variations in mission length and launch time are accounted for in figures 17a through 17h. From these curves the total USA coverage time and total number of passes over the USA for any length mission, any launch date and time can be determined. No constraints other than the 30°/20° lighting constraint are imposed.

Estimates using these figures are given for the following Skylab mission definition: launch on November 9 at 9:30 a.m. EST with subsequent launches on days 1, 71, and 173. Given the initial SL-1 launch date and time, the launch times of day for the subsequent SL-2, SL-3, and SL-4 missions are derived using a procedure found in Appendix C.

Launch Date	Mission	Launch Day	Duration (days)	Launch Time* (EST)	Total USA Coverage Time (hr)	Total USA Passes
Nov. 9	SL-1	0	--	9:30 a.m.	--	--
Nov. 10	SL-2	1	28	9:06 a.m.	4.5	66
Jan. 19	SL-3	71	56	4:42 a.m.	8.5	125
May 1	SL-4	173	56	11:06 a.m.	13.4	168
				TOTAL	26.4	359

*Assumes planar launches.

The appropriate curves to use for the SL-2 mission would be those of figure 17c (9:00 a.m. launch). Reading above the date of November 10, and interpolating when necessary, the values of 4.5 hours of total USA coverage and 66 total passes over the USA can be read. Totals for the SL-3 mission are estimated by interpolating between the 50- and 60-day curves of figure 17b above the date of January 19. Likewise, the SL-4 estimates come from figure 17d.

Any continuous mission can be read from one appropriate figure, summing the 60-day values until mission completion or to the last even multiple of 60 days. Interpolation between the given launch time intervals can also be made if such accuracy is desired (e.g., for a 10:30 a.m. launch). Mission lengths which are a fraction of the regression cycle would be read from the same figure, but from a curve or interpolation of curves representing less than 60 days length. Hence, launch times corresponding to any launch interval can be determined, and total coverage times, for any length mission (with no constraint other than lighting), can be read from the appropriate curves.

These curves can indicate the optimum positioning of individual missions which rendezvous with the experiment carrier. Assume that three 60-day missions were planned. Considering no other limitations, launching in May or early June for three consecutive years would optimize earth resources daylight USA coverage. For total durations less than two years, the optimum would be one mission (first or last) centered over one summer and the other two shared over the other summer. For durations less than a year, at least one mission is penalized by poorer lighting. Depending upon minimum launch interval and time between recovery of one mission and launch of the next, the middle mission would be placed optimally over the summer with the other two on each side as close as possible; or two of the missions would share the better lighting period with the remaining mission falling as close as constraints allow.

E. Definition of Orbit Selection Criteria

The preceding discussion and figures concerned total daylight USA availabilities considering no β constraints. If an earth resources package were on a steerable platform or in a "free-flying" mode independent of the orbital assembly attitude, these numbers are applicable. However, if the experiment package is rigidly mounted in the orbital assembly as it is in the Skylab program, the entire assembly must be maneuvered each data-taking period to the earth-viewing attitude Z-LV(E). This earth-viewing attitude is usually limited in terms of frequency, duration, and time of performance during the mission due to such considerations as power, thermal, pointing accuracy, and attitude control. In the Skylab program, these considerations are relevant because of the non-steerable solar array system used to power the orbital assembly. In the Z-LV(E) attitude, figure 13, designated for Skylab earth viewing, the solar arrays experience a varying sun incident angle (angle between normal to solar arrays and the sun line). The larger the sun incident angle on the solar arrays, the smaller the amount of electrical power generated by the solar cells. Depending upon the electrical load during the Z-LV(E) attitude, this reduced electrical power generation capability can result in excessive discharge of the SWS batteries. Correspondingly,

during this attitude hold, areas that are not normally exposed receive direct sunlight and thus experience a more severe thermal environment. The acceptable frequency of using the Z-LV(E) attitude is related in this study to the beta angle (β). The larger the magnitude of β at the time a maneuver is made to Z-LV(E), the less direct the sun's rays will be on the solar panels while the cluster is in this attitude, and thus, reduced power generation capability.

The Skylab reference orbit produces a β history which is a 60-day cyclic function ranging between +73.5° to -26.5° at the summer solstice (June 22), ±50° during the fall and spring equinoxes, and +26.5° to -73.5° at the winter solstice (December 22). The β magnitude ranges between these bounds in a sinusoidal fashion every 60 days. The USA daylight coverage cycles are, in fact, directly related to the β cycles. The β curve reaches a minimum every 60 days, and at this time, the middle of a daylight USA coverage cycle occurs.

Up to six daylight passes per day over the USA are possible. However, with rigidly mounted earth resources sensors, the number of passes that can actually be used are fewer because of system limitations. Criteria for the Z-LV(E) attitude are that it can be attained every other orbit, or held for two consecutive orbits if β is between ±50° and if followed by at least 4 orbits in the solar inertial mode. Therefore, on a given day when β is between ±50° and when five passes over the USA satisfy the lighting constraint, passes 1, 3, 4, or 2, 4, and 5, or 1, 3, and 5 may be chosen for a total of three usable passes possible on that day. Likewise, if six passes were in daylight, as many as four passes are possible using the combination 1, 3, 5, and 6 followed by four orbits in the solar inertial mode. A maximum of one pass is assumed possible (if available) on days when β is greater than 50°. To analyze the effect of this particular system limitation, the maximum number of orbits possible to select on any given mission day was related to both β angle magnitude and the total number of daylight passes available that day. All adequately illuminated passes available each day are filtered through the orbit selection criteria defined in table 1.

Table 1. Orbit Selection Criteria

Number of daylight passes available	1	2	3	4	5	6
Number of passes selected when $\beta \leq 50°$	1	2	2	3	3	4
Number of passes selected when $\beta > 50°$	1	1	1	1	1	1

Figures 18 and 19 show the penalty per regression cycle (in terms of USA earth resources opportunities) of constraining available opportunities through the orbit selection filter. Coverage times and passes for earth resources experiments which are on a steerable platform or independent module are represented by the total time and passes curves which are constrained by lighting only. Hard-mounted designs are penalized as indicated by the curves which have been filtered through the previously identified orbit selection criteria.

F. USA Coverage Constrained by Orbit Selection Criteria

Total coverage time and passes, including both the 30°/20° lighting constraint and the orbit selection criteria, can also be estimated for any mission length. Figures 20a through 20h present these constrained values for different launch times and various mission durations for any launch date. Again using a Skylab mission definition with a 9:30 a.m. EST launch on November 9 as an example, the following estimation is derived for USA coverage:

	Constrained Time (hrs)	Constrained Passes
SL-2	2.0	34
SL-3	4.8	76
SL-4	8.5	111
TOTAL	15.3	219

The total of 219 passes would be further reduced by crew availability and target cloud cover constraints. However, the present Skylab requirements of 45 passes would be expected to be met.

Total time per day for a 9:30 a.m. EST launch on November 9, Skylab mission, is shown in figure 21. Days when the β angle is $> 50°$ are represented by the striped areas. Here the relative position of the manned portion of the individual SL-1/2, 3, and 4 missions can be seen. Mission totals are close to those which can be estimated from the previous figures. In the determination of these totals, the first and last days of each manned mission are assumed to be unavailable for earth resources data-taking. From the perspective of figure 21, moving the launch date of SL-1 later is advantageous to earth resources. Launching later in the day can also help.

The effect of launch date on a representative Skylab mission is shown in figure 22 for various SL-1 launch times. The launch intervals are held constant with CSM launches occurring on days 1, 71, and 173. March appears to be the optimum launch month. This date places the SL-3 mission over the better summer cycles, and the Skylab mission is over before the winter period of poor USA viewing. Throughout the year, afternoon launches between ≈ 1:00 and 3:30 produce optimum USA daylight coverage. (Optimum coverage defined as being within one hour of the maximum total mission USA daylight coverage time constrained by the orbit selection criteria.) However, wider windows are available on any given launch day, particularly in the winter where the smallest coverage cycle of the year falls during the shortest (28-day SL-2) mission.

A present candidate launch time for the Skylab mission is April 30 at 12:30 a.m. EST, with launches on days 0, 1, 85, and 181. The estimates derived from this report are as follows:

Mission (day)	1973 Launch Date	Approximate Launch Time	USA Daylight Coverage (hrs)	USA Daylight Passes	Constrained USA Daylight Coverage Time	Constrained USA Daylight Passes
SL-1 (0)	4/30	12:30 p.m.	--	--	--	--
SL-2 (1)	5/1	12:00 noon	10.7	128	7.0	85
SL-3 (85)	7/24	2:30 a.m.	10.7	144	7.4	103
SL-4 (181)	10/28	11:15 a.m.	7.2	110	3.4	57
			28.6	382	17.8	245

G. Influence of Orbital Inclination

The effect of other inclinations on daylight USA coverage is shown in figures 23, 24, and 25. These curves give the average observation time/day over the year for various inclinations, again with 30°/20° lighting and 435 km altitude. With inclinations less than 49° (the upper latitude boundary of the USA), the shoulders on the daylight coverage cycles disappear. The coverage cycle shoulders produced by the 50° inclined orbits are caused by the exclusion (as coverage time) of that part of the orbit which extends above the USA and into Canada. At the lower inclinations, a greater percentage of the orbit, particularly the upper latitude portion, passes over the USA. Hence, the time over the USA per pass is longer. The lighting and β constraints are also less penalizing because the maximum angle between the uppermost latitude of the orbit and the earth-sun line is smaller. (With the earth-sun line ranging between ±23.5° to the equator, a 50° inclined orbit produces beta angles up to ±73.5°; whereas, a 46° inclined orbit produces extreme

β angles of $\pm 69.5°$.) Greater maximum average time/day over the USA then is the result of lower inclinations. This is only true up to a point. The advantages of lower inclinations are offset by the fact that USA coverage can cover only up to latitudes equal to the orbit inclination. As an extreme example, a 25° inclined orbit would not cover any of the continental USA. For a 435 km altitude circular orbit, daylight USA coverage time is maximized at an inclination of 46°-48° orbit. This produces an increase of approximately 15 percent in total USA coverage time. With the 46° inclination, however, USA areas above 46° latitude accrue no coverage time, a fact which must be considered if targets above a 46° latitude are desired. An additional factor is that, although the total coverage time per cycle increases with somewhat lower inclinations (see figure 26), the total number of daylight passes possible per cycle decreases (figure 27). This is due to the reduced duration of the regression cycle.

The length, in days, of a regression cycle varies with inclination. For orbits inclined from 50° to 44°, the length of the regression cycle varies by $\approx$ -1 day per degree of lower inclination. The adjustment for launch time of day increases as inclination declines from 50° to 44° by $\approx$ .4 minutes per degree of inclination. For example, the 50° inclination produces regression cycles every $\approx$ 60 days (with planar launches possible 24 minutes earlier each day thereafter), and a 48° inclination completes a regression cycle every $\approx$ 58 days (with rendezvous compatible launch time regressing 24.8 minutes per day). Similarly, the cycle lengths for 46° and 44° inclinations are $\approx$ 56 and 54 days, respectively.

H. Influence of Orbital Altitude

Within the altitude range of 370 km (200 n.mi.) to 556 km (300 n.mi.) for the 50° inclination, the total USA daylight coverage time per regression cycle increased $\approx$ 1/2 hour per 92.6 km (50 n.mi.) increase in orbital altitude. Coverage time then can be increased through the use of higher orbits (about 1 1/2 percent increase in time per 50 km increase in altitude). Higher altitude orbits produce fewer but longer passes per day. The viewing swath width is also wider with the higher altitude. However, higher altitude brings with it lower resolution for the same sensor and causes the orbiting assembly to fly through higher proton levels of the Van Allen radiation belt.

I. Coverage with Respect to Target Latitude

Latitude (in the context of this section) implies a certain solar lighting history and is therefore a prime factor in the coverage accessibility of targets. Certain latitudes (as evidenced by months of continuous darkness or daylight at the polar latitudes) experience, during

various times of the year, little or no sunlight. The higher the latitude, the more apt the target will be to have inadequate illumination at some time during the year (e.g., high northern latitudes during late fall and early winter). Since the target-viewing opportunities are restricted to being contained within the flight plane, those targets that are higher in latitude than the inclination of the orbit are effectively inaccessible. These two factors (solar lighting history and target viewing opportunities) point up the difficulty of viewing extreme latitude targets. Offsetting this is the fact that, when compared to coverage near the equator, a large portion of the orbit is near the northern and southern latitudes equal to the orbital inclination; i.e., a 50° inclined orbit results in a disproportionate amount of time in the 49° to 50° latitude range. Figure 28 depicts the time/cycle spent in bands up to the 50° latitude. Canada is included as a target in this figure. These coverage times per cycle can be broken into percentages of the cycle above specific latitudes. Since these percentages vary with season, three curves representing cycles centered over sun declinations near -23° (winter), 0° (spring and fall) and +23° (summer) are shown on figure 29.

The percentage of daylight coverage time per cycle between any USA latitude band can be derived from figure 29 by taking the delta percentage between the two latitudes. For example, 50 percent of a summer coverage cycle is at latitudes above 45°. Twenty-three percent of the coverage time occurs over latitudes between 40° and 45°, 13 percent between latitudes 35° and 40°, and 14 percent over latitudes less than 35°. These percentages are shown in figure 30 in latitude bands of 5°. The portion of the cycle over Canada in the 45° to 50° latitude band is so indicated. In the summer, over 30 percent of a combined target coverage time cycle represents time over Canada, thus increasing the daylight coverage time per cycle from $\approx$ 14.2 hours for only USA coverage to $\approx$ 20.2 hours (figure 28) for the combined target.

J. Coverage of Other Target Areas

It is expected that other areas besides the USA will be targets in any earth resources mission. Because USA is of prime interest, most of this analysis considered the continental USA only. Daylight coverage of Brazil and Australia is included to represent briefly other potential targets of interest.

Figure 31 gives the average time over Brazil per 60-day cycle over the year. For approximately 50 days out of each cycle, two daylight passes per day are possible with occasionally a short, less than 2-minute, third pass. An average of $\approx$ 12 minutes of daylight coverage per day is obtained except when broken by days with dark passes only. Being close

to the equator, Brazil as a target is almost insensitive to the seasonal changes with the 30°/20° elevation angle constraint.

Coverage time per cycle for Australia is shown in figure 32. Coverage over Australia, except during its summer, is very similar to that of Brazil. A period of days (≈ 20 consecutive days) in which two or three descending passes satisfy the lighting constraint is followed by a comparable period in which only the ascending passes are in daylight. Australia is more sensitive to seasonal changes than Brazil, but the 30°/20° lighting constraint almost evens out the coverage time over the year.

A composite of USA, Brazil, and Australia coverage time/day is shown in figure 33 for the November 9, 9:30 a.m. launch. Daylight coverage of at least one of the three targets is seen to be available almost every day. The Brazil coverage cycles begin with a 25-day period of daylight descending passes which are the extensions of descending passes over the USA. For approximately the first half of this period, daylight passes over the USA are also possible (days 10 through 24, 70 through 80, etc., on figure 33). The USA/Brazil daylight coverage overlaps during ascending passes (days 46-60, 106-120, etc.) are produced from separate orbits.

K. Conclusions

Certain conclusions have become evident with respect to earth resources opportunities from an orbiting assembly:

1. The imposition of a target lighting constraint creates a sensitivity of the target to season, or more specifically, to the sun declination. This sensitivity increases with magnitude of the target latitude and with increase in the lighting constraint (implemented through a required sun elevation angle at the target). The USA as a target, with latitudes up to 49°, is quite sensitive to season. Even with the minimum sun elevation angle at the target relaxed from 30° to 20° in the "winter," daylight coverage in the summer is more than double the daylight coverage time possible in the winter. The continent of Australia, with southern latitudes to ≈ -39° is thus less sensitive to season. The winter lighting constraint relaxation almost eliminates the seasonal sensitivity. Brazil, on the equator, is essentially insensitive to the season.

2. Constraining acceptable coverage time to days when β is less than some geometrically obtainable value decreases USA coverage time. The lower the magnitude of acceptable β angles, the greater the penalty.

3. Constraining the daily number of viewing opportunities through orbit selection criteria lessens the seasonal effect, penalizing summer coverage more than winter coverage. In the summer, more passes are candidates for selection than can be chosen. The winter yields fewer candidates.

4. Launch time of day lessens as a coverage time parameter as the mission length approaches or becomes a multiple of the regression cycle.

5. Lowering the orbital inclination from 50° to as low as 44° increases total USA daylight coverage time per regression cycle but decreases the total number of passes per cycle.

6. For missions approaching or exceeding one year in duration, a uniform distribution of targets in terms of latitude yields the best in earth resources opportunities.

7. The optimum time of year for USA earth resources opportunities is that date which centers the greatest portion of the mission over the better summer coverage cycles, and if possible, eliminating the worst winter cycle or cycles.

8. The quantity of observation time available per year increases with the magnitude of the target latitude while the quality, in terms of adequate lighting, decreases.

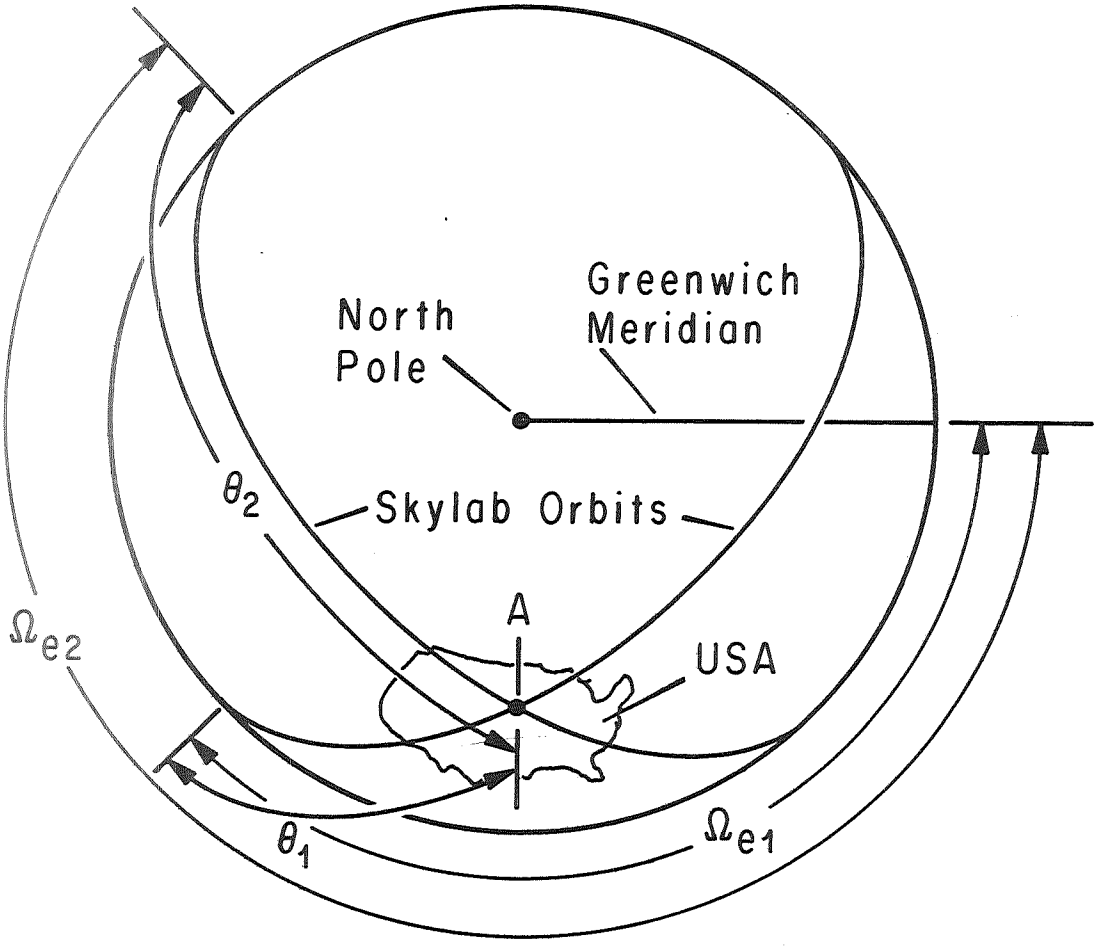

FIG. 1. DEFINITION OF Ω_e AND θ

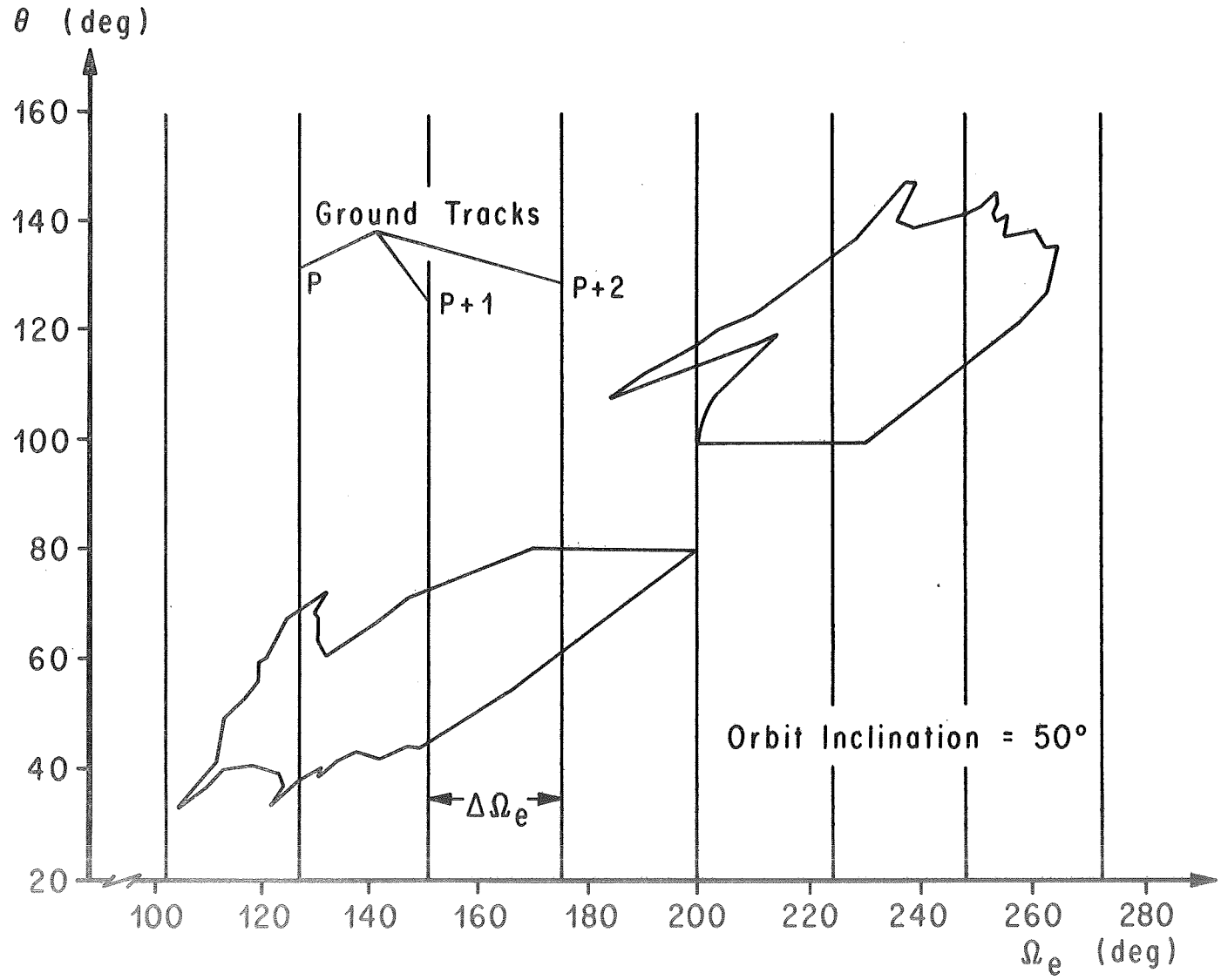

FIG. 2. MAP OF USA IN Ω_e, θ COORDINATES

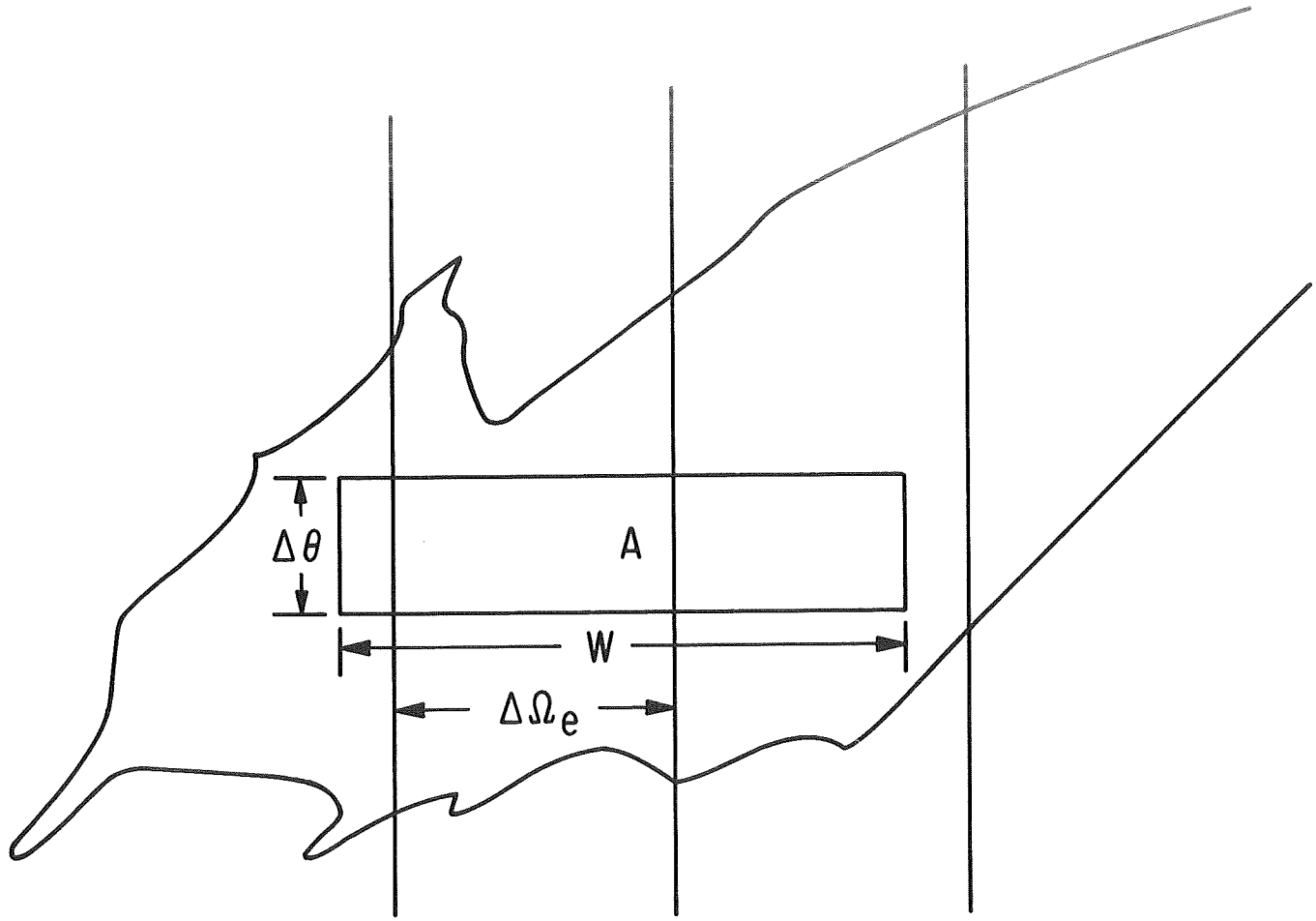

FIG. 3. OBSERVATION TIME OVER AN AREA

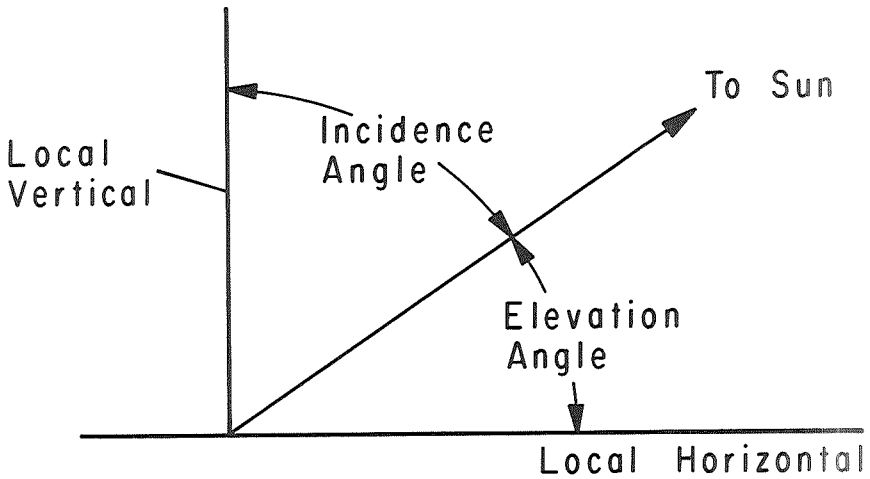

FIG. 4. DEFINITION OF ELEVATION ANGLE

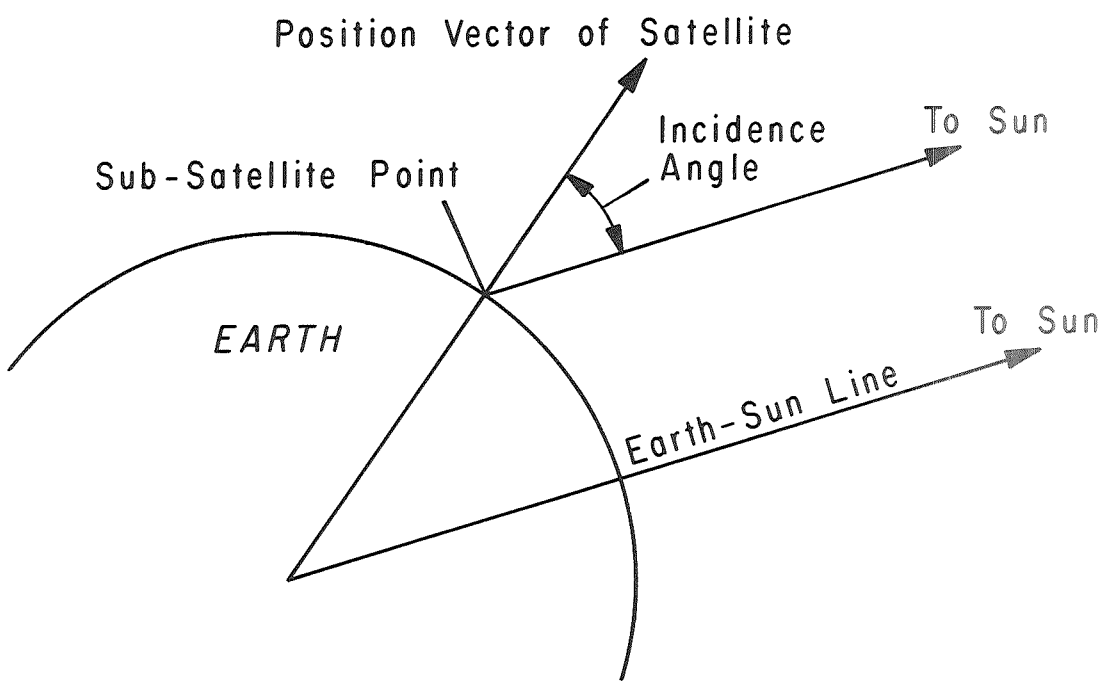

FIG. 5. CALCULATION OF SUN INCIDENCE ANGLE

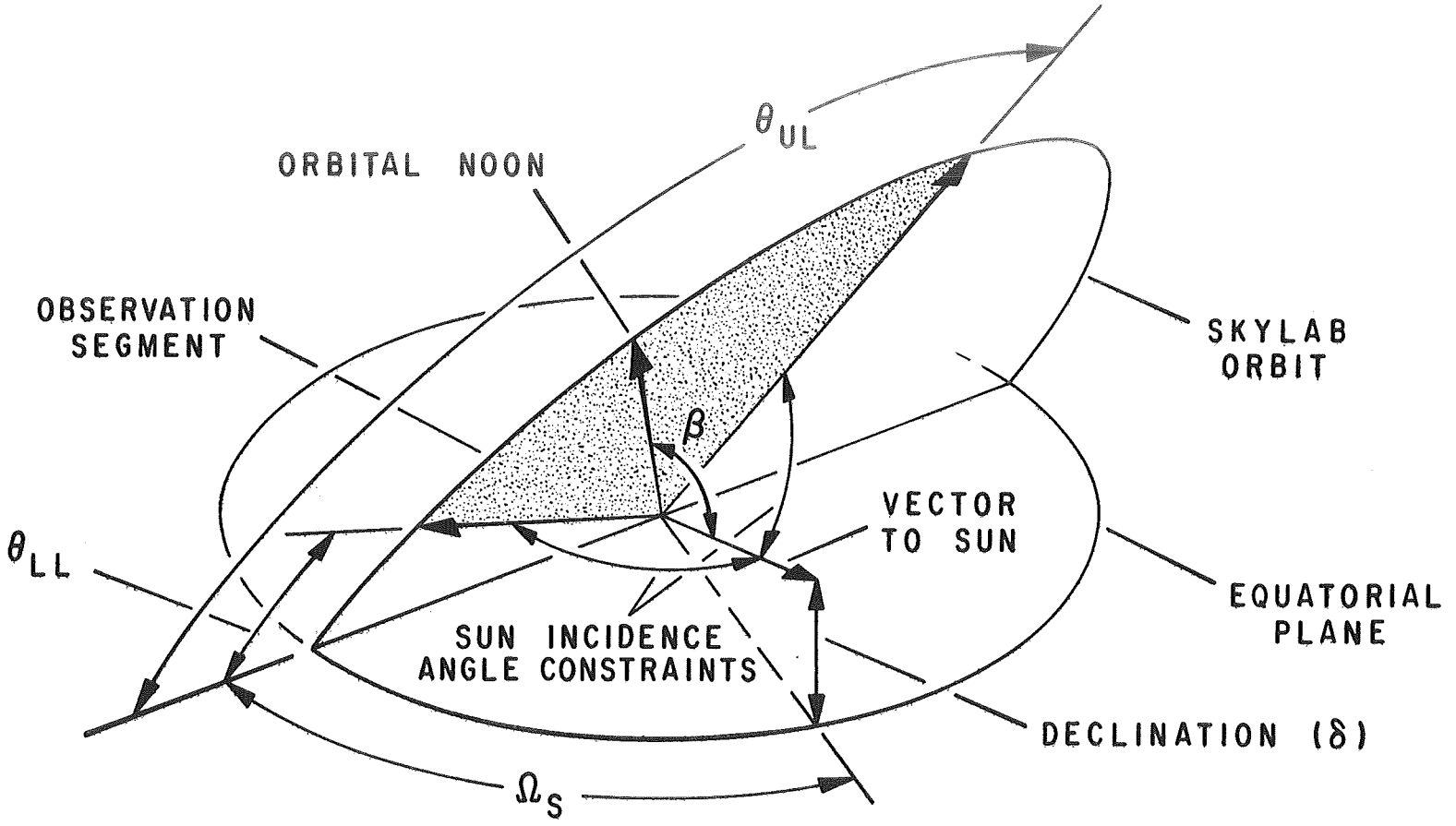

FIG. 6. OBSERVATION SEGMENT

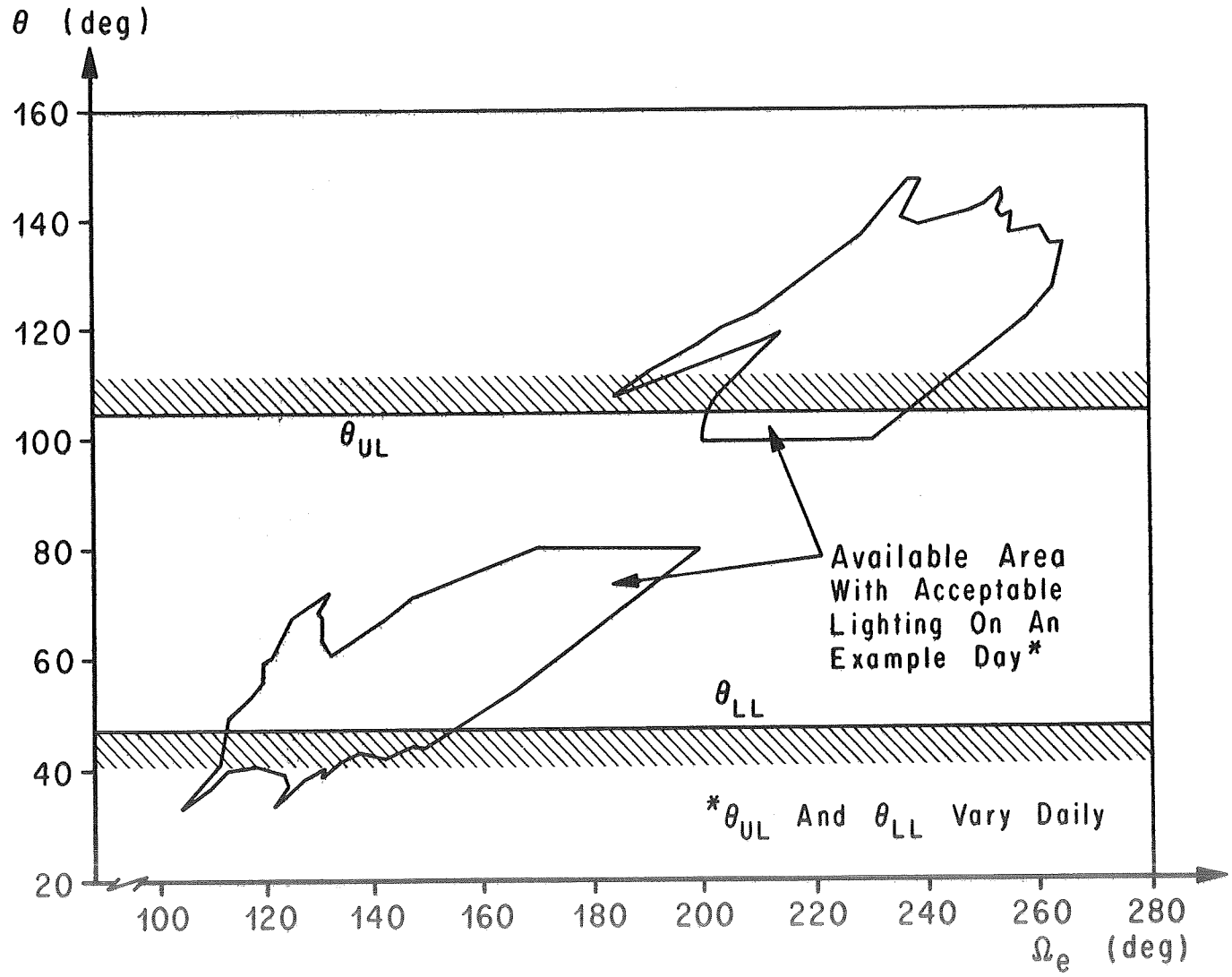

FIG. 7. AREA OF USA AVAILABLE FOR OBSERVATION

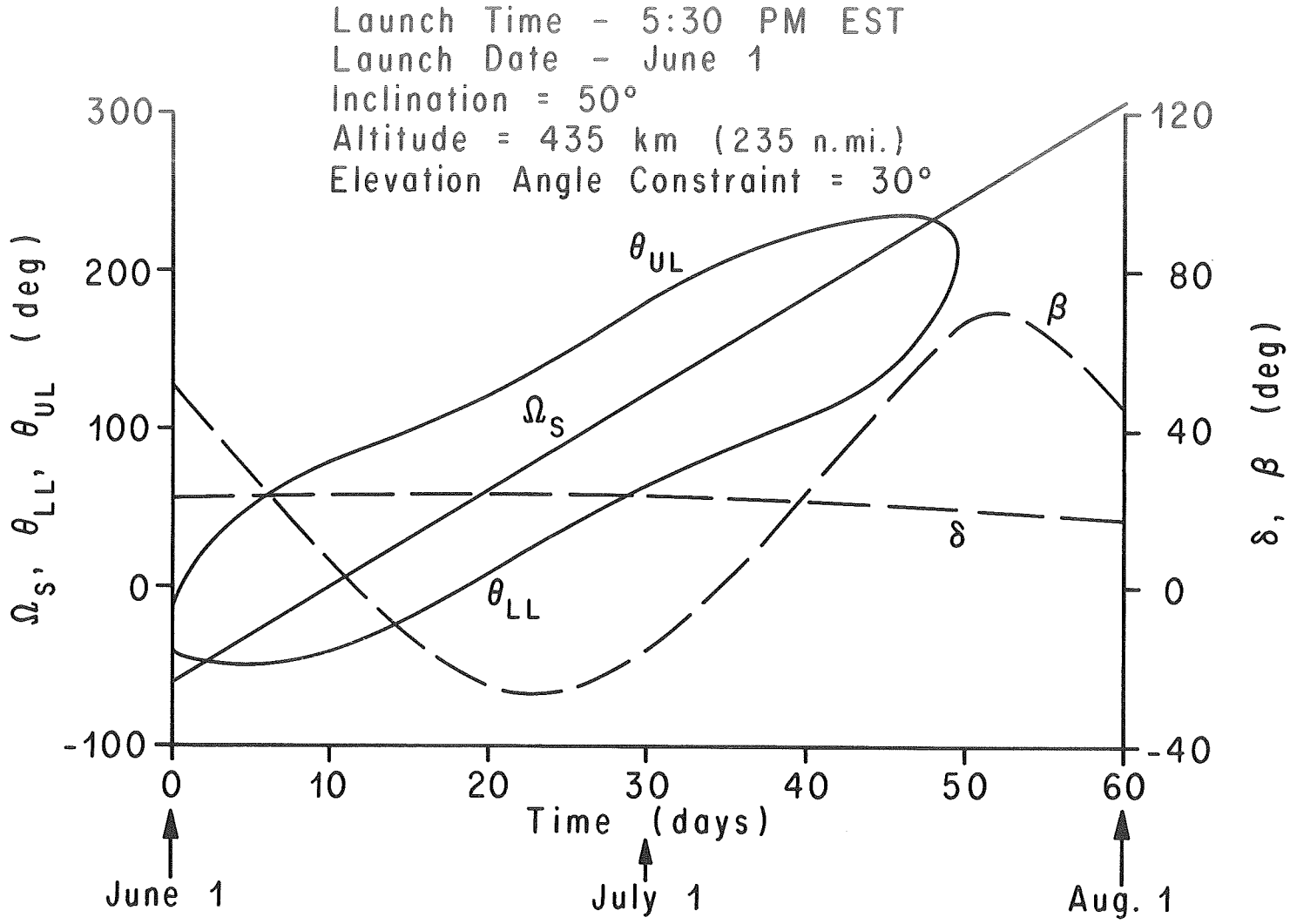

FIG. 8. TYPICAL TIME HISTORY OF θ_{LL}, θ_{UL}, Ω_S, δ, AND β

Launch Time - 5:30 P.M. EST
Launch Date - June 1
Inclination = 50°
Altitude = 435 km (235 n. mi.)
Elevation Angle Constraint = 30°

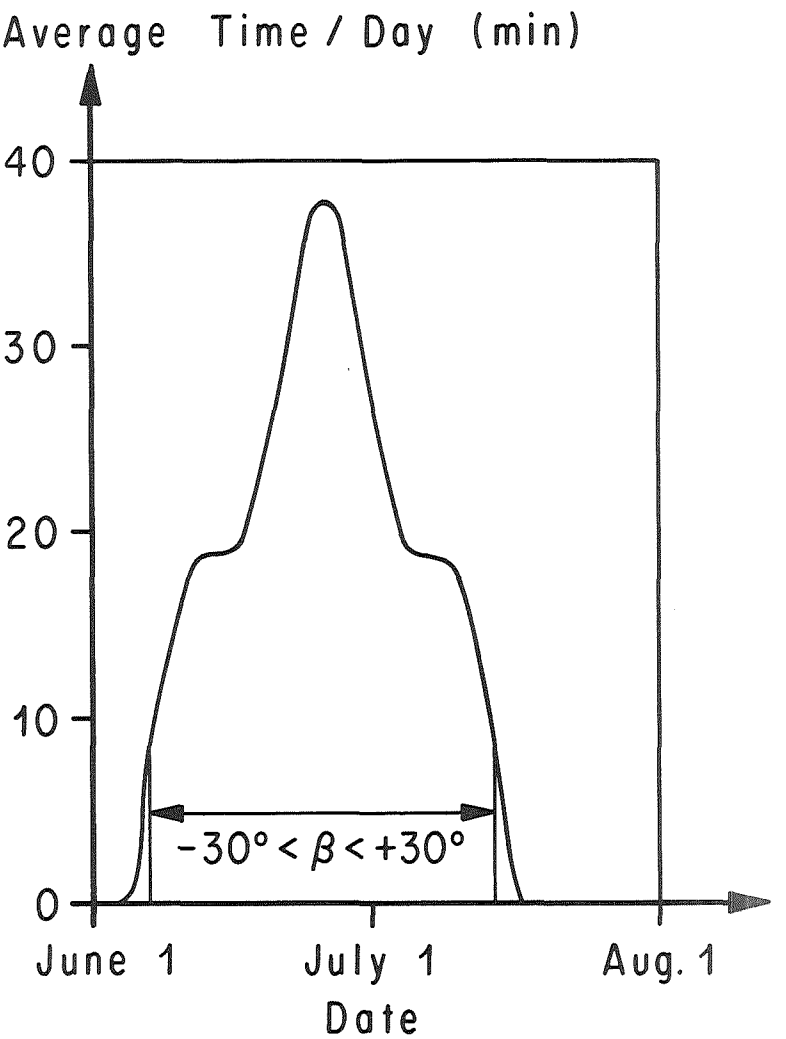

FIG. 9. OBSERVATION TIME PER DAY (ONE CYCLE)

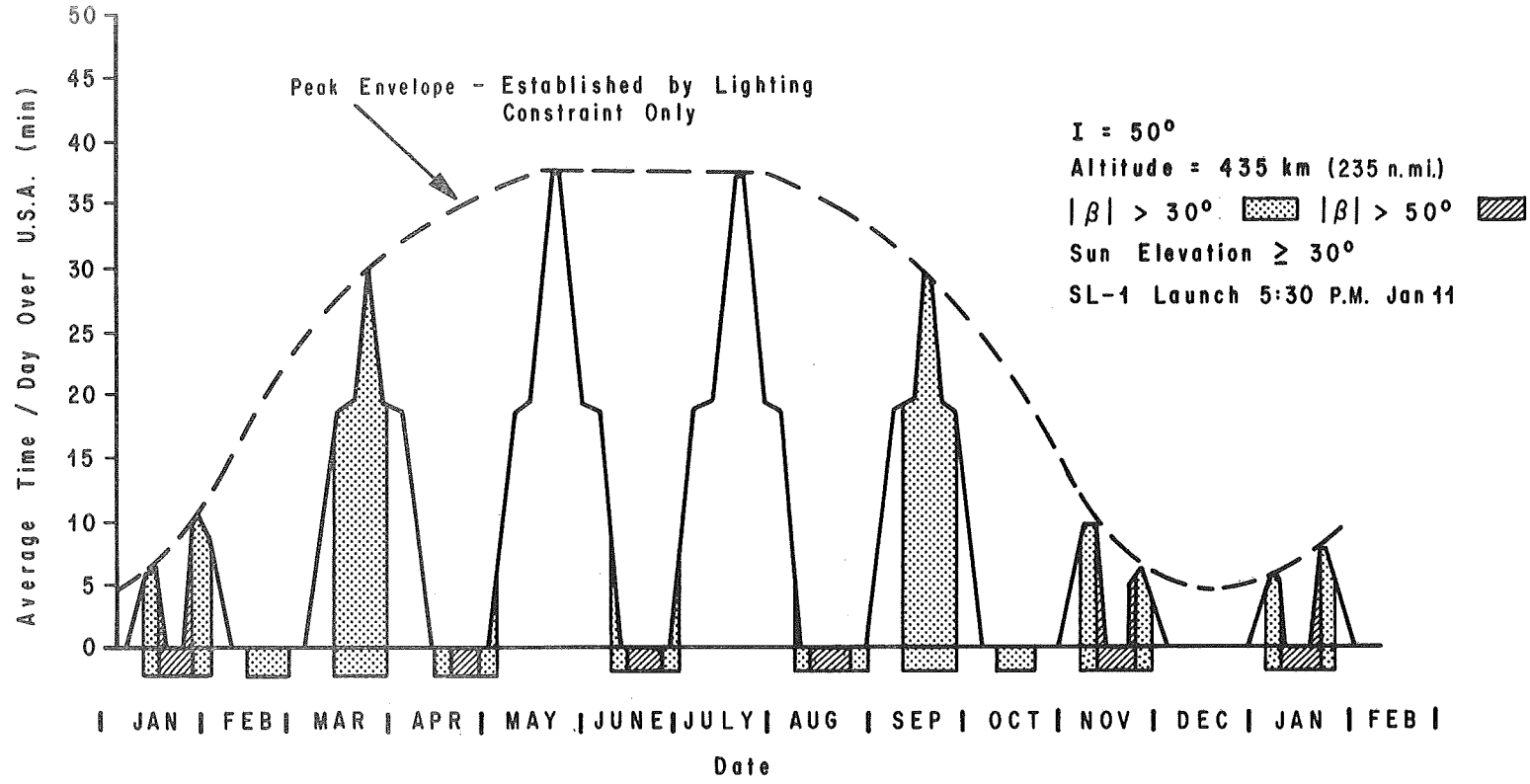

FIG. 10. DAILY VARIATIONS IN USA COVERAGE TIME

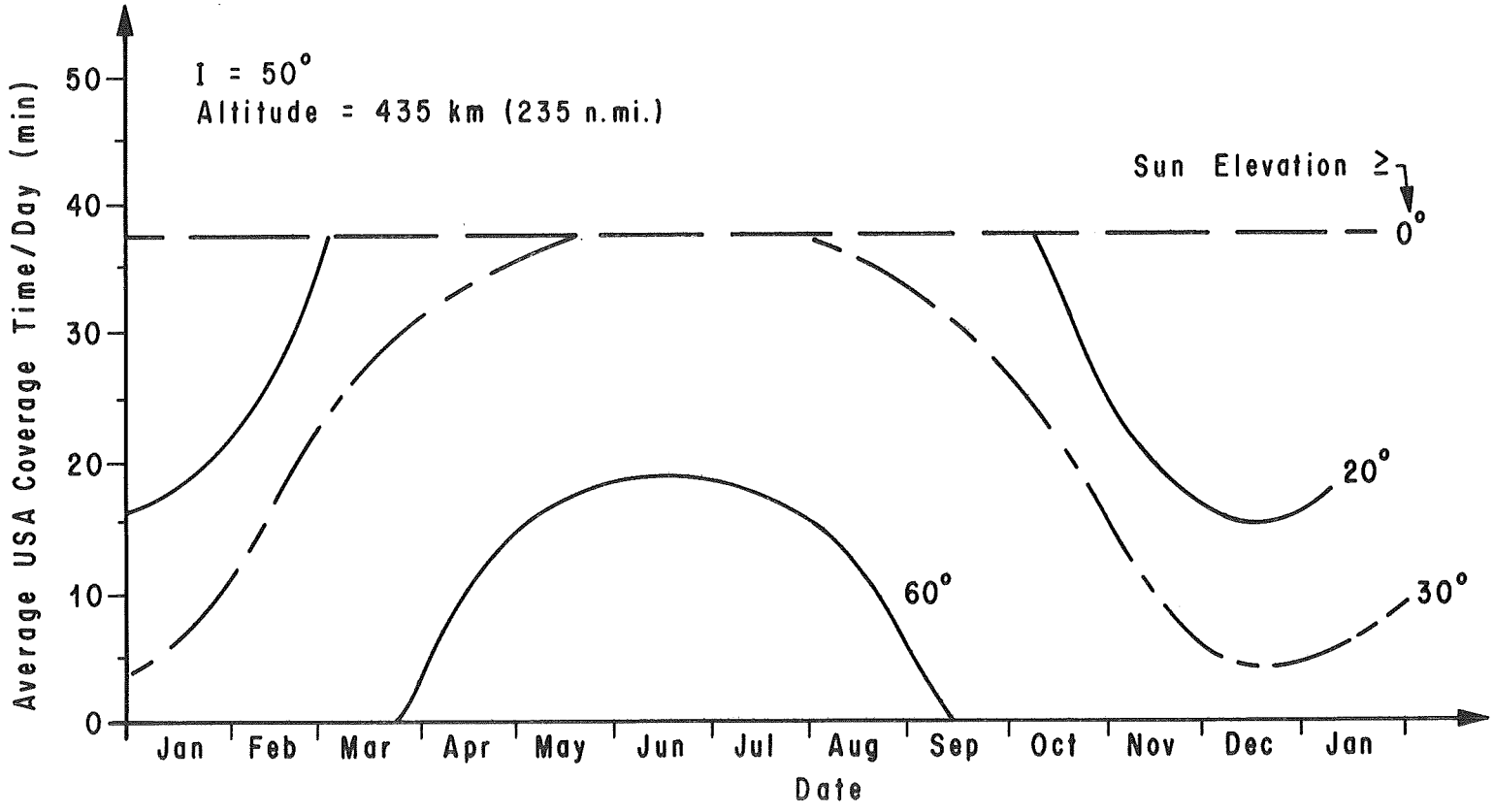

FIG. 11. INFLUENCE OF LIGHTING CONSTRAINT ON ENVELOPE OF COVERAGE CYCLE PEAKS

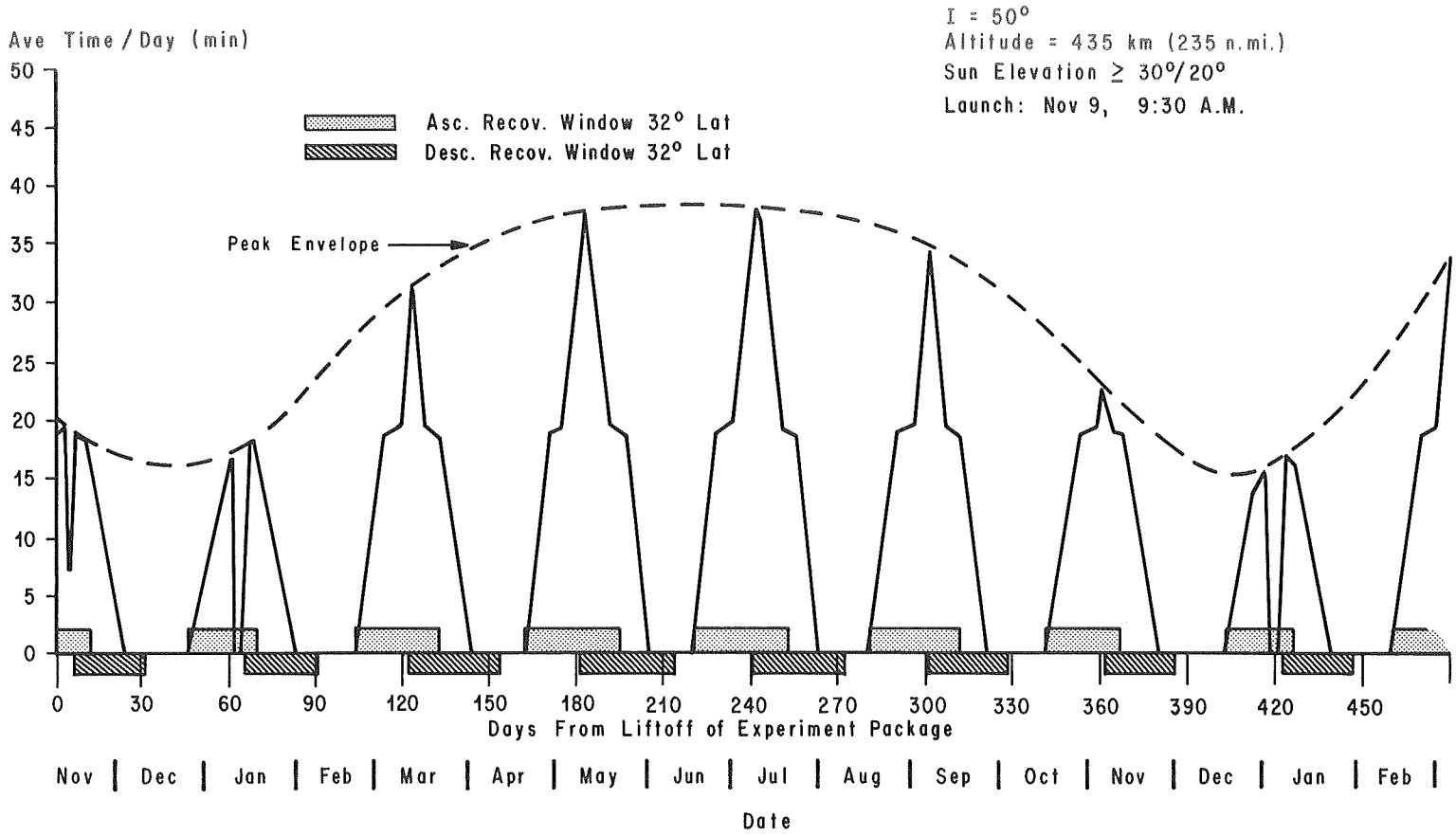

FIG. 12. DAILY VARIATIONS IN USA COVERAGE TIME / DAY "30/20" LIGHTING CONSTRAINT

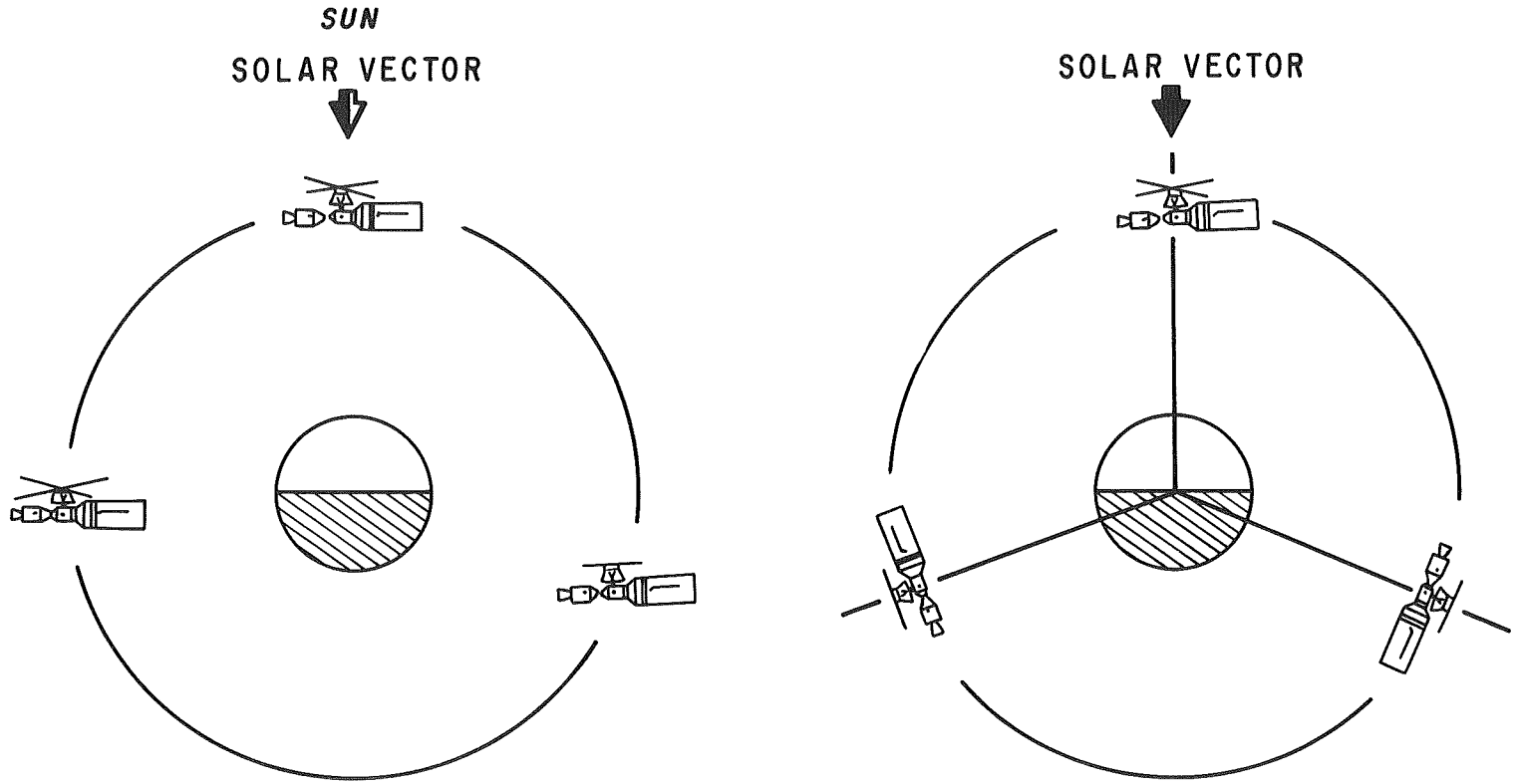

FIG. 13. ORBITAL ASSEMBLY ATTITUDES

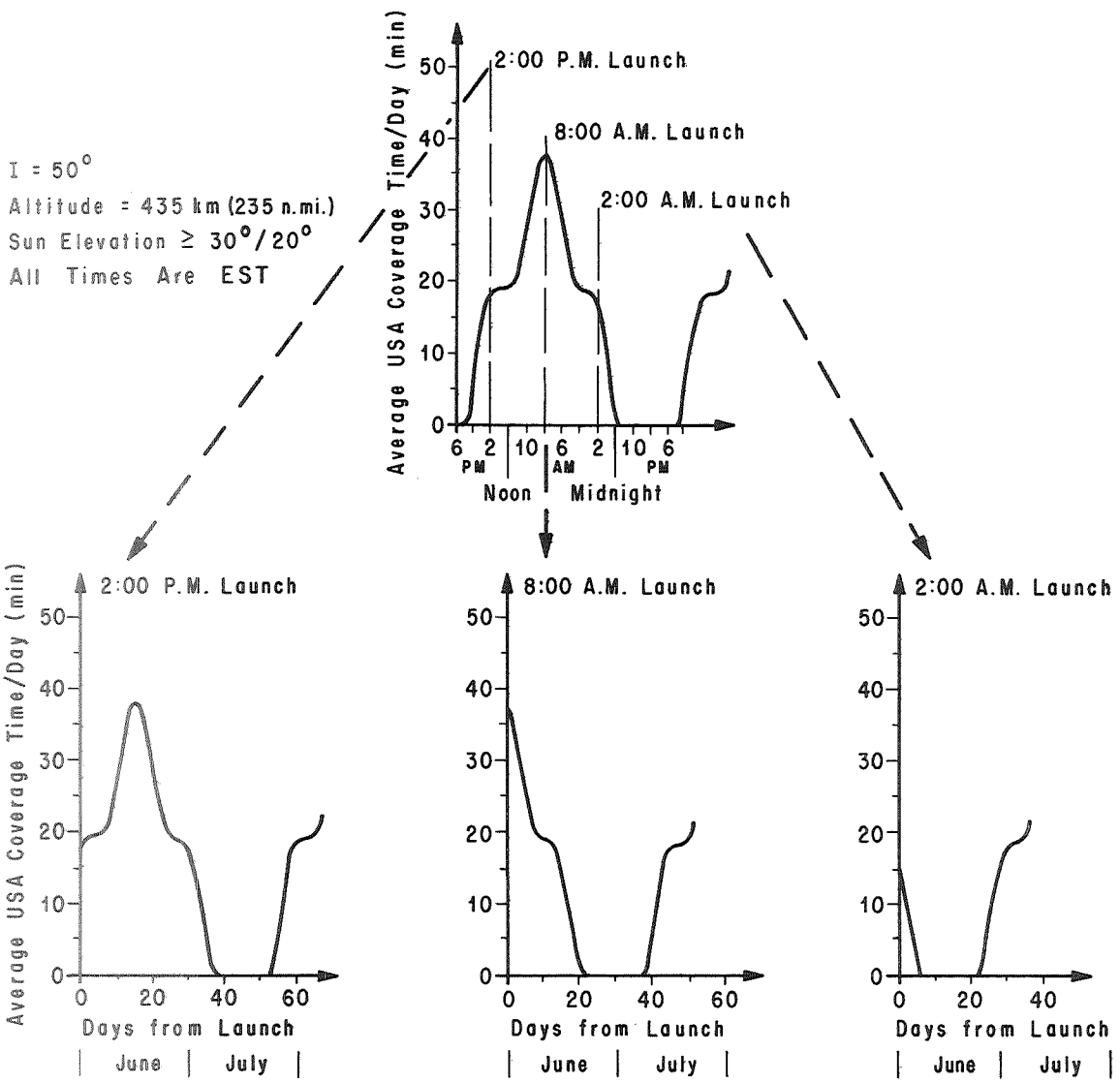

FIG. 14. LAUNCH TIME OF DAY EFFECT ON INITIAL POSITION OF USA COVERAGE CYCLE

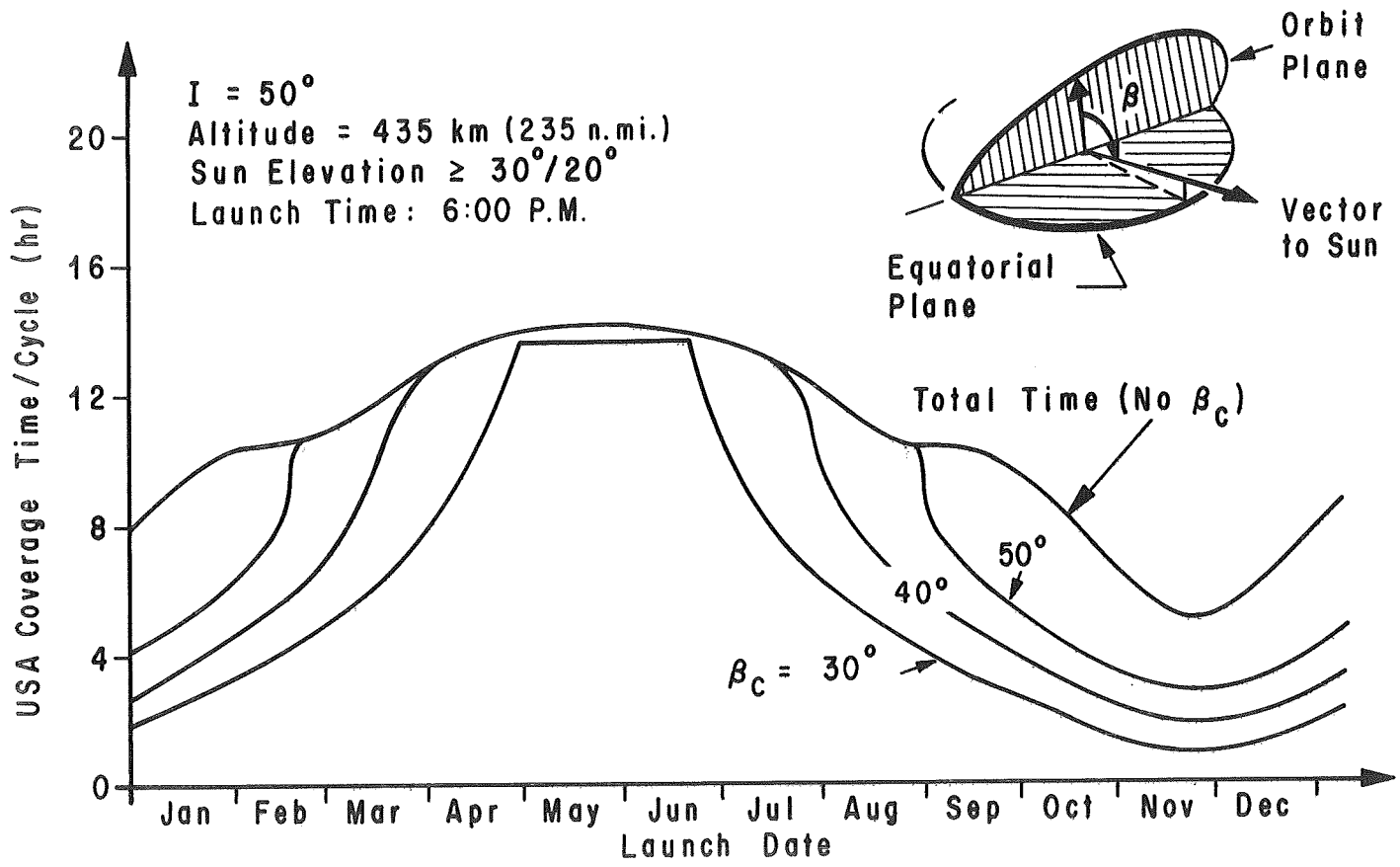

FIG. 15. BETA INDUCED VARIATION IN USA COVERAGE TIME (PER REGRESSION CYCLE) AS A FUNCTION OF LAUNCH DATE

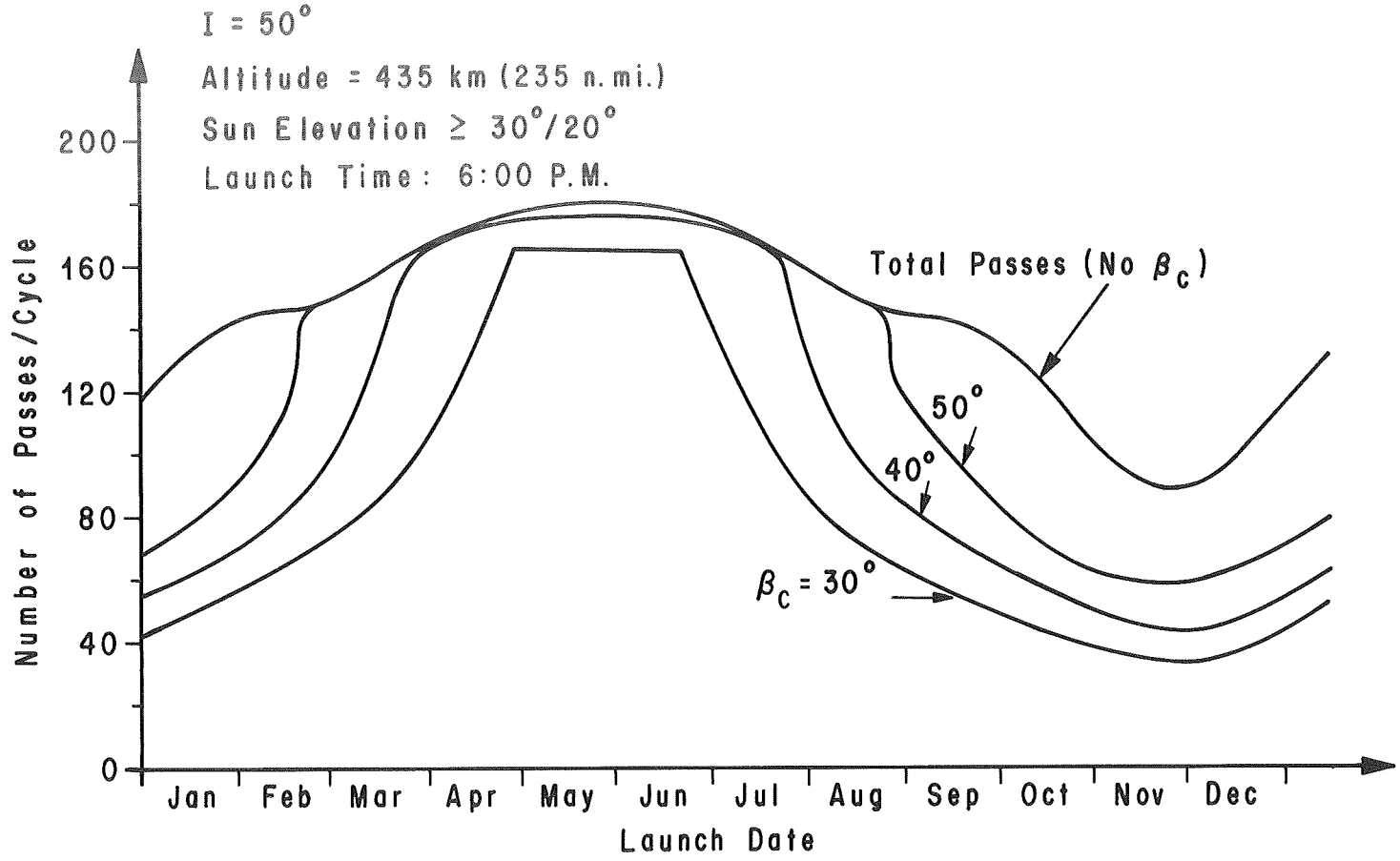

FIG. 16. BETA INDUCED VARIATION IN NUMBER OF DAYLIGHT PASSES OVER THE USA (PER REGRESSION CYCLE) AS A FUNCTION OF LAUNCH DATE

I = 50°
Launch Time: 3:00 A.M.
Sun Elevation: ≥ 30°/20°
Altitude = 435 km (235 n.mi.)

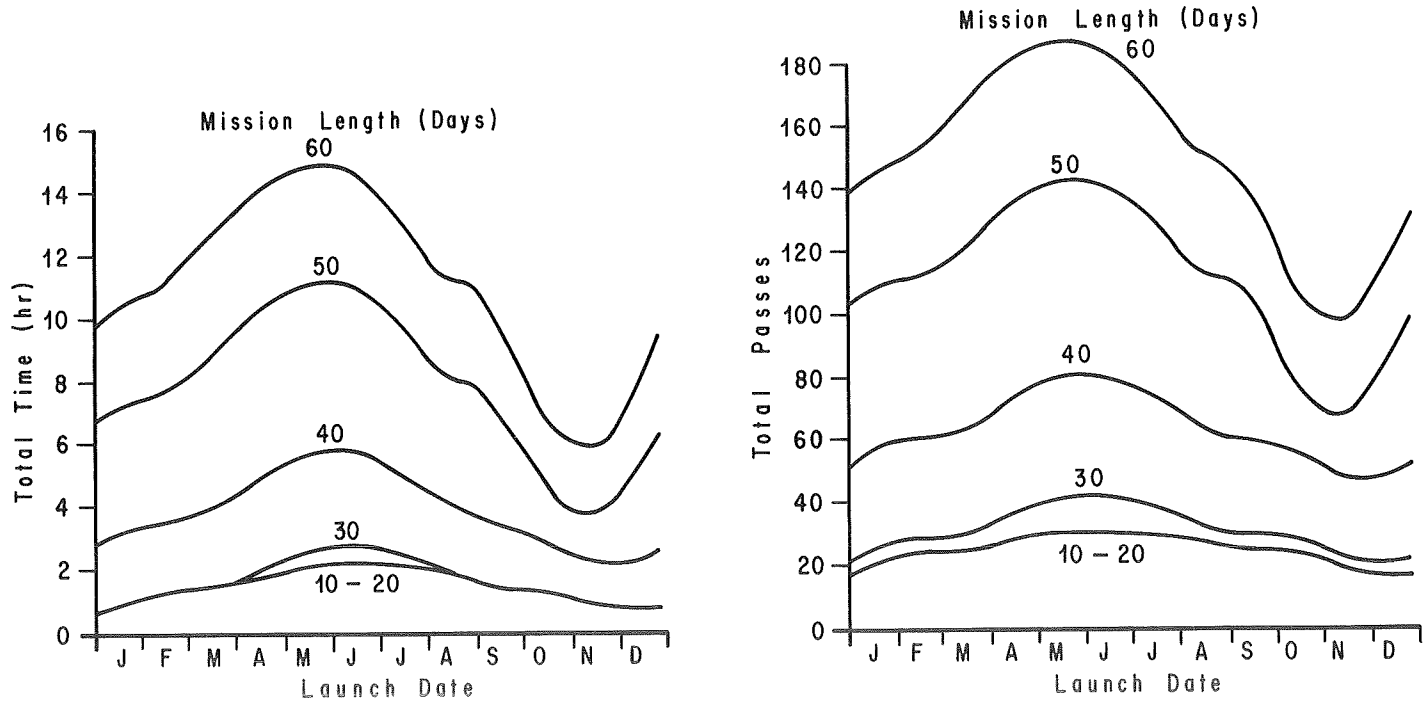

FIG. 17a. TOTAL USA COVERAGE TIME AND PASSES (PER MISSION LENGTH) AS A FUNCTION OF LAUNCH DATE (3 A.M. LAUNCH)

I = 50°
Altitude: 435 km (235 n.mi.)
Launch Time: 6:00 A.M.
Sun Elevation: ≥ 30°/20°

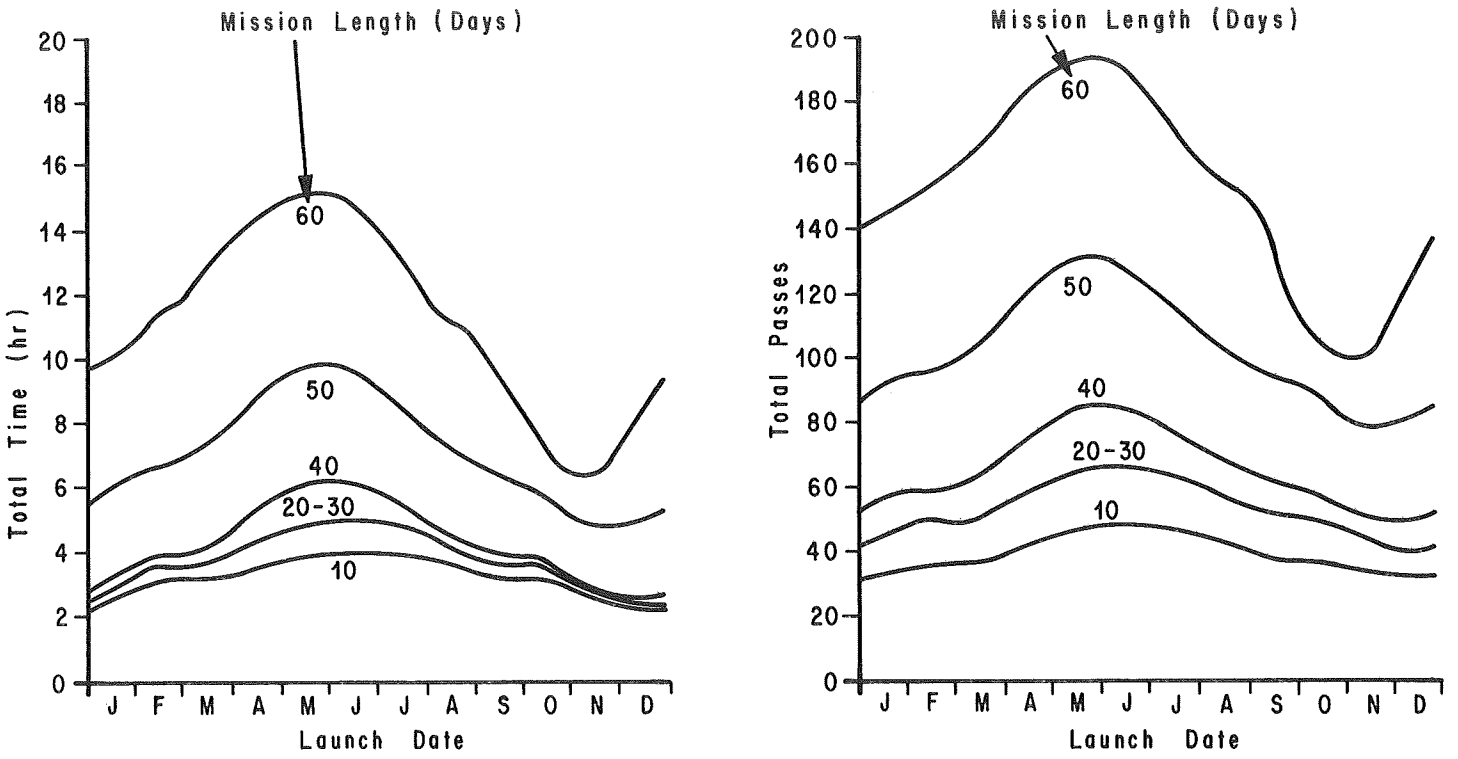

FIG. 17b. TOTAL USA COVERAGE TIME AND PASSES (PER MISSION LENGTH) AS A FUNCTION OF LAUNCH DATE (6 A.M. LAUNCH)

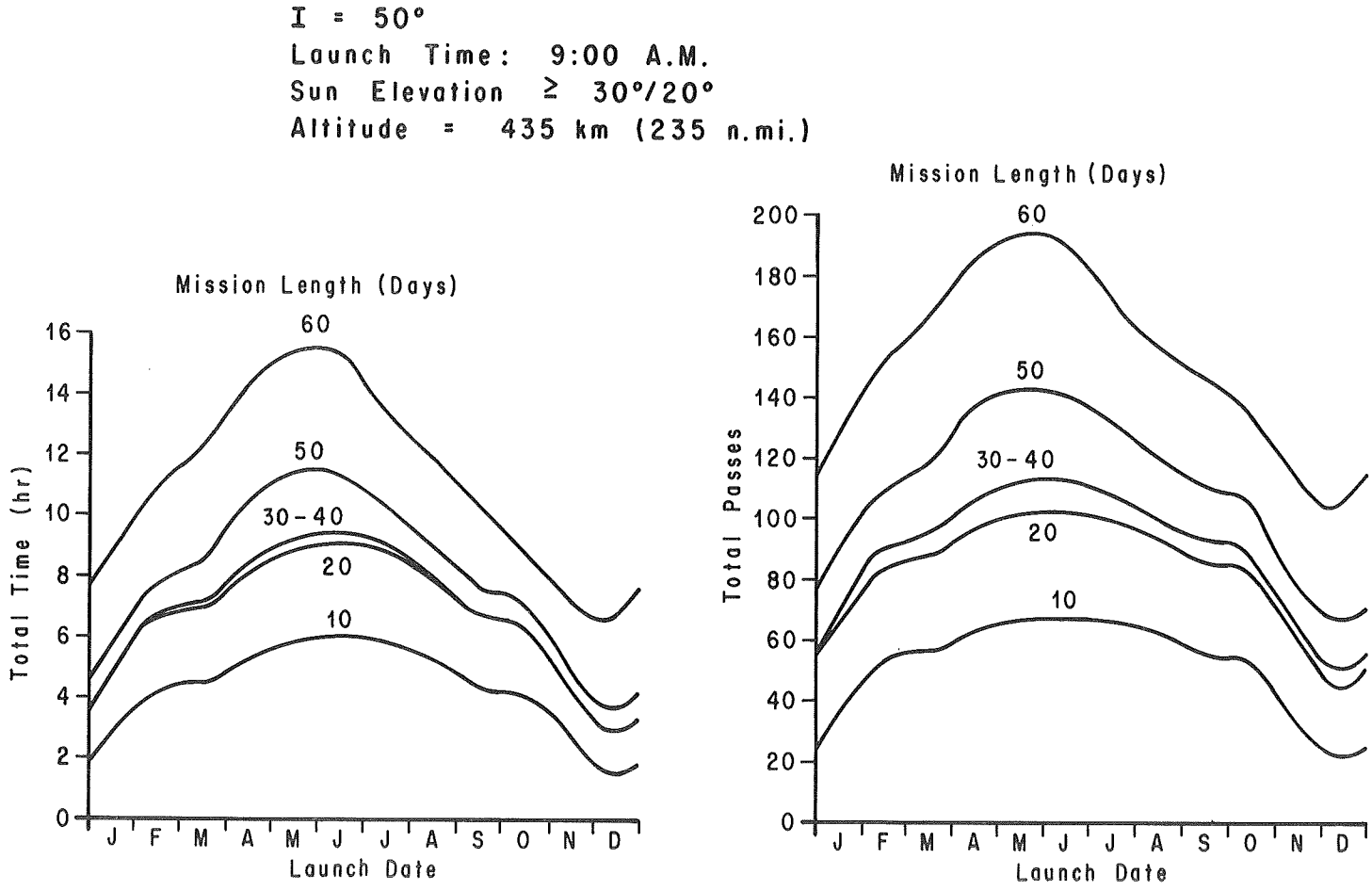

FIG. 17c. TOTAL USA COVERAGE TIME AND PASSES (PER MISSION LENGTH) AS A FUNCTION OF LAUNCH DATE (9 A.M. LAUNCH)

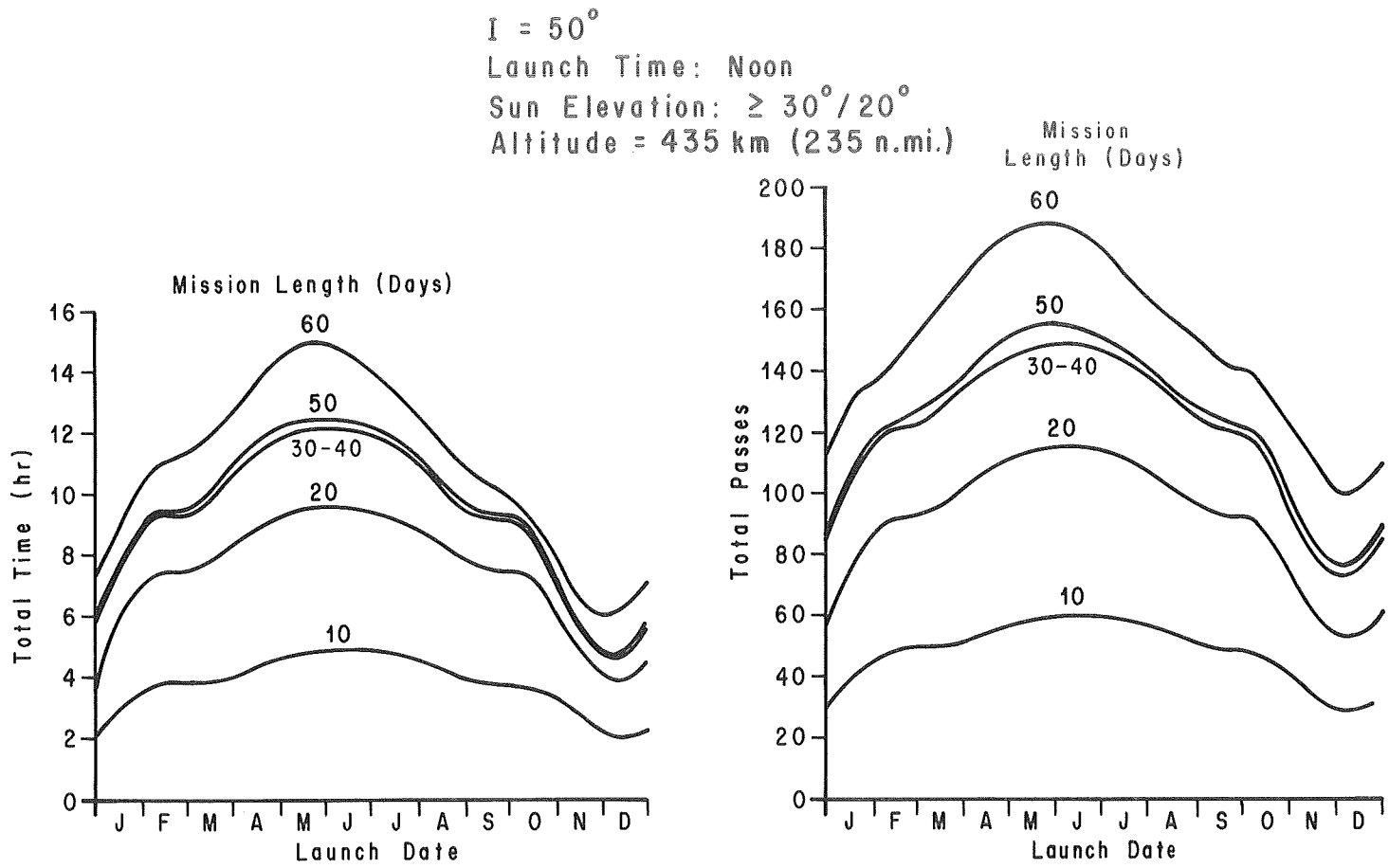

FIG. 17d. TOTAL USA COVERAGE TIME AND PASSES (PER MISSION LENGTH) AS A FUNCTION OF LAUNCH DATE (NOON LAUNCH)

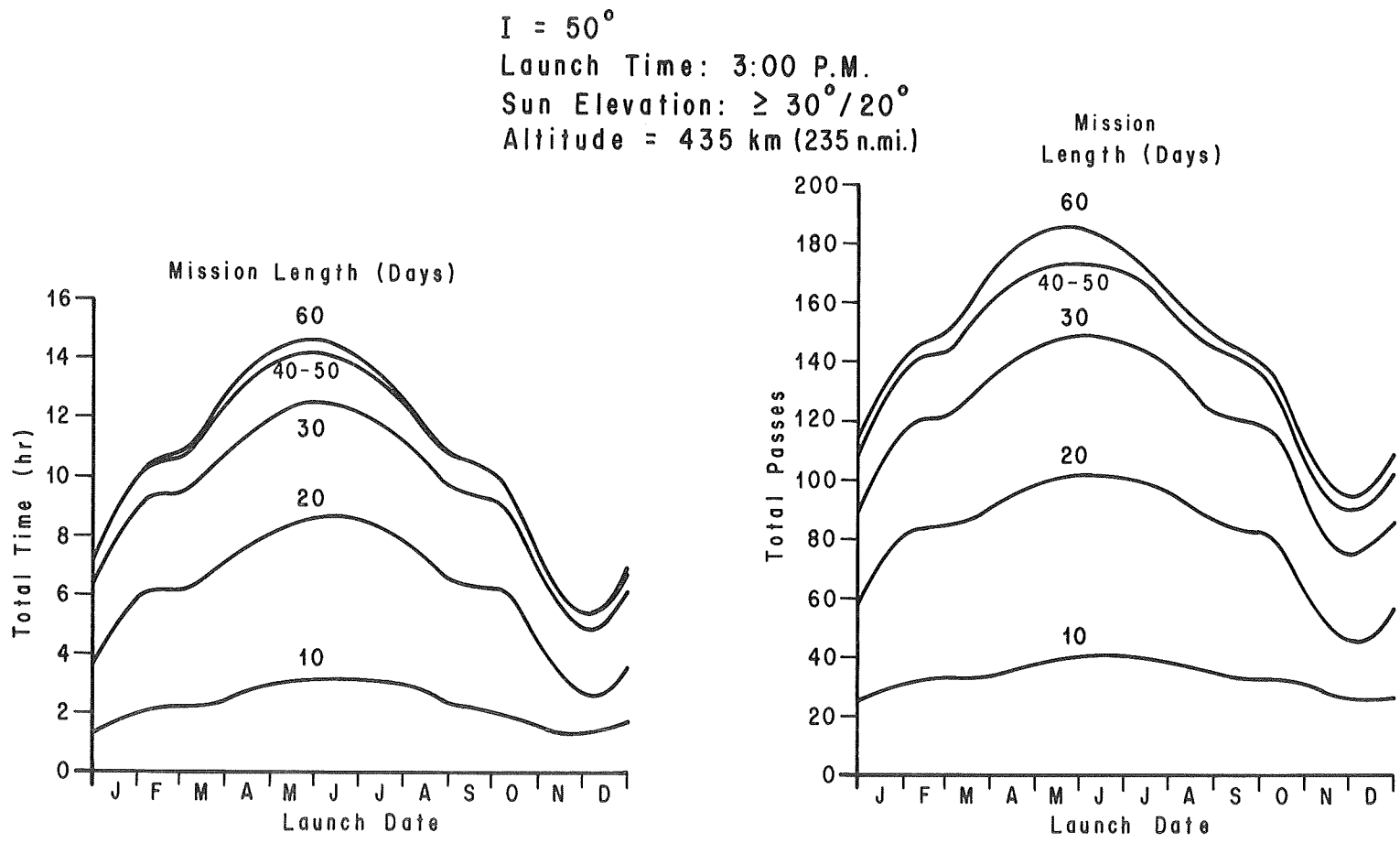

FIG. 17e. TOTAL USA COVERAGE TIME AND PASSES (PER MISSION LENGTH) AS A FUNCTION OF LAUNCH DATE (3 P.M. LAUNCH)

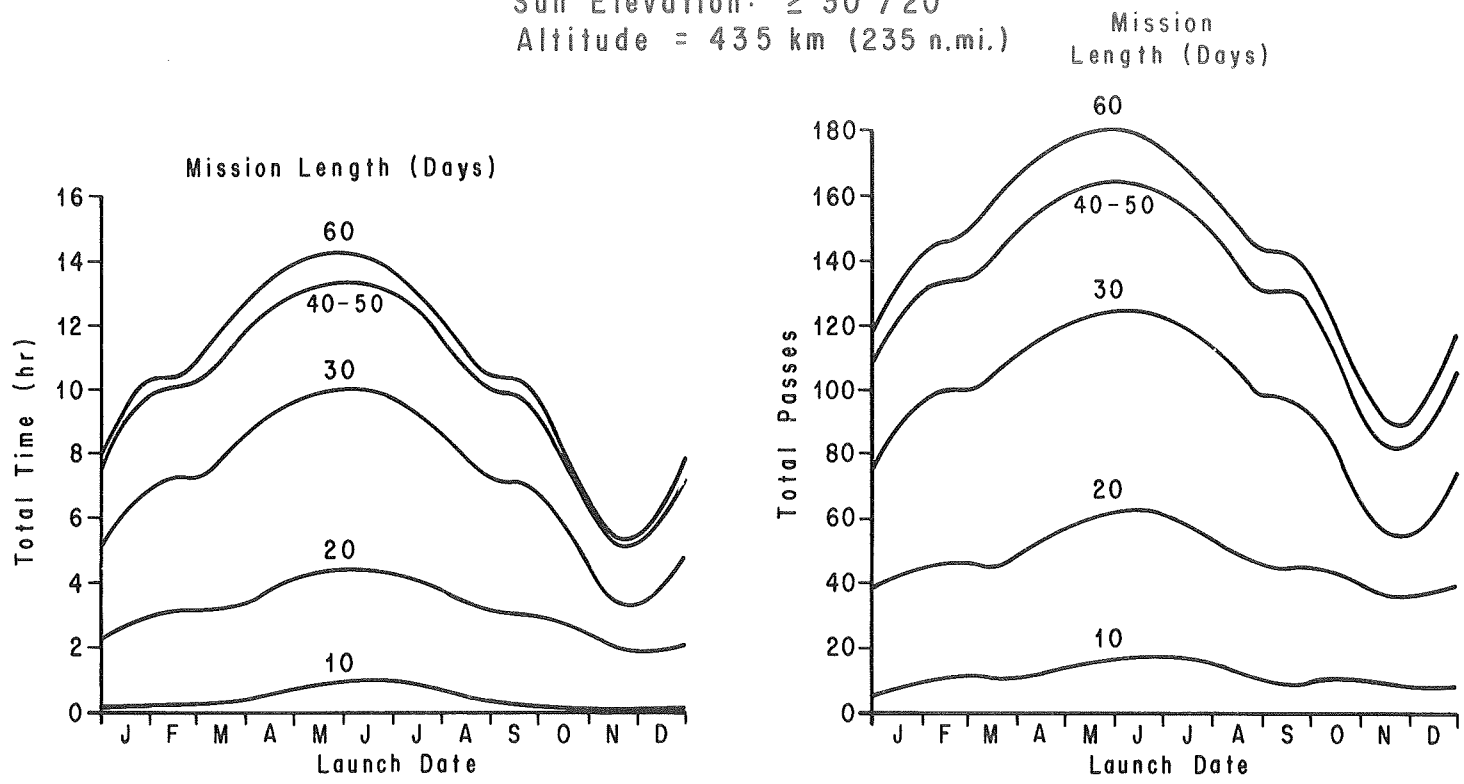

FIG. 17f. TOTAL USA COVERAGE TIME AND PASSES (PER MISSION LENGTH) AS A FUNCTION OF LAUNCH DATE (6 P.M. LAUNCH)

I = 50°
Launch Time: 9:00 P.M.
Sun Elevation: ≥ 30°/20°
Altitude = 435 km (235 n.mi)

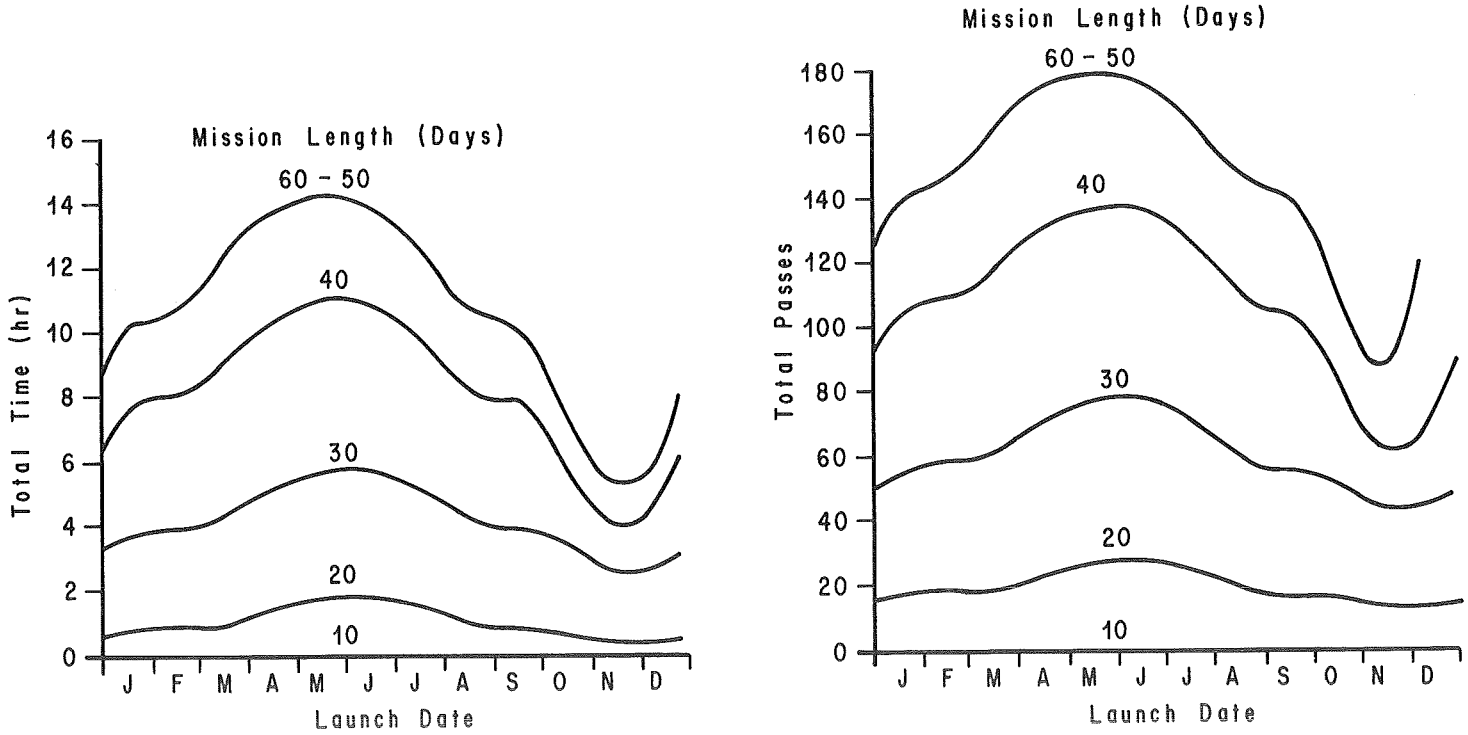

FIG. 17g. TOTAL USA COVERAGE TIME AND PASSES (PER MISSION LENGTH) AS A FUNCTION OF LAUNCH DATE (9 P.M. LAUNCH)

I = 50°
Launch Time: Midnight
Sun Elevation: ≥ 30°/20°
Altitude = 435 km (235 n.mi.)

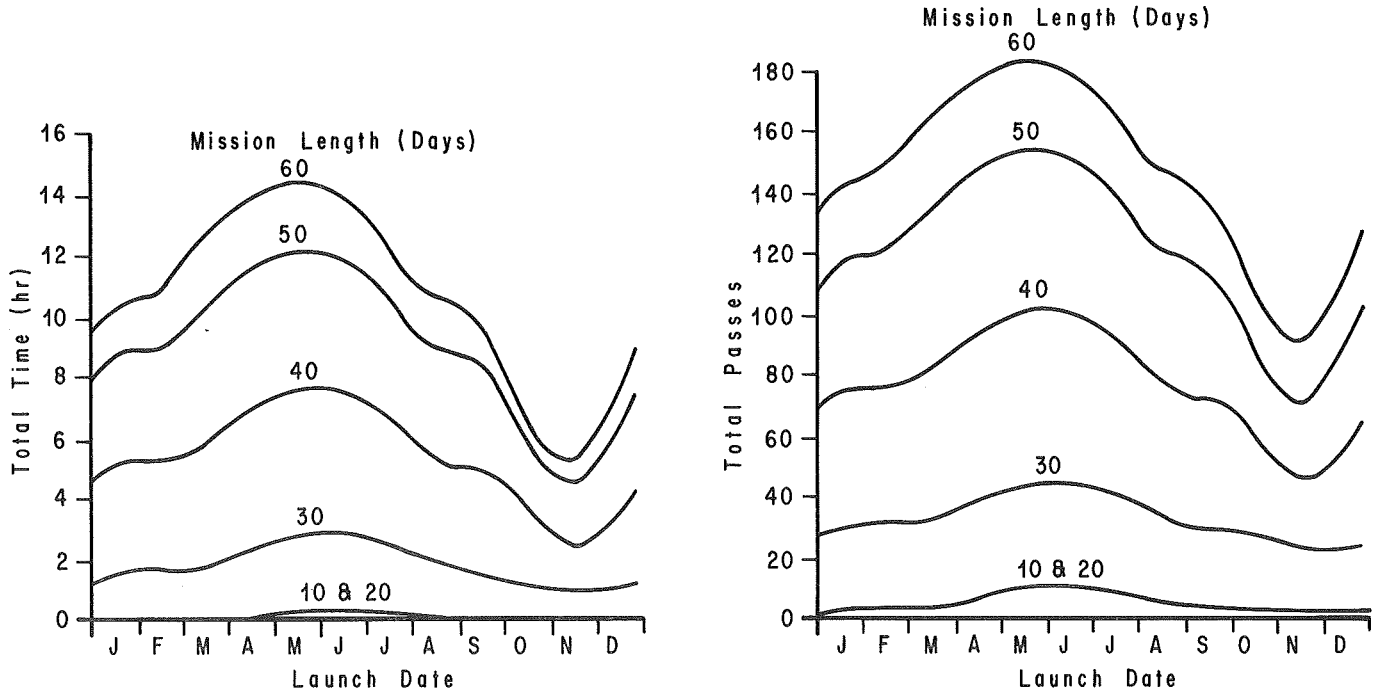

FIG. 17h. TOTAL USA COVERAGE TIME AND PASSES (PER MISSION LENGTH) AS A FUNCTION OF LAUNCH DATE (MIDNIGHT LAUNCH)

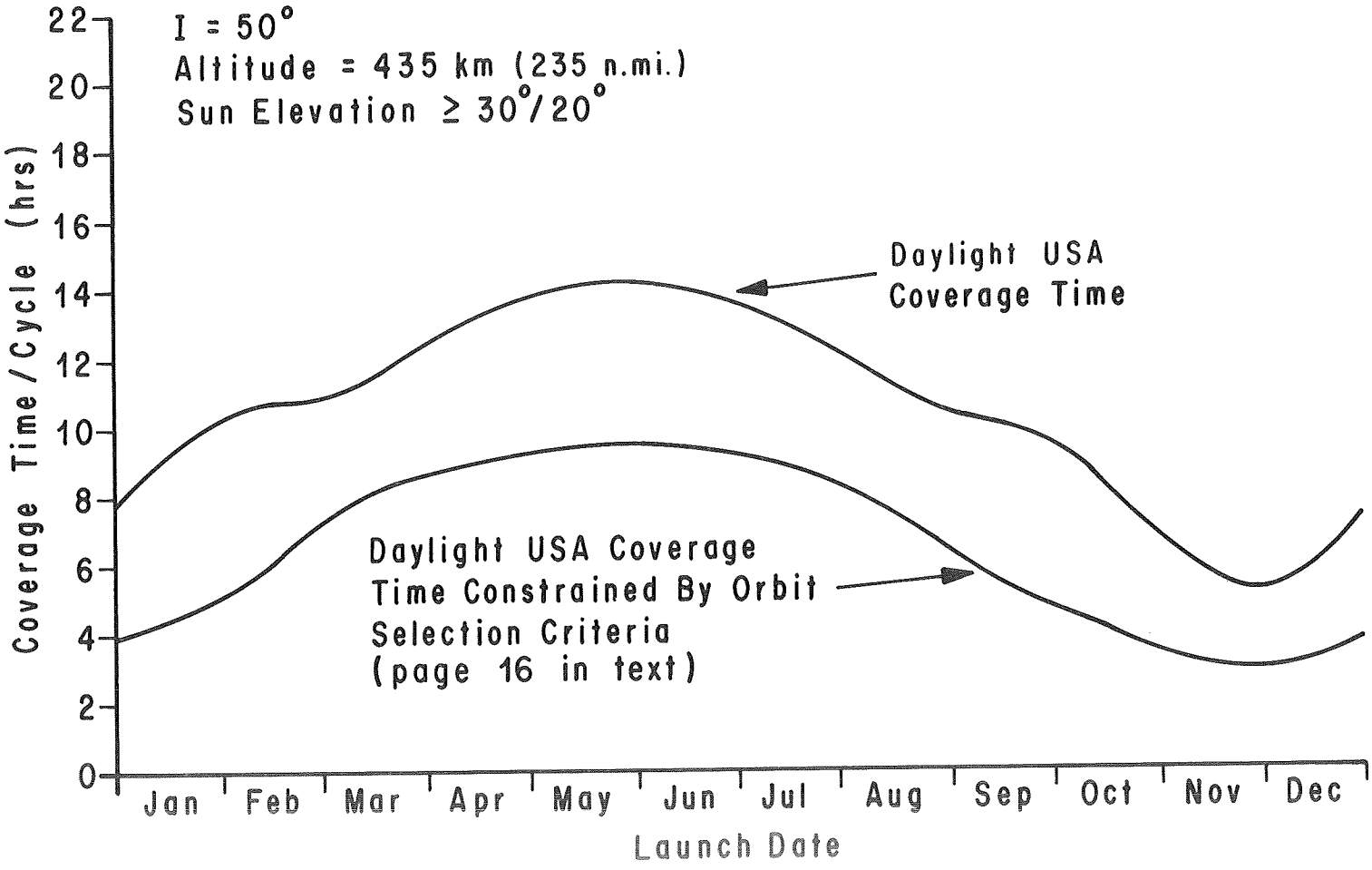

FIG. 18. INFLUENCE OF ORBIT SELECTION CRITERIA ON USA COVERAGE TIME (PER REGRESSION CYCLE)

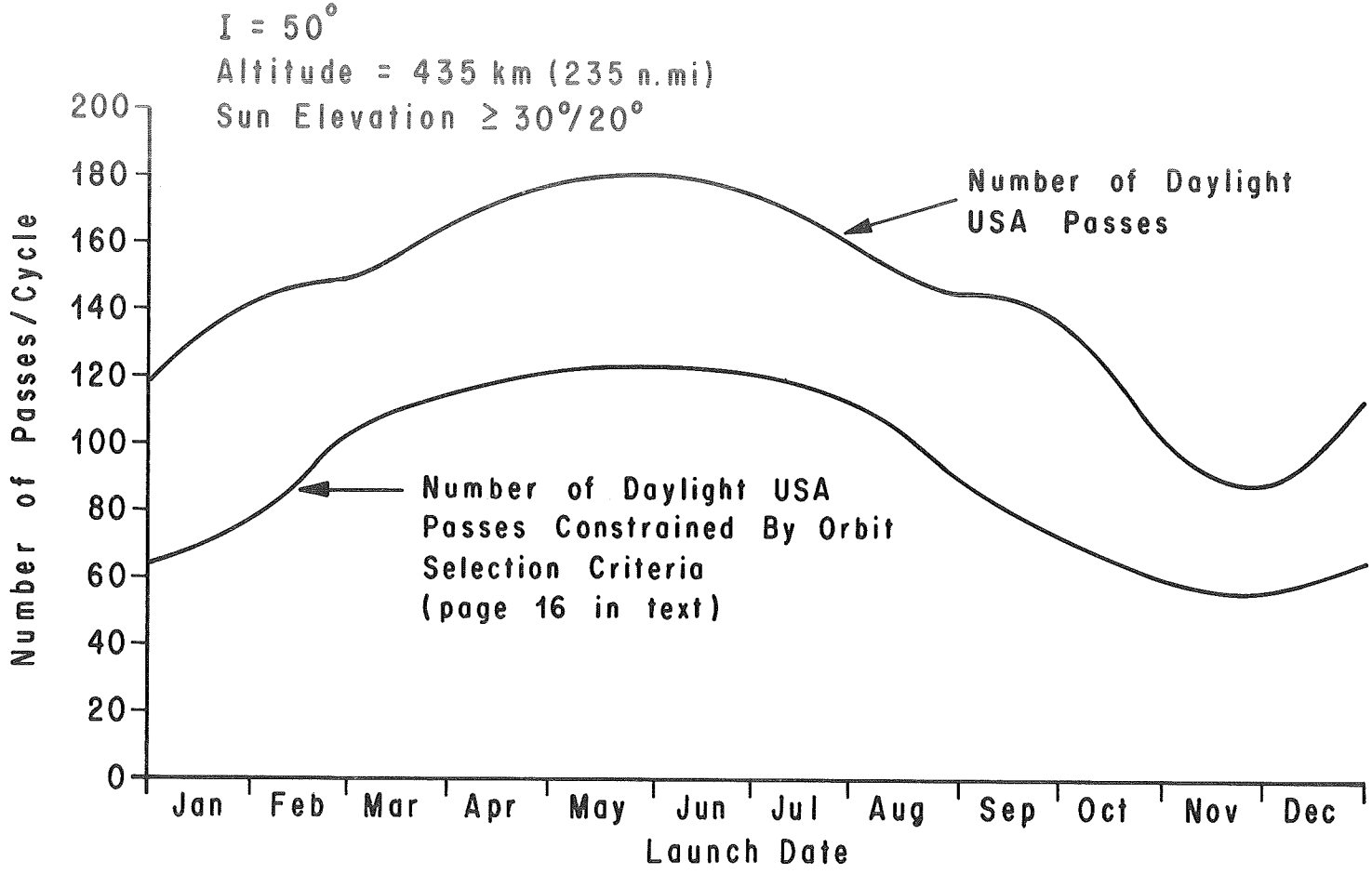

FIG. 19. INFLUENCE OF ORBIT SELECTION CRITERIA ON NUMBER OF DAYLIGHT PASSES OVER THE USA (PER REGRESSION CYCLE)

I = 50°
Altitude = 435 km (235 n.mi.)
Launch Time: 3:00 A.M.
Sun Elevation: ≥ 30°/20°

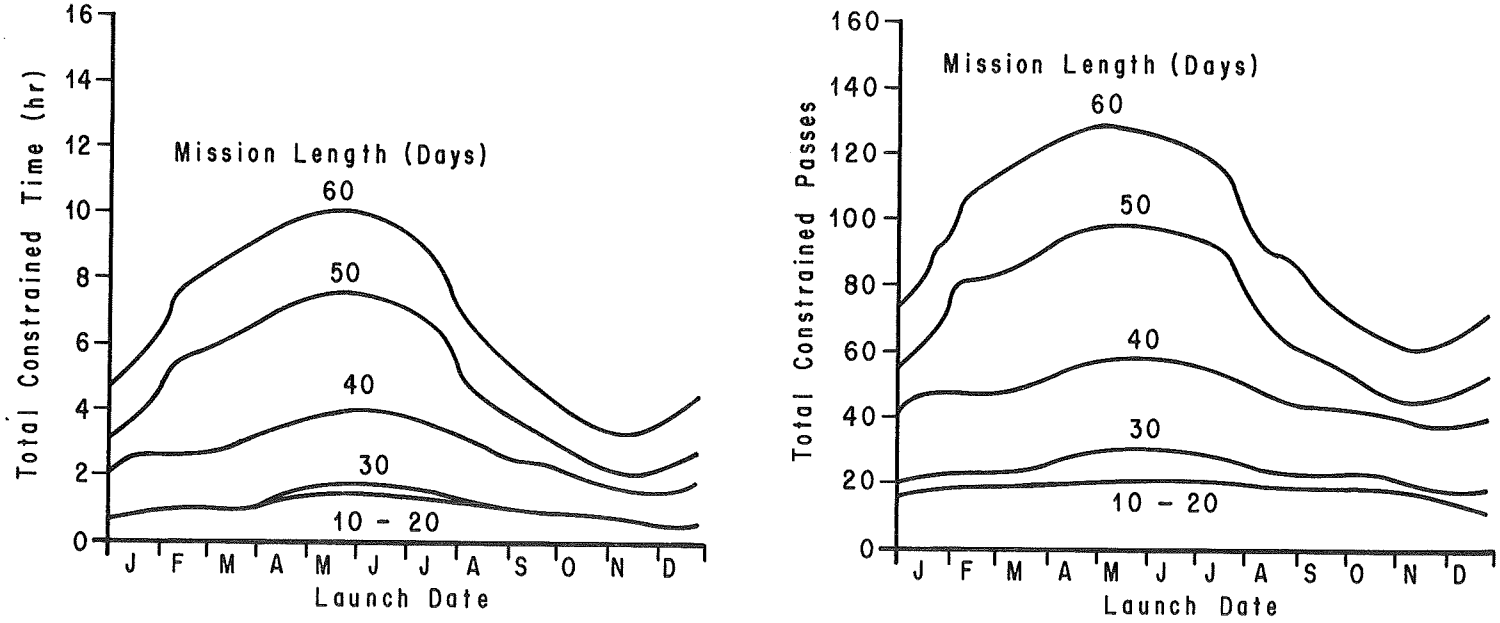

FIG. 20a. TOTAL CONSTRAINED USA COVERAGE TIME AND PASSES (PER MISSION LENGTH) AS A FUNCTION OF LAUNCH DATE (3:00 A.M. LAUNCH)

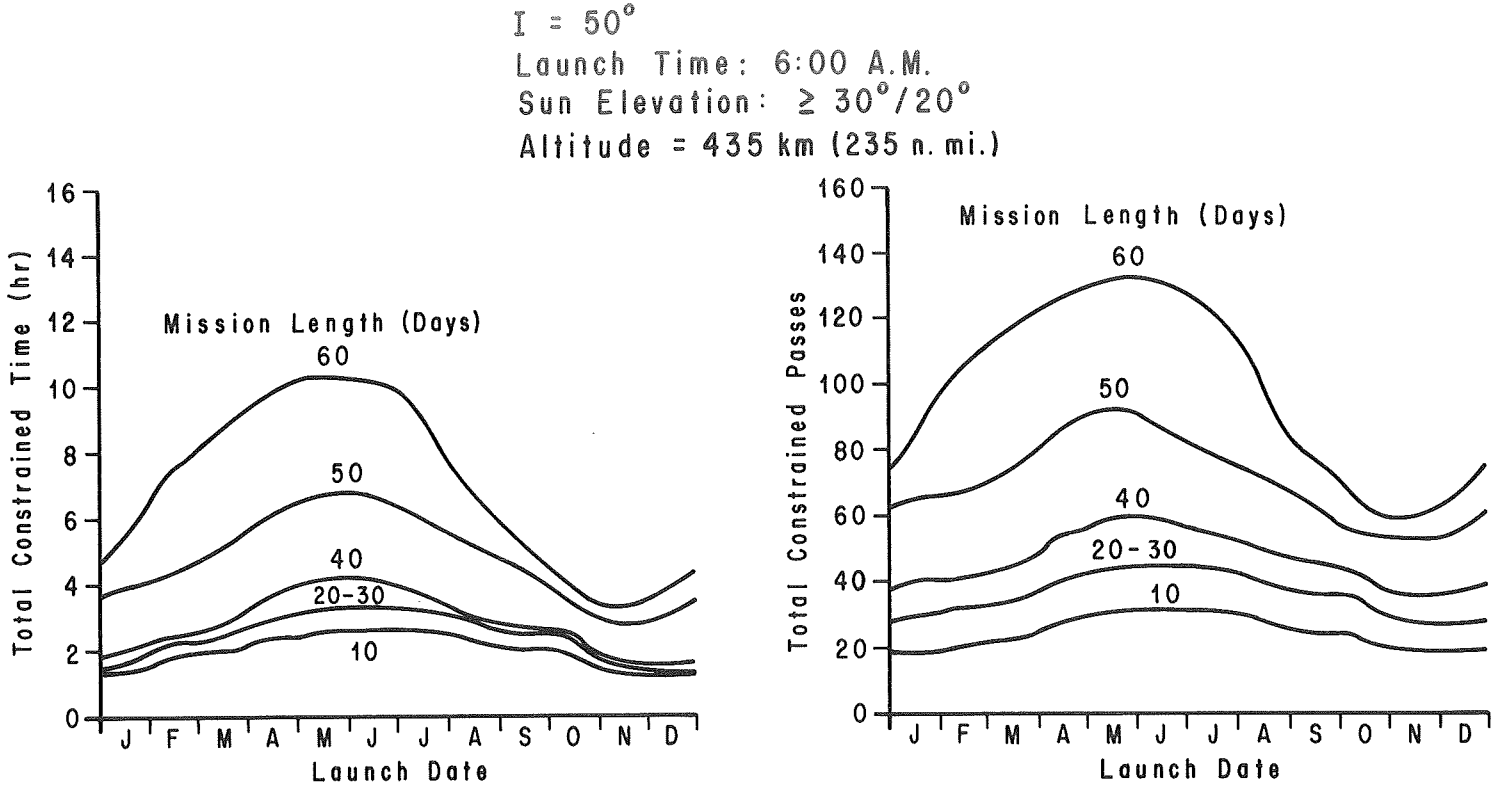

FIG. 20b. TOTAL CONSTRAINED USA COVERAGE TIME AND PASSES (PER MISSION LENGTH) AS A FUNCTION OF LAUNCH DATE (6:00 A.M. LAUNCH)

I = 50°
Altitude: 435 km (235 n.mi.)
Launch Time: 9:00 A.M.
Sun Elevation: ≥ 30°/20°

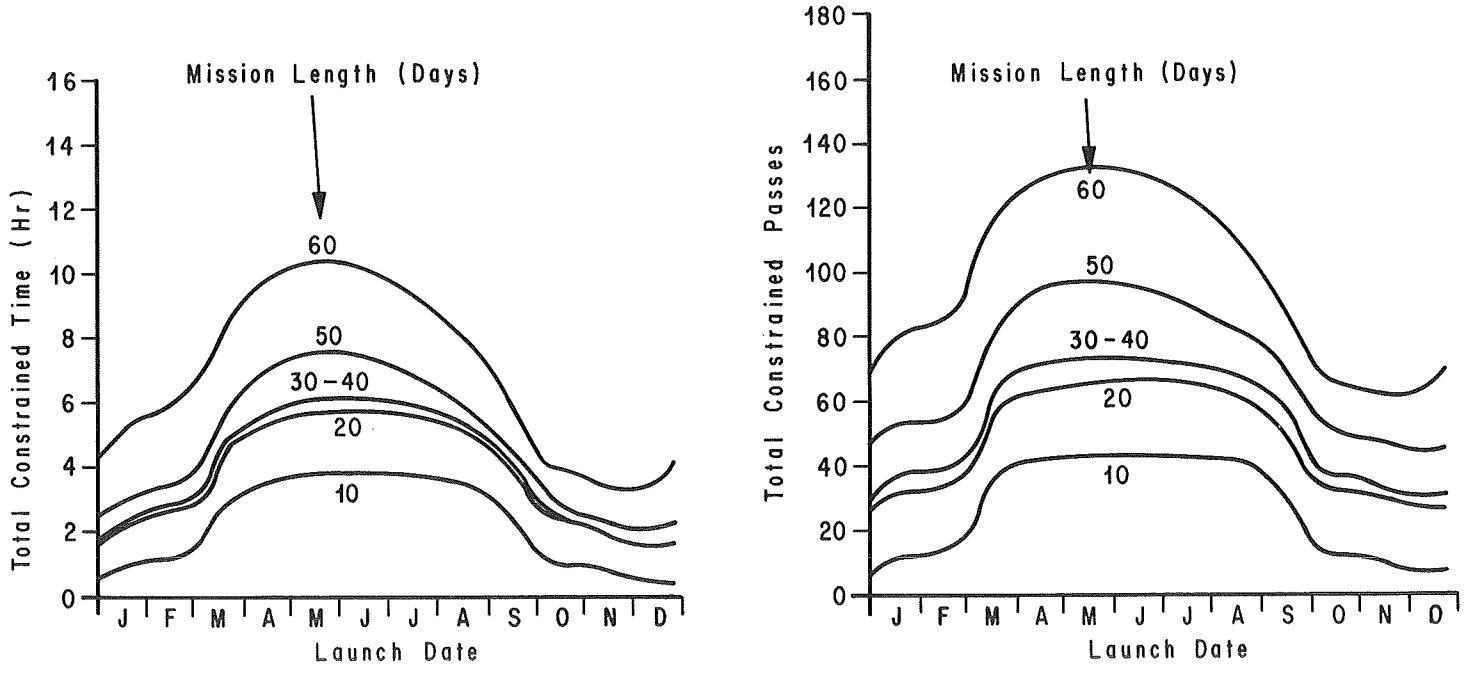

FIG. 20c. TOTAL CONSTRAINED USA COVERAGE TIME AND PASSES (PER MISSION LENGTH) AS A FUNCTION OF LAUNCH DATE (9 A.M. LAUNCH)

I = 50°
Altitude = 435 km (235 n.mi.)
Launch Time: Noon
Sun Elevation: ≥ 30°/20°

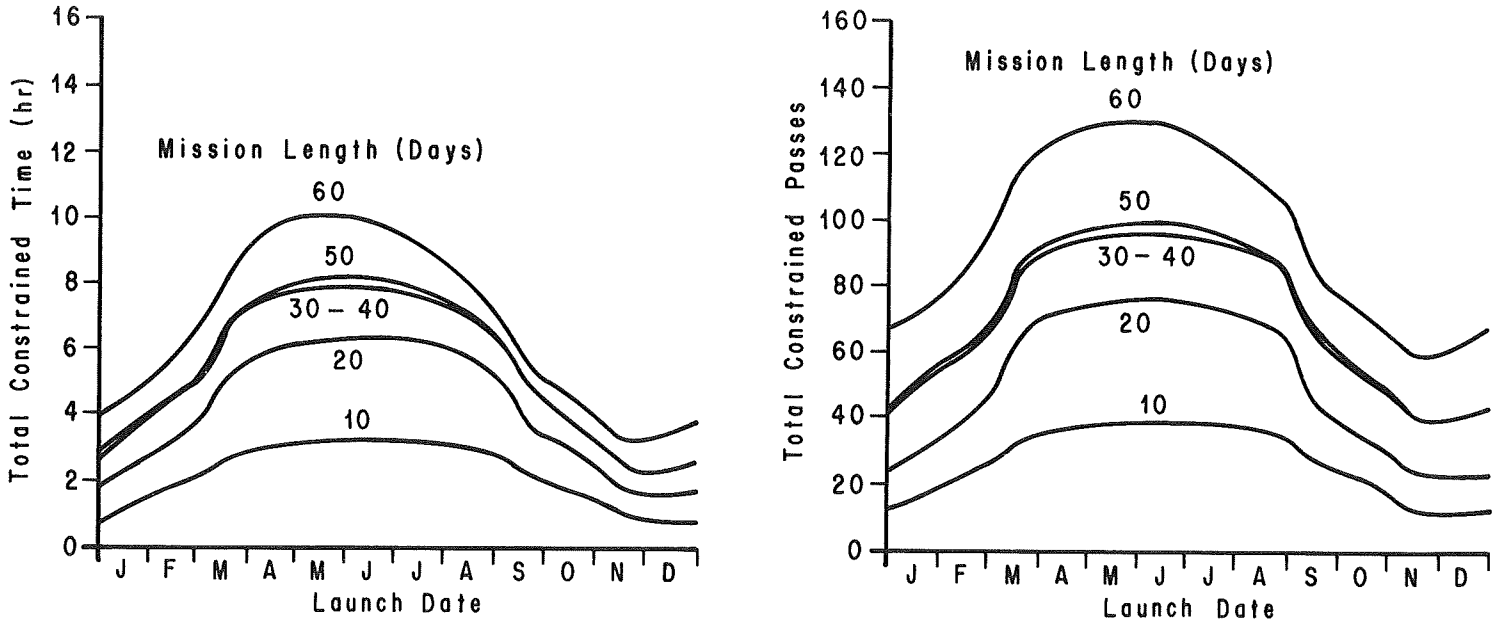

FIG. 20d. TOTAL CONSTRAINED USA COVERAGE TIME AND PASSES (PER MISSION LENGTH) AS A FUNCTION OF LAUNCH DATE (NOON LAUNCH)

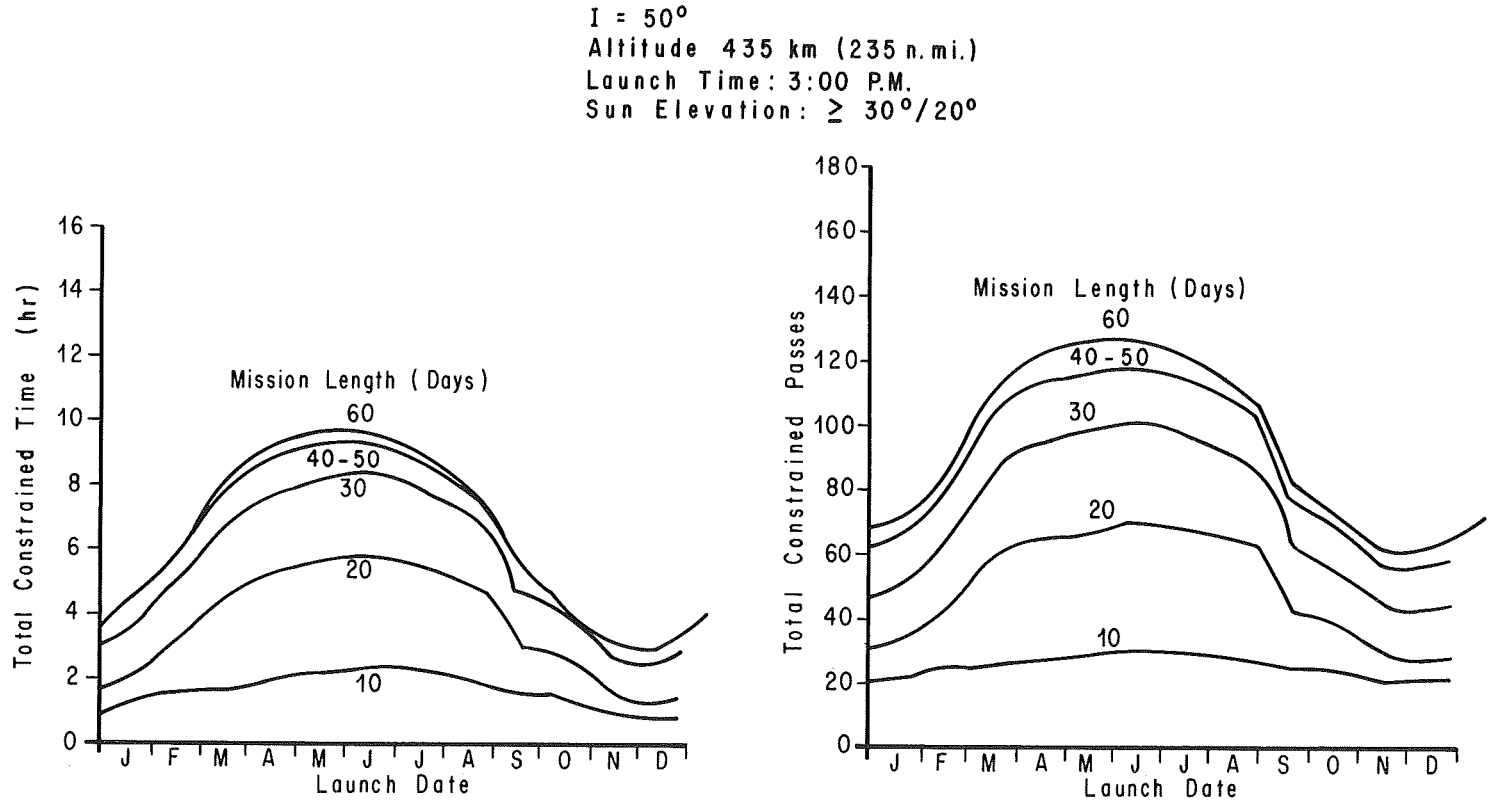

FIG. 20e. TOTAL CONSTRAINED USA COVERAGE TIME AND PASSES (PER REGRESSION CYCLE) AS A FUNCTION OF LAUNCH DATE (3:00 P.M. LAUNCH)

I = 50°
Altitude = 435 km (235 n.mi)
Launch Time: 6:00 P.M.
Sun Elevation: ≥ 30°/20°

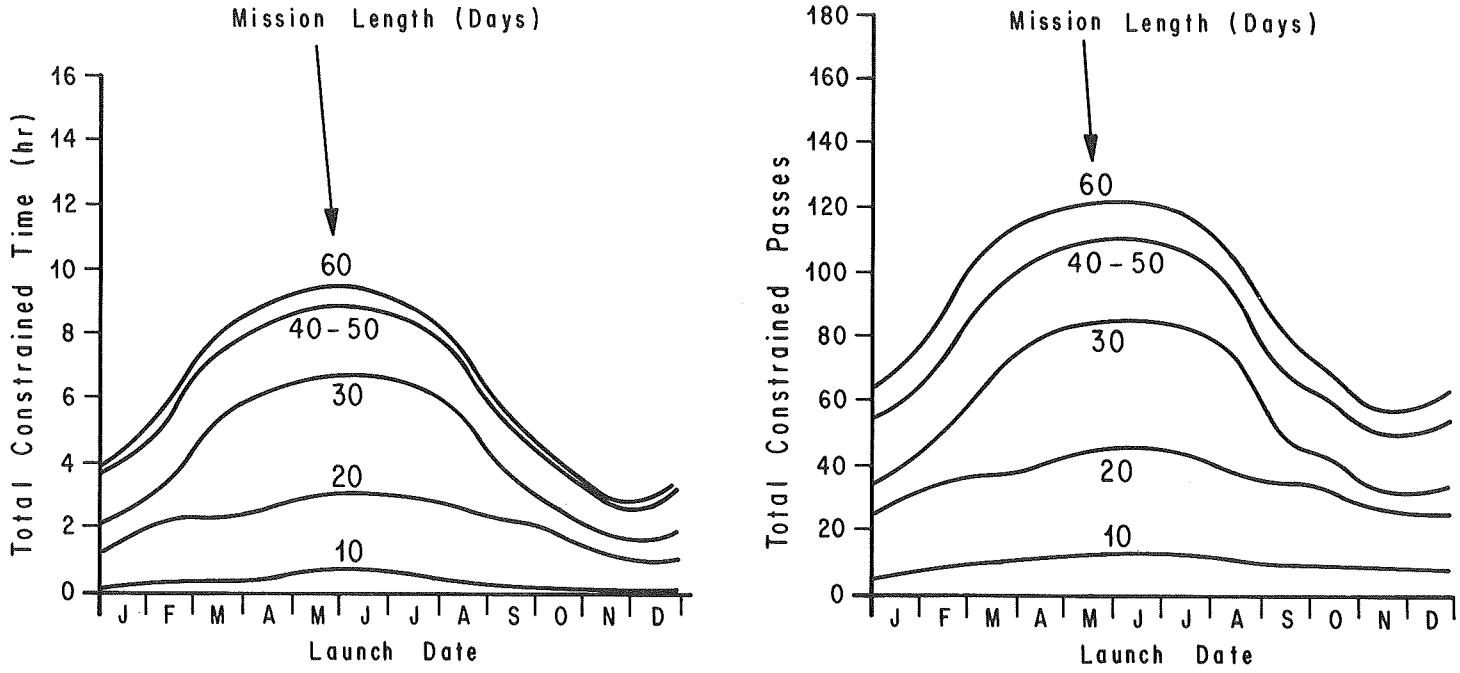

FIG. 20f. TOTAL CONSTRAINED USA COVERAGE TIME AND PASSES (PER REGRESSION CYCLE) AS A FUNCTION OF LAUNCH DATE (6 P.M. LAUNCH)

I = 50°
Altitude = 435 km (235 n.mi.)
Launch Time: 9:00 P.M.
Sun Elevation: ≥ 30°/20°

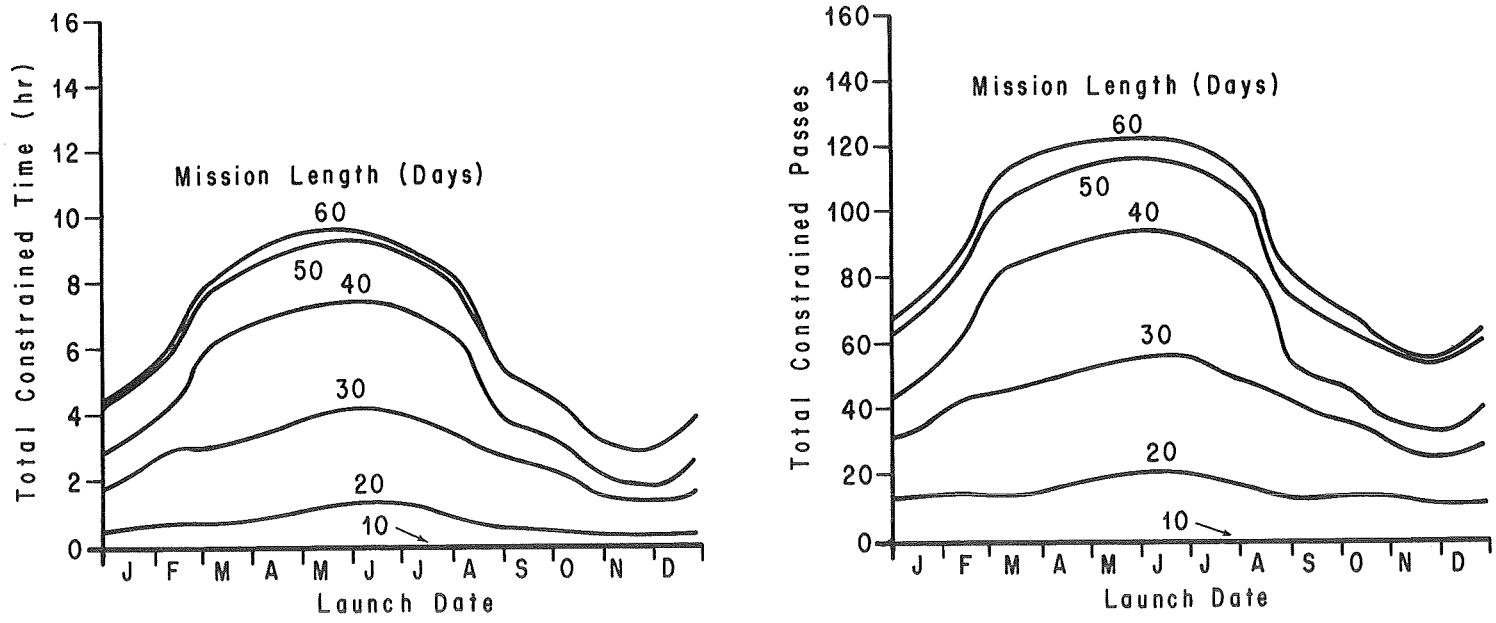

FIG. 20g. TOTAL CONSTRAINED USA COVERAGE TIME AND PASSES (PER MISSION LENGTH) AS A FUNCTION OF LAUNCH DATE (9:00 P.M. LAUNCH)

I = 50°
Altitude = 435 km (235 n.mi.)
Launch Time: Midnight
Sun Elevation: ≥ 30°/20°

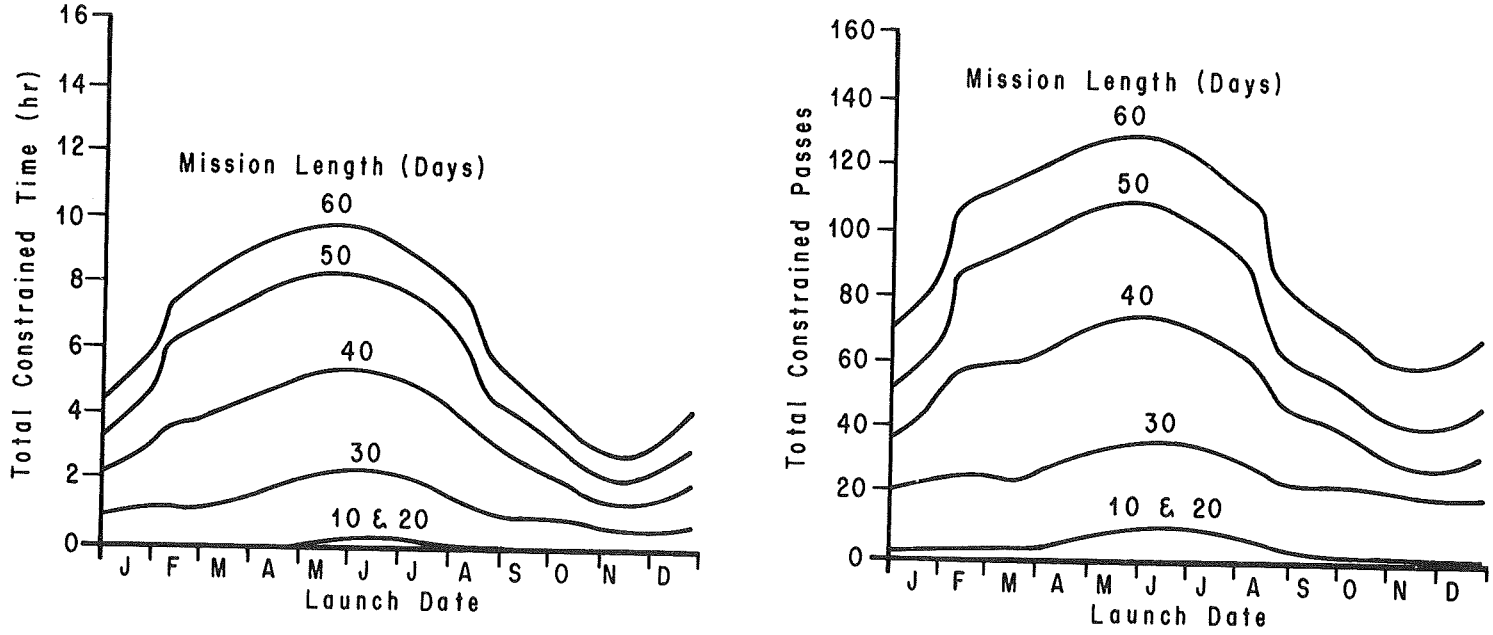

FIG. 20h. TOTAL CONSTRAINED USA COVERAGE TIME AND PASSES (PER MISSION LENGTH) AS A FUNCTION OF LAUNCH DATE (MIDNIGHT LAUNCH)

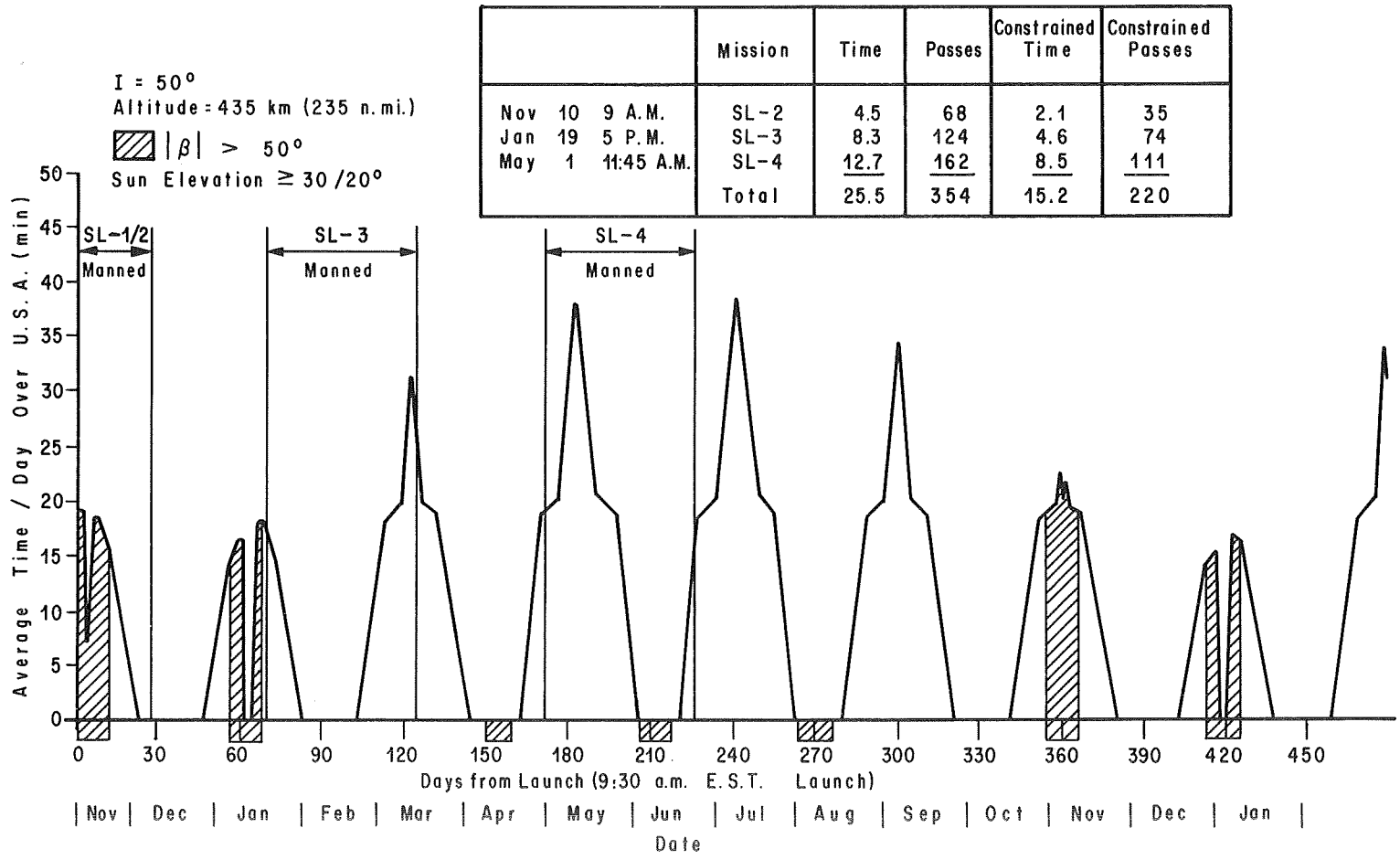

	Mission	Time	Passes	Constrained Time	Constrained Passes
Nov 10 9 A.M.	SL-2	4.5	68	2.1	35
Jan 19 5 P.M.	SL-3	8.3	124	4.6	74
May 1 11:45 A.M.	SL-4	12.7	162	8.5	111
	Total	25.5	354	15.2	220

FIG. 21. SKYLAB A MISSION – DAILY VARIATIONS IN U.S.A. COVERAGE TIME / DAY

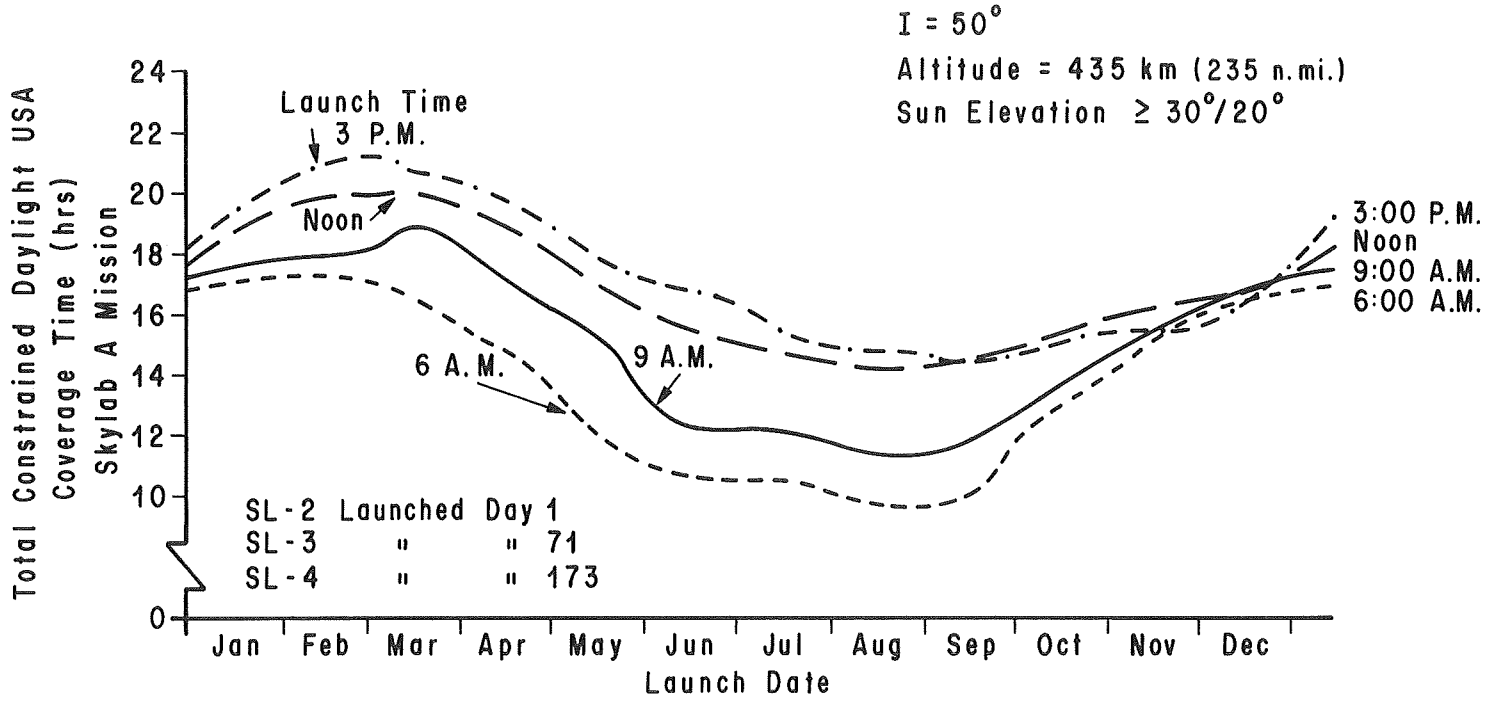

FIG. 22. CONSTRAINED COVERAGE TIME FOR SKYLAB A MISSION AS A FUNCTION OF LAUNCH DATE

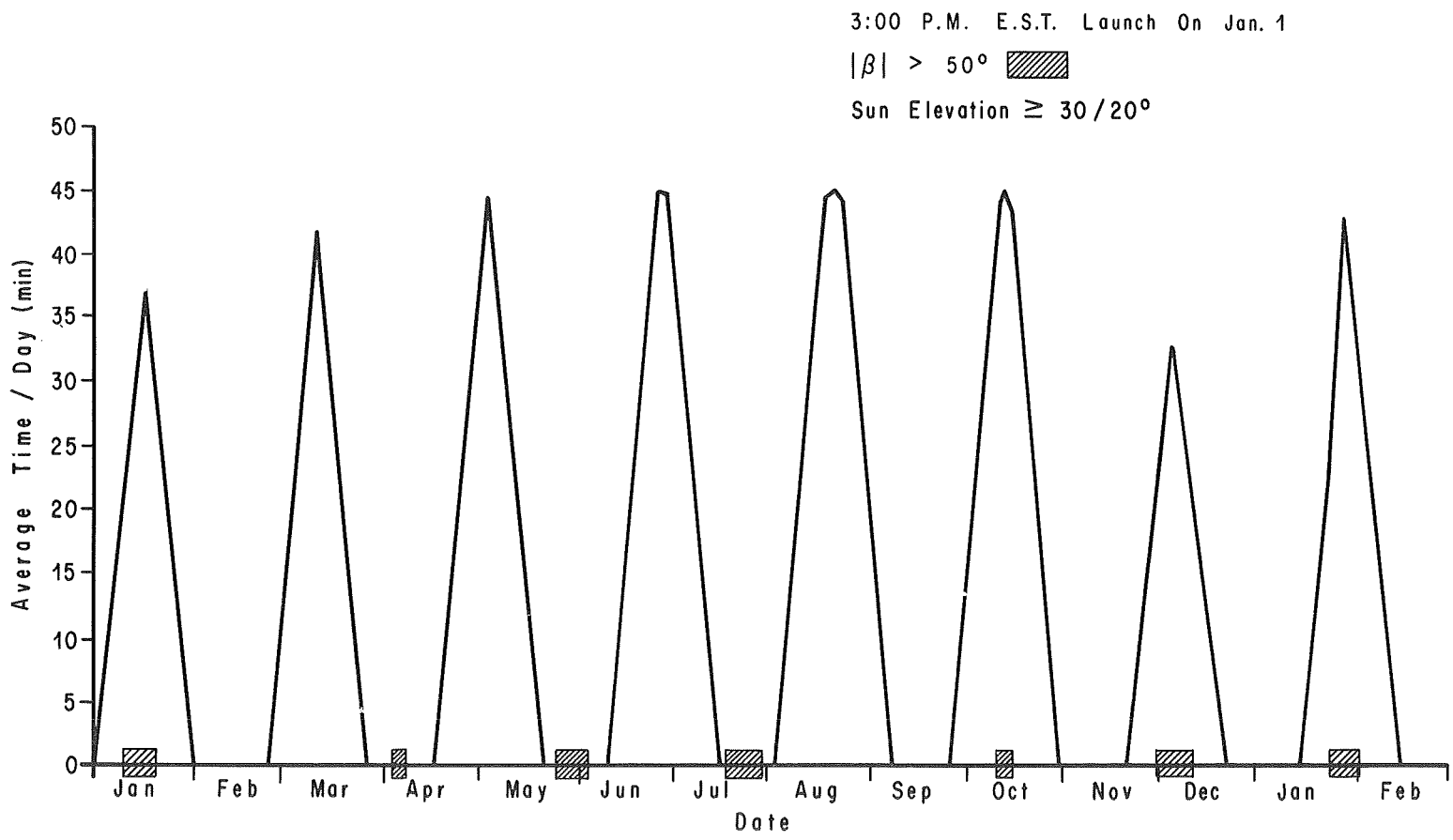

FIG. 23. DAILY VARIATIONS IN U.S.A. COVERAGE TIME FOR A 44° INCLINED CIRCULAR ORBIT AT 435 KM (235 N.MI.) ALTITUDE

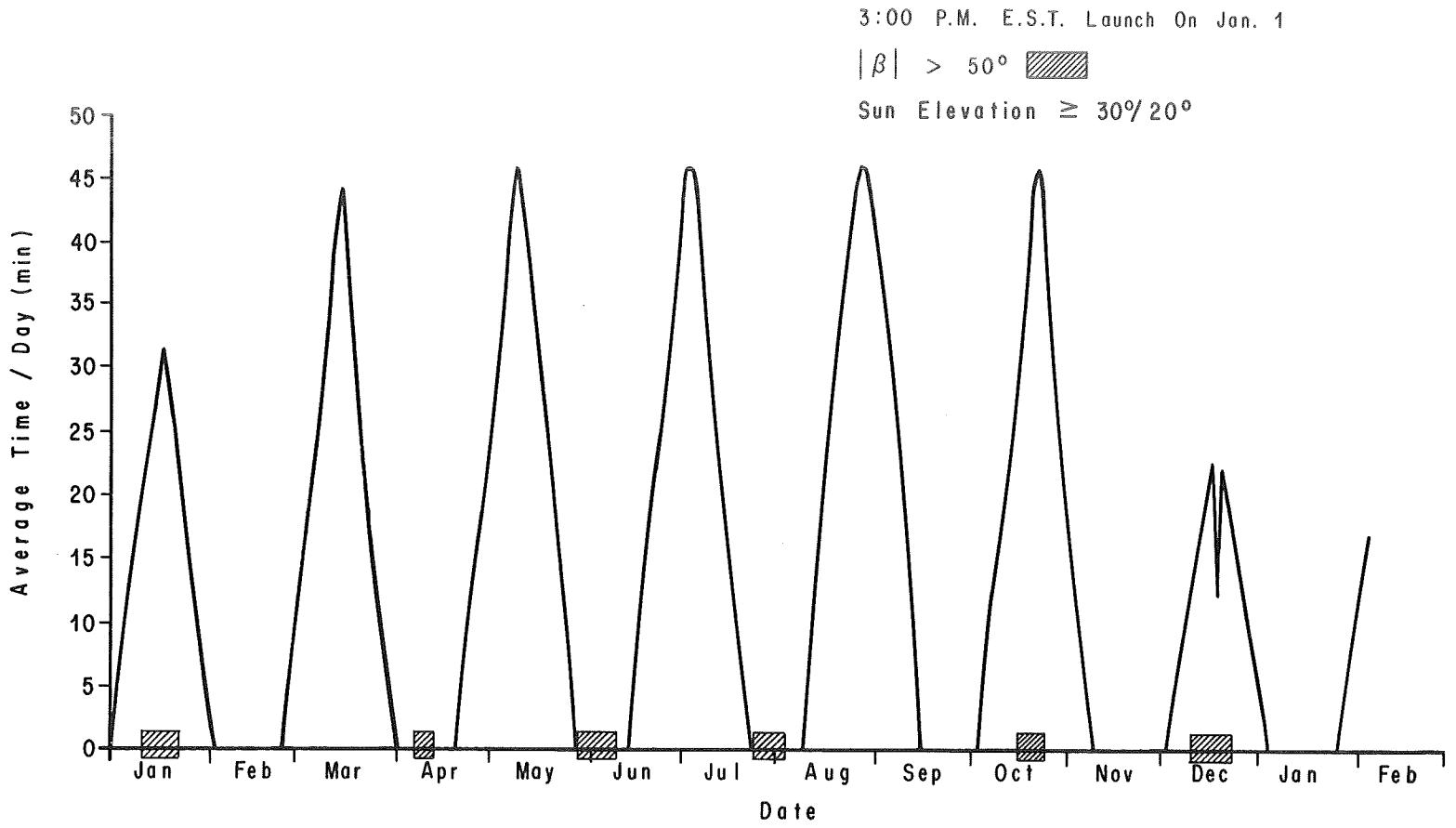

FIG. 24. DAILY VARIATIONS IN U.S.A. COVERAGE TIME FOR A 46° INCLINED CIRCULAR ORBIT AT 435 KM (235 N.MI.) ALTITUDE

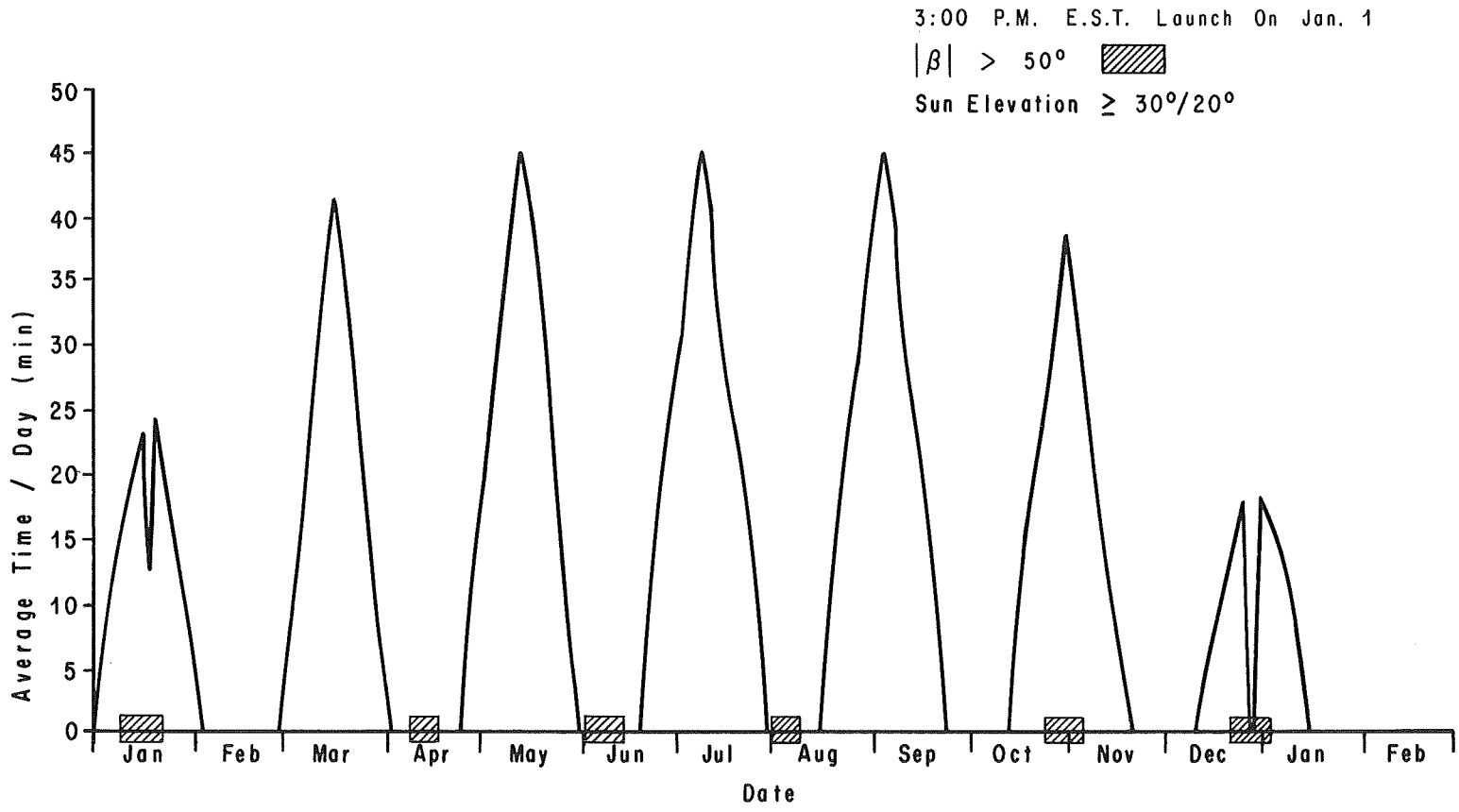

FIG. 25. DAILY VARIATIONS IN U.S.A. COVERAGE TIME FOR A 48° INCLINED CIRCULAR ORBIT AT 435 KM (235 N.MI.) ALTITUDE

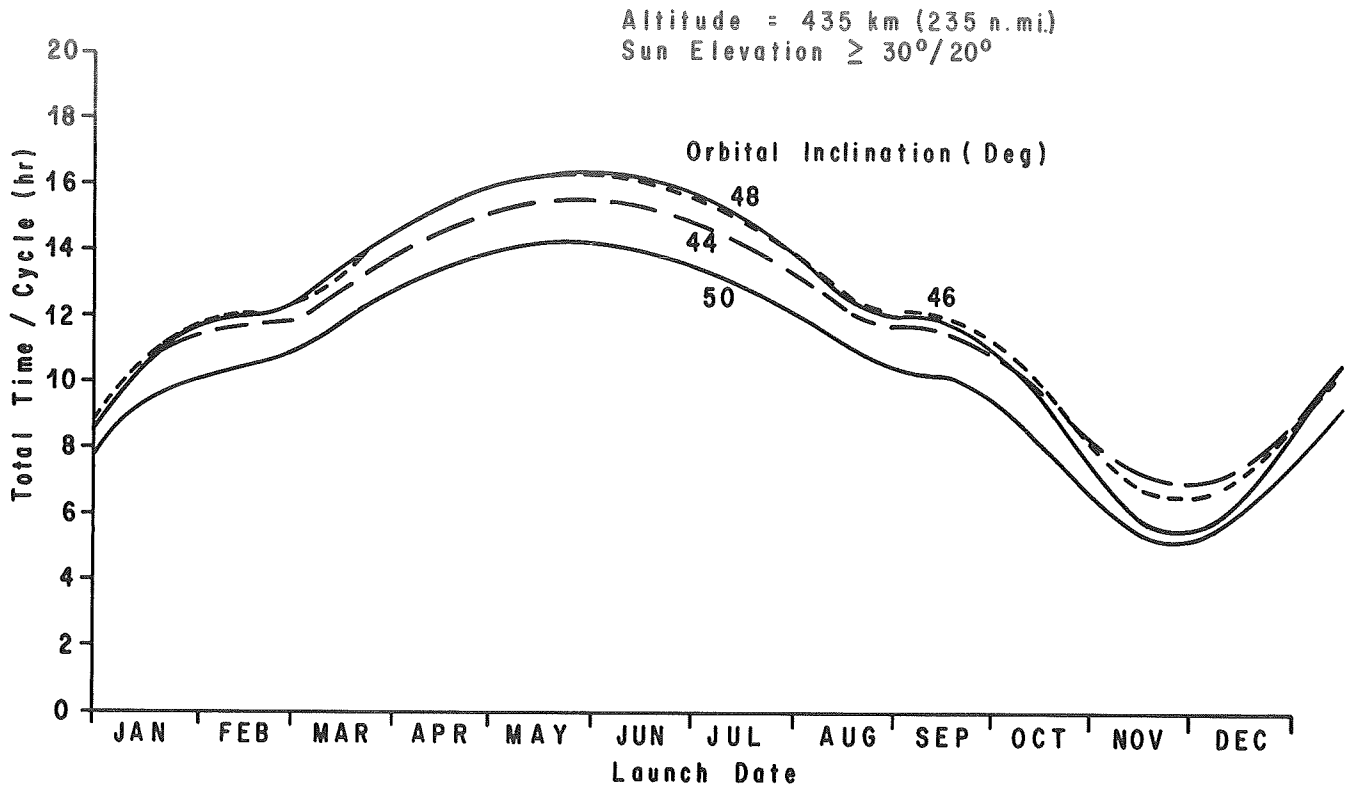

FIG. 26. TOTAL USA DAYLIGHT COVERAGE TIME (PER REGRESSION CYCLE) AS A FUNCTION OF INCLINATION

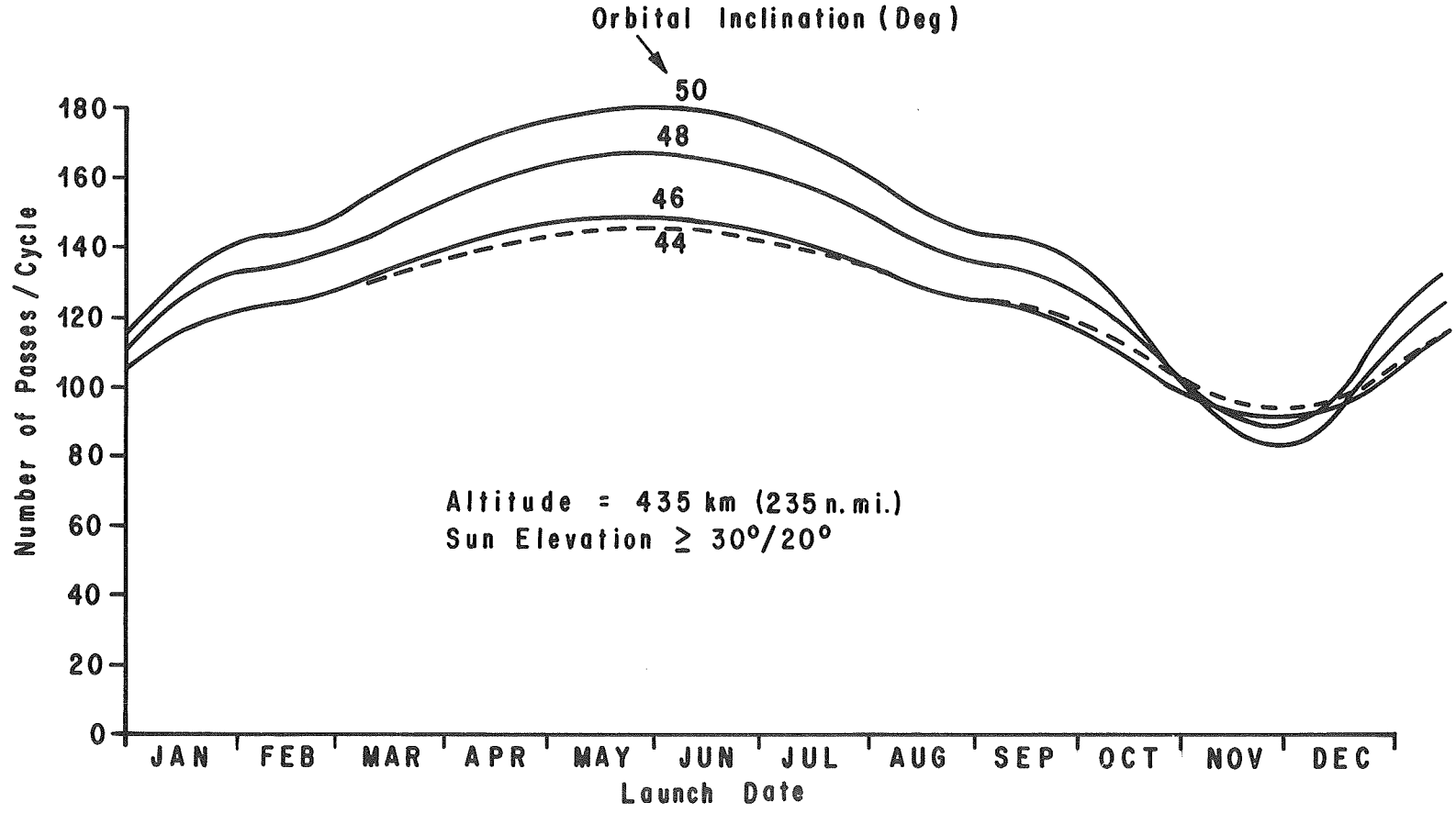

FIG. 27. TOTAL NUMBER OF USA PASSES (PER REGRESSION CYCLE) AS A FUNCTION OF INCLINATION

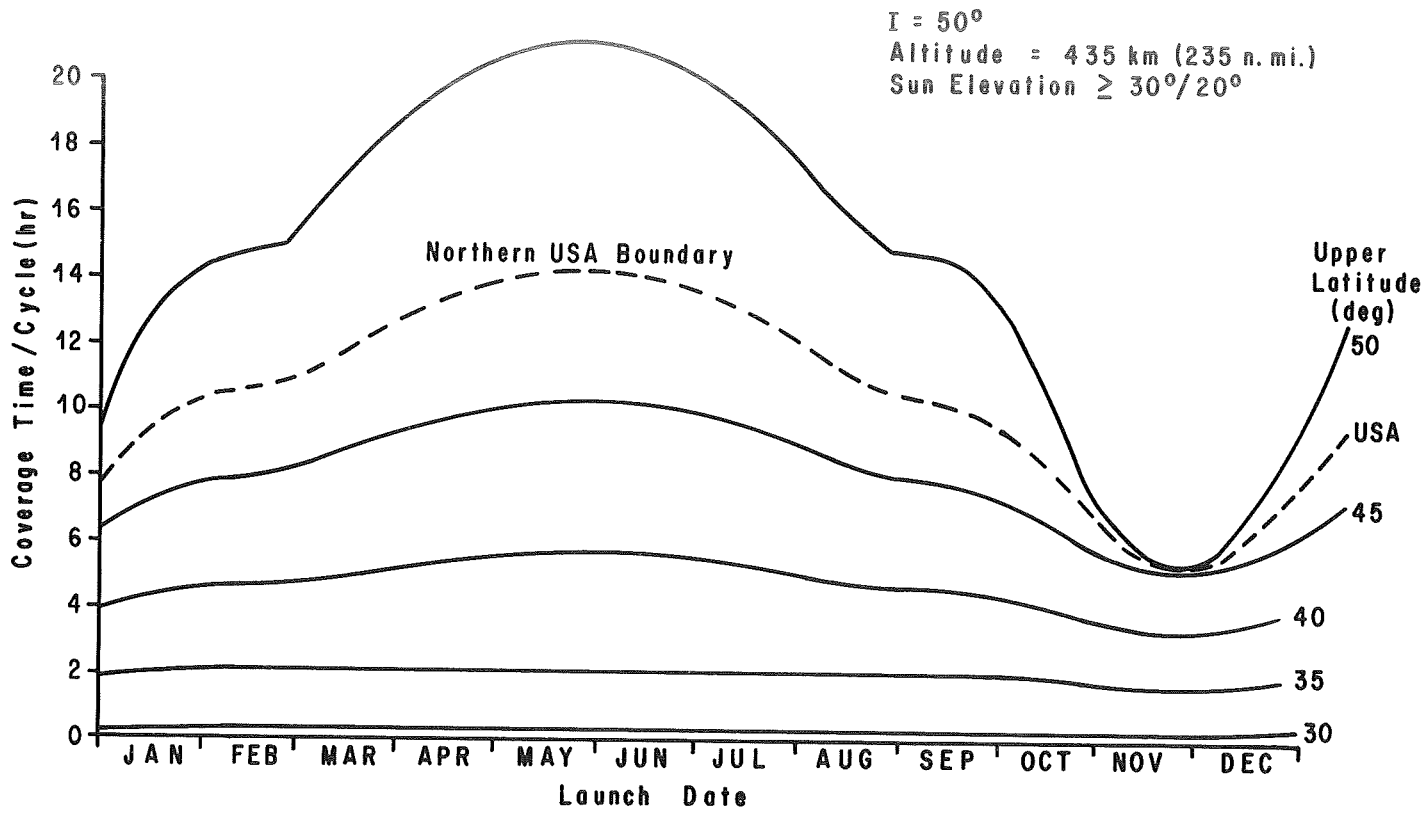

FIG. 28. COVERAGE TIME (PER REGRESSION CYCLE) FOR VARIOUS LATITUDE UPPER LIMITS

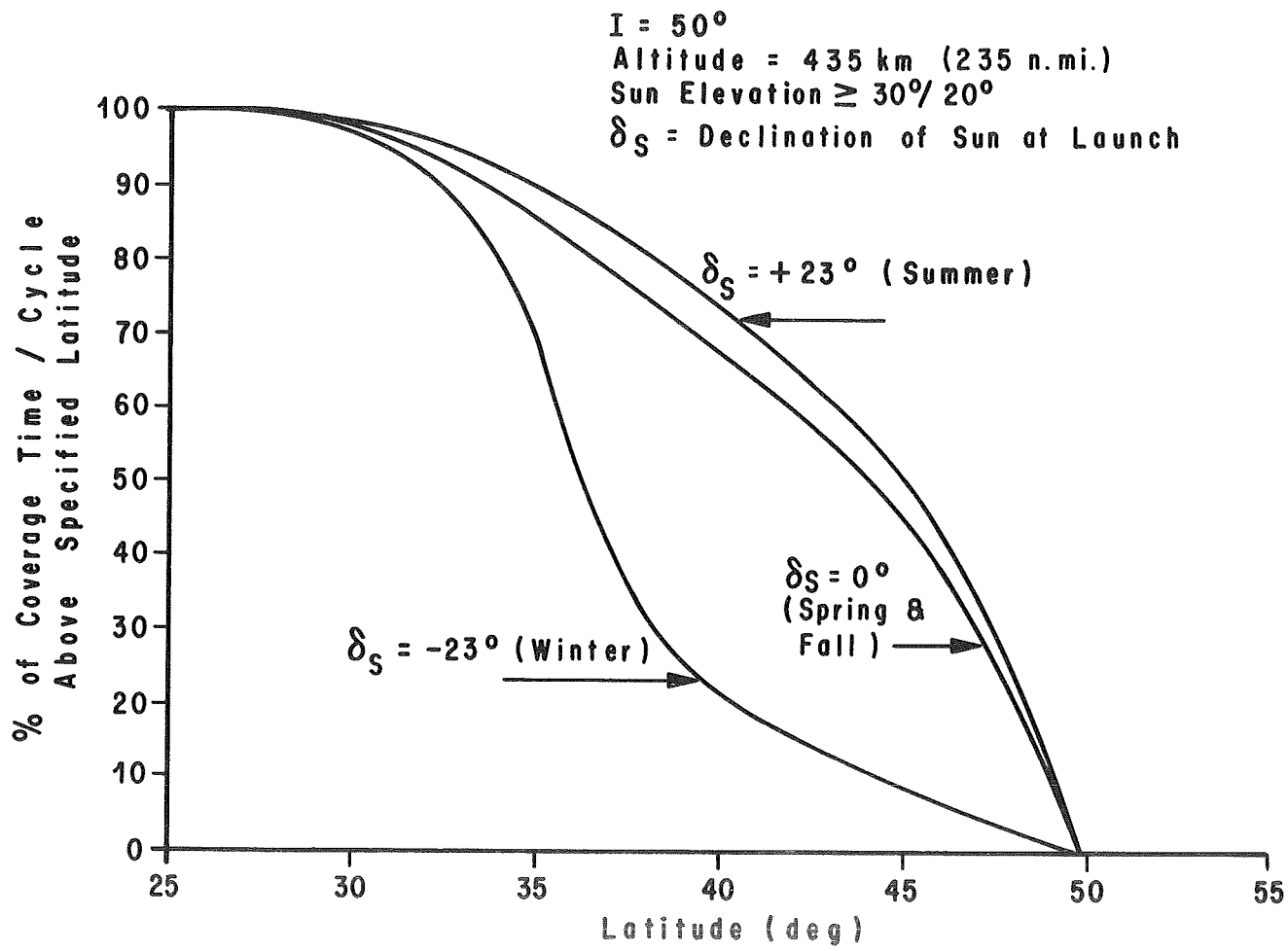

FIG. 29. SEASONAL INFLUENCE ON % OF COVERAGE CYCLE ABOVE SPECIFIED LATITUDES

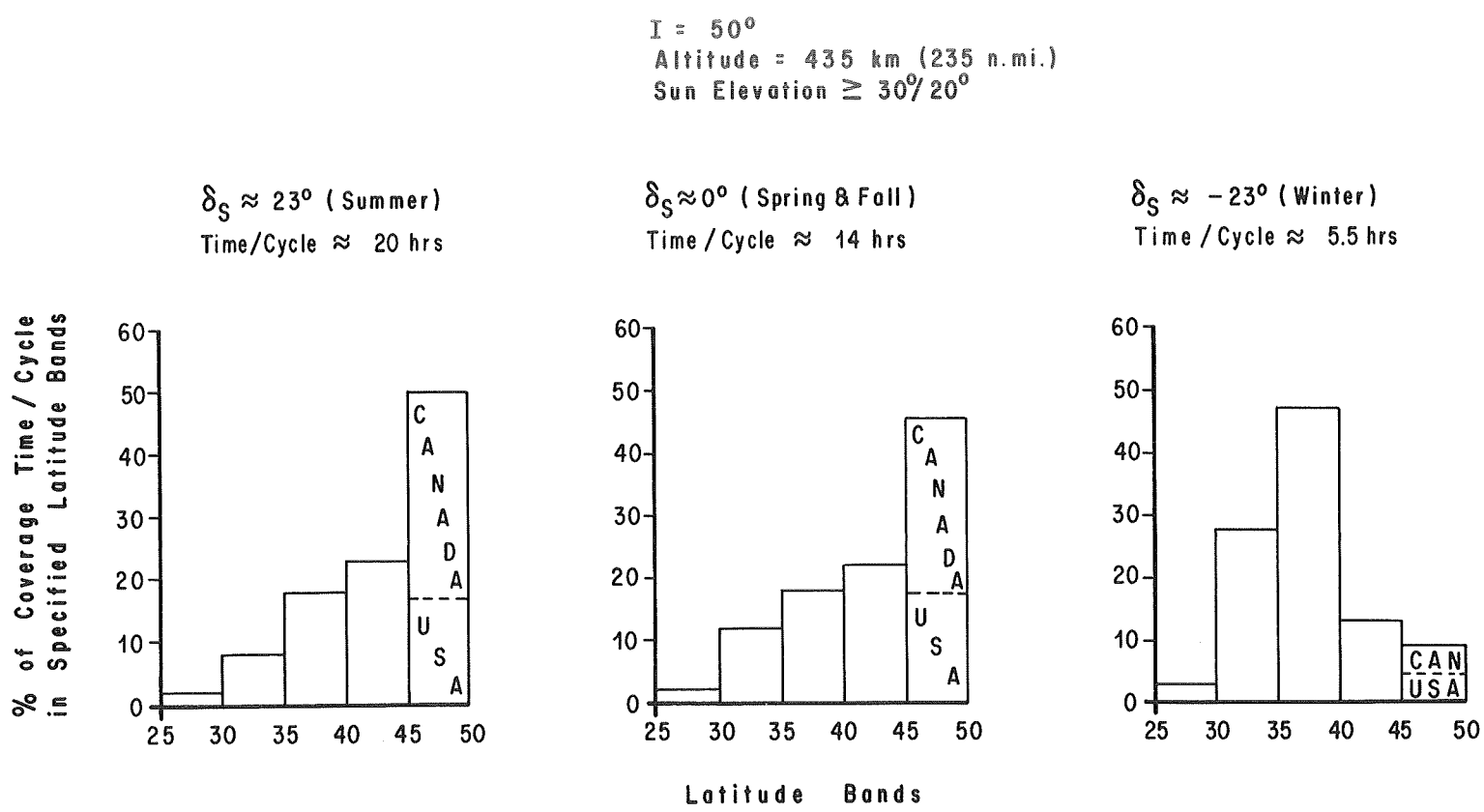

FIG. 30. PERCENTAGE OF COVERAGE CYCLES WITHIN SPECIFIED LATITUDE BANDS

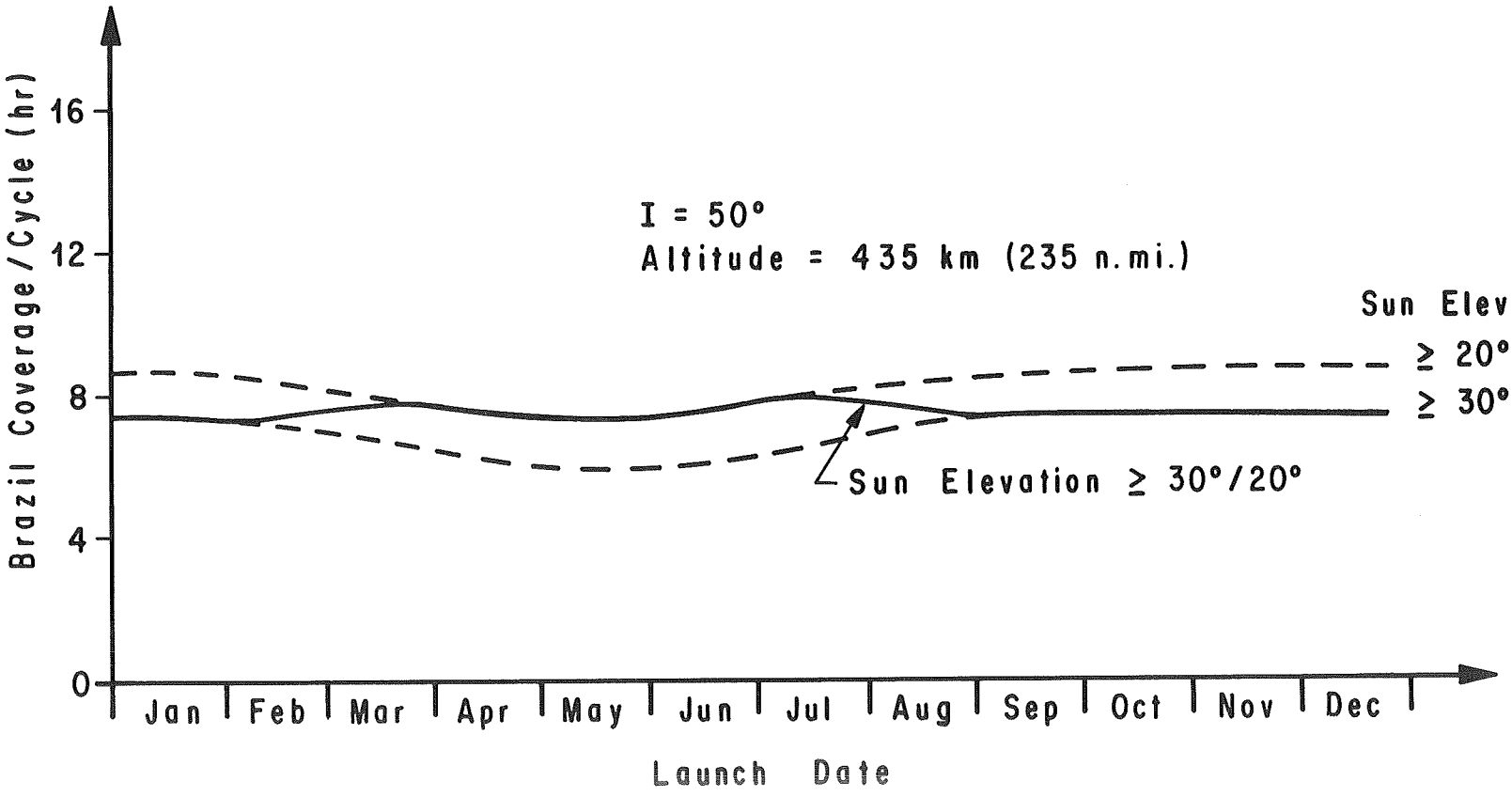

FIG. 31. BRAZIL COVERAGE PER REGRESSION CYCLE

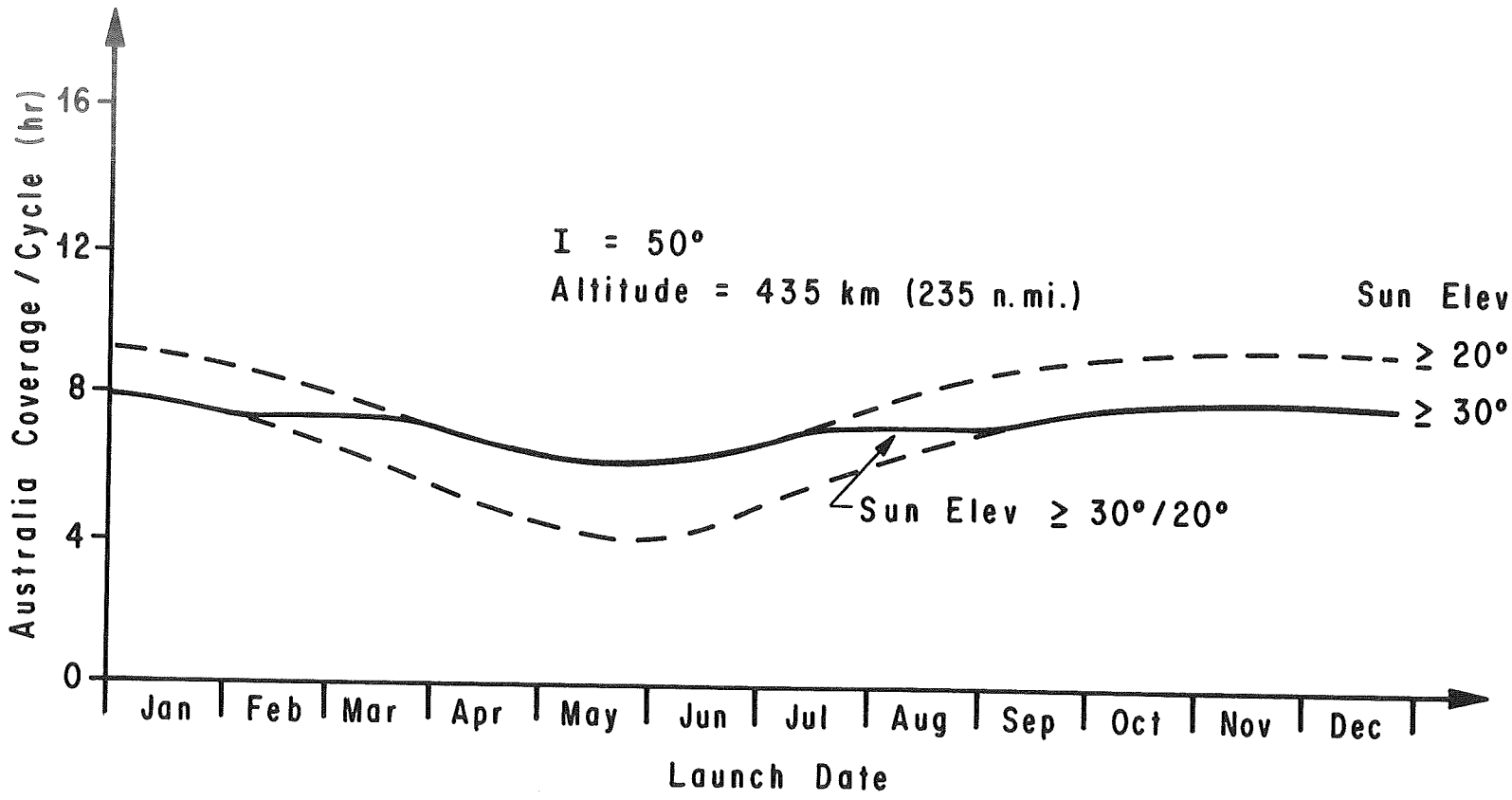

FIG. 32. AUSTRALIA COVERAGE PER REGRESSION CYCLE

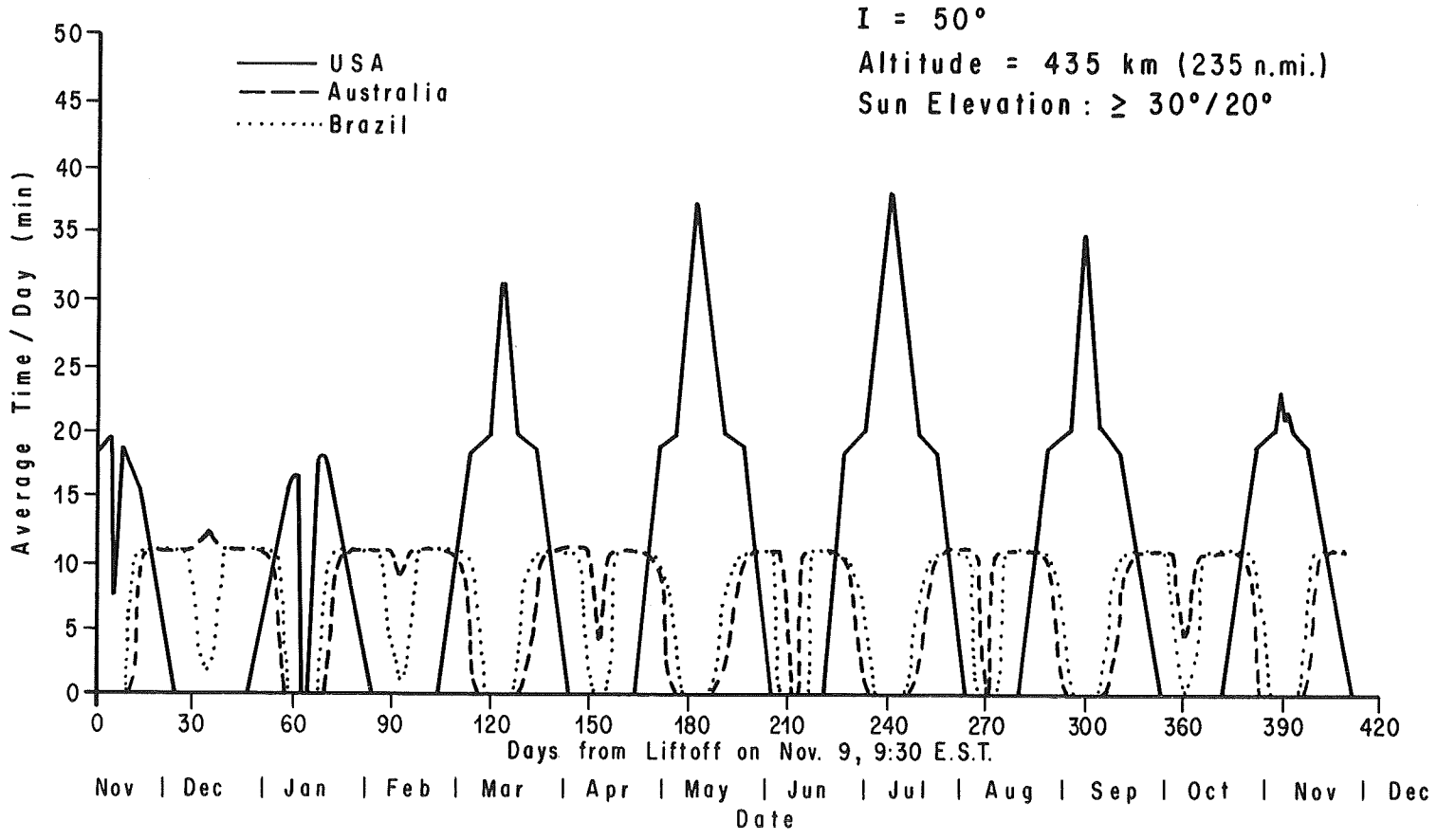

FIG. 33. DAILY VARIATION IN COVERAGE TIME FOR USA, AUSTRALIA, AND BRAZIL

APPENDIX A

Transformation to (Ω_e, θ) Space

Figure A1 shows the spherical triangle necessary for the calculation of θ_1 and Ω_{e1}. Arc AB represents a portion of the orbit. Arc BC represents a portion of the equator. The satellite is at point A. Point D is a point fixed to the rotating earth which was directly beneath the satellite as it crossed the equator. Using Napier's rules, it is found that

$$\theta_1 = \sin^{-1}\left[\frac{\sin \text{ lat}}{\sin i}\right]$$

and $X = \tan^{-1}[\cos i \tan \theta_1]$.

The amount of time it takes the satellite to travel from the equator to point A is θ_1/ω_o. Since the angular rate of the earth with respect to the descending node is $\omega_e + \dot{\Omega}$, the arc BD is $(\omega_e + \dot{\Omega})\theta_1/\omega_o$. Thus, the angle from the prime meridian to point D is

$$\Omega_{e1} = \text{longitude}^* + X - \frac{\omega_e + \dot{\Omega}}{\omega_o}\theta_1.$$

Substituting for X,

$$\Omega_{e1} = \text{longitude} + \tan^{-1}[\cos i \tan \theta_1] - \frac{\omega_e + \dot{\Omega}}{\omega_o}\theta_1.$$

By inspection of Figure 1, it can be seen that θ_2 is merely the supplement of θ_1:

$$\theta_2 = \pi - \theta_1.$$

Ω_{e2} can be obtained by substituting θ_2 for θ_1 in the equation for Ω_{e1}:

$$\Omega_{e2} = \text{longitude} + \tan^{-1}[\cos i \tan \theta_2] - \frac{\omega_e + \dot{\Omega}}{\omega_o}\theta_2.$$

*Where longitude is longitude of subpoint A.

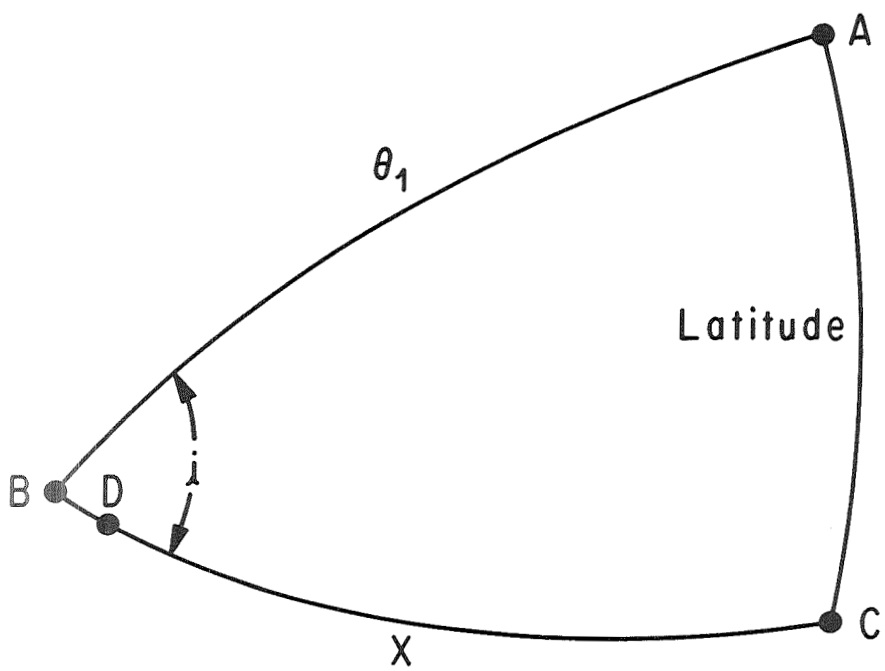

FIG. A1. CALCULATION OF θ_1 AND Ω_{e1}

APPENDIX B

Calculation of θ_{LL} and θ_{UL}

Construct an orthogonal coordinate system centered in the earth with the X axis out the ascending node of the orbit, the Z axis out the north pole of the earth and the Y axis forming a right-handed system Figure B1. A unit vector normal to the orbit in this coordinate system is

$$\hat{N} = \begin{pmatrix} 0 \\ -\sin i \\ \cos i \end{pmatrix}.$$

In Figure B1 the direction of a unit vector, $\hat{S}$ to the sun is described by two angles, Ω_S and δ. It can be shown that

$$\hat{S} = \begin{pmatrix} \cos\delta \cos\Omega_S \\ \cos\delta \sin\Omega_S \\ \sin\delta \end{pmatrix}.$$

The projection of $\hat{S}$ on the orbit plane will define the location of orbital noon. The angle between $\hat{S}$ and its projection on the orbit is the β angle. β would be negative as shown in Figure B1. Since β is the complement of the angle between $\hat{S}$ and $\hat{N}$

$$\beta = \sin^{-1}(\hat{N} \cdot \hat{S}).$$

In order to find the location of orbital noon define a vector $\hat{V}$ which lies in the orbit plane perpendicular to both $\hat{N}$ and $\hat{S}$,

$$\hat{V} = \frac{\hat{S} \times \hat{N}}{|\hat{S} \times \hat{N}|}.$$

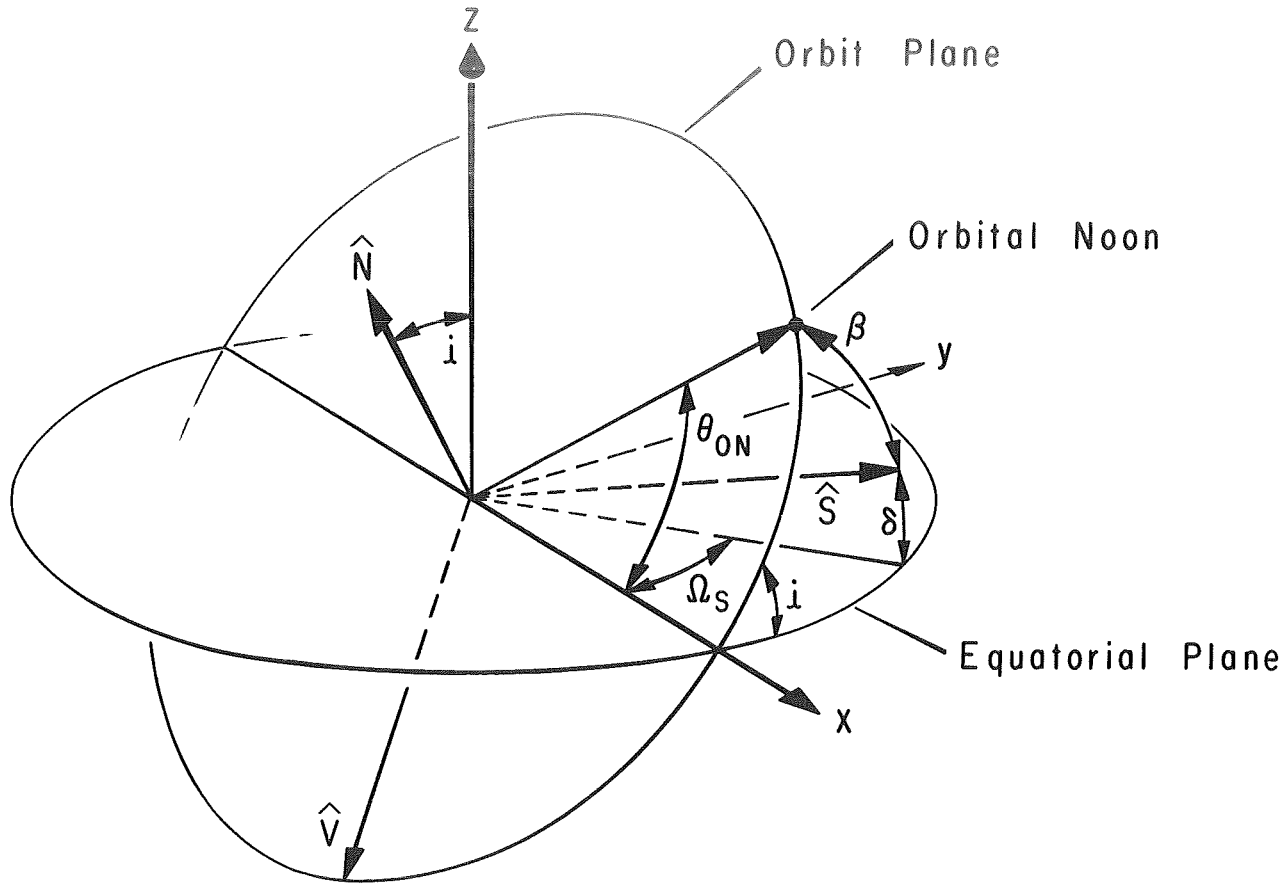

FIG. B1. POSITION OF THE SOLAR VECTOR WITH RESPECT TO THE ORBIT PLANE

The angle between the X axis and orbital noon, θ_{ON} is the complement of the angle between the X axis and $\hat{V}$. Therefore,

$$\theta_{ON} = \sin^{-1}(V_X)$$

where V_X is the X component of $\hat{V}$.

The region, $\Delta\theta_c$, about orbital noon for which the sun incidence angle constraint, φ_c, is satisfied can now be calculated from Figure B2. Since projecting the solar vector onto the orbit plane forms a right spherical triangle, Napier's rules can be used to calculate $\Delta\theta_c$:

$$\Delta\theta_c = \cos^{-1}\left(\frac{\cos\varphi_c}{\cos\beta}\right).$$

Thus, the lower and upper limits on θ can be calculated:

$$\theta_{LL} = \theta_{ON} - \Delta\theta_c$$

$$\theta_{UL} = \theta_{ON} + \Delta\theta_c.$$

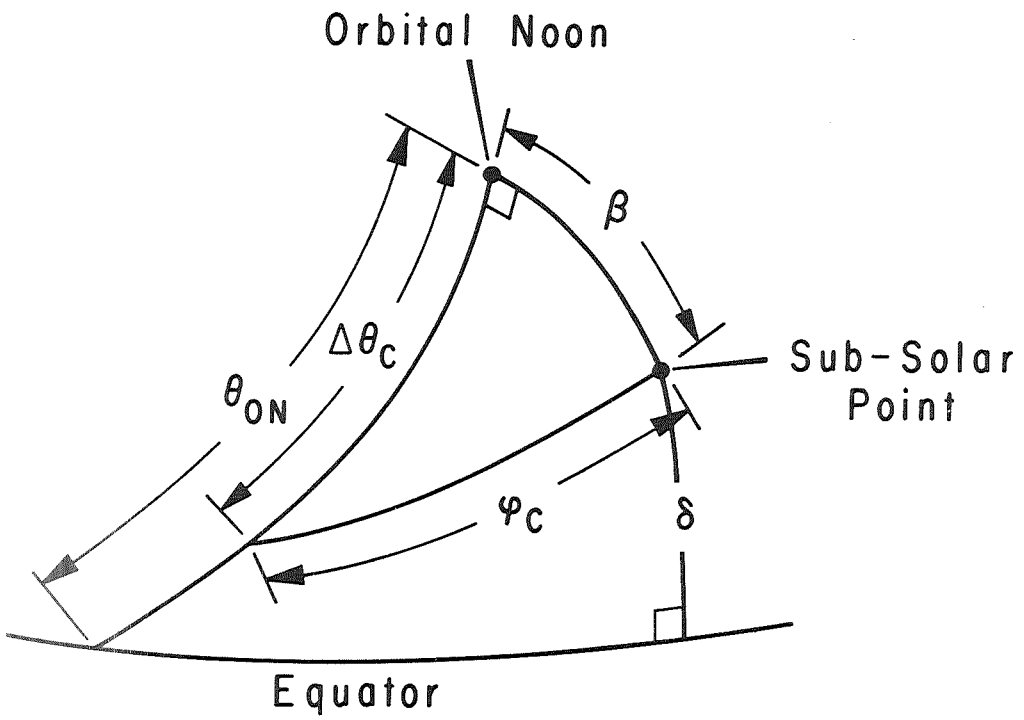

FIG. B2. CALCULATION OF $\Delta\theta_c$

APPENDIX C

Determination of Subsequent Mission Launch Times into a 50° Inclination, 435 km Circular Orbit

Once the initial launch date and time are established, the launch time for any subsequent in-plane launch intended for rendezvous with the orbiting assembly can also be determined. The space-fixed orbital plane for a 50° inclination, 435 km orbit regresses ≈ 6° each day relative to the sun, passing through Cape Kennedy ≈.4 hour or 24 minutes earlier each day. (This assumes that any orbital decay is insignificant which is valid for a nominal decay of the Skylab at 435 km altitude.) Launch time for any subsequent mission (utilizing the same launch direction) is established by subtracting the product of .4 hours times the number of days from the initial launch of the orbiting assembly. Each 60 days this product equates to 24 hours. Hence, the launch time would be the same as the initial launch time but 24 hours earlier, or on day 59. (Since launch opportunities occur each ≈ 23.6 hours, one day out of approximately every 59 contains two launch opportunities.) To launch on day 60 then, another subtraction of .4 hours (1 day) is necessary. Thus, each multiple of 60 days from launch represents .4 hours earlier launch time. This cursory evaluation of subsequent mission launch time determination is a reasonably accurate approximation. A thorough discussion on determining launch time of day is beyond the scope of this document.

REFERENCES

1. Sherr, P. E., et al., "World-Wide Cloud Cover Distributions for Use in Computer Simulations," NASA CR-61226, June 14, 1968, NASA, MSFC.

2. Brown, S. C., "Simulating the Consequence of Cloud Cover on Earth-Viewing Space Mission," American Meteorology Society Bulletin, Vol. 51, No. 2, February 1970, pp. 126-131.

3. Mission Requirements Document, Skylab/Mission SL-1/SL-2, NASA 1-MRD-001D, April 1, 1971.

APPROVAL

AN EVALUATION OF EARTH RESOURCES OBSERVATION OPPORTUNITIES FROM AN ORBITING SATELLITE

by E. H. Bauer and B. S. Perrine

The information in this report has been reviewed for security classification. Review of any information concerning Department of Defense or Atomic Energy Commission programs has been made by the MSFC Security Classification Officer. This report, in its entirety, has been determined to be unclassified.

This document has also been reviewed and approved for technical accuracy.

J. W. Cremin
Chief, Operations Analysis Branch

R. H. Benson
Chief, Orbital Mechanics Branch

J. P. Lindberg
Chief, Mission Planning and Analysis Division

E. D. Geissler
Director, Aero-Astrodynamics Laboratory

DISTRIBUTION

DIR
DEP-T
A&TS-PAT, Mr. Wofford
PM-PR-M, Mr. Goldston
A&TS-MS-H
A&TS-MS-IP
A&TS-MS-IL (8)
A&TS-TU, Mr. Wiggins (6)
AD-S, Dr. Stuhlinger

S&E-DIR
Mr. Weidner
Dr. McDonough (5)

S&E-CSE
Dr. Haeussermann
Mr. Mack
Mr. Hagood
Mr. Lester (5)
Mr. Berry
Mr. Hammers
Mr. Ledford
Mr. Aberg
Mr. Curry
Mr. DeSanctis
Mr. Tinius
Mr. Marmann

S&E-ASTR
Mr. Noel
Mr. Cox
Mr. Brooks
Mr. Stroud
Mr. Scofield
Mr. Atherton
Mr. Duffy
Mr. Aden
Mr. Wood
Mr. Thornton
Mr. Rupp
Mr. Brown
Mr. McMahen
Mr. Thompson
Mr. Erickson

S&E-ASTN
Mr. Heimburg
Mr. Isbell
Mr. Barnes
Mr. Sells
Mr. Stevens
Mr. Poe

PM
Mr. Rives
Mrs. McNair
Mr. Hamner
Mr. Kurtz
Mr. Naumcheff
Mr. Recio
Mr. Beaman
Mr. Grant
Mr. Boyanton
Mr. White
Mr. Humphreys
Mr. Thomas
Mr. Waite
Mr. Hardy
Mr. Powell
Mr. Shipman
Mr. Chambers
Mr. Comer
Mr. Belew

PD
Mr. Goldsby (3)
Mr. Downey
Mr. Carey
Mr. Craft
Mr. Palaoro
Mr. Lavender

S&E-SSL-DIR
Mr. Heller

S&E-AERO
Dr. Geissler
Mr. Horn
Dr. F. Krause (5)
Mr. Lindberg (2)
Mr. L. Stone
Mr. Cremin (2)

S&E-AERO (Cont'd)
Mr. Mabry
Mrs. Bauer (20)
Mr. Telfer
Mr. Benson (2)
Mr. Perrine (20)
Mr. Haussler
Mr. Glaser
Mr. Coulter
Mr. Hardage
Mr. Dahm
Dr. Lovingood
Mr. Ryan
Mr. Rheinfurth
Dr. Worley
Mr. Baker
Mr. Deaton
Mr. Sims
Mr. Teague
Mr. Jackson
Mr. W. Vaughan (5)
Mr. Brown
Mr. O. Vaughan
Mr. V. Buckelew
Mrs. Hightower

NASA-MSC
Houston, Texas
Attn: A. A. Bishop/KM
F. C. Littleton/KM
W. L. Brady/PM-MO-F
Dr. M. Holter/TF
G. L. Hunt/FM
P. J. Stull/TK
M. G. Kennedy/FC5
S. G. Bales/FC5
W. P. Gatlin/FC2
G. E. Coen/FC3
R. D. Duncan/FM5
J. C. O'Loughlin/KW
H. E. Whitacre/KM
R. A. Berglund/HA
D. E. Fielder/HA
A. L. Grandfield/TF
C. R. Hicks/FA-4
J. D. Hodge/HA
K. Young/FM6
J. Mayer/FM
R. Hergert/TF5

NASA-MSC (Cont'd)
Attn: W. E. Koons/FA
R. O. Piland/TF
A. Watkins/TK
B. Ernull/FA
H. Whitacre/KM
G. Hull/FM13
J. Saultz/FC9
W. Eaton/TF3
R. Duncan/FM5
J. Llewellyn/FC5
D. Evans/TF

Sci. & Tech. Info. Facility (25)
P. O. Box 33
College Park, MD 20740
Attn: NASA Rep. (S-AK/RKT)

NASA-KSC
Attn: W. B. Shapbell, AA-SVO-3
J. Twigg, LV
R. Arbic, LO-PLN-2
C. Mars, LS-ENG-8
L. Bell, LS-ENG-9
J. Perkinson, LV-GDS-32
J. Bardwell, IN-DAT-2
W. Cooper, IN-TEC
F. Dudley, IN-TEL-21
W. Brown, IS-TSM
F. Hartman, SF

NASA Headquarters
Attn: Dr. von Braun
Mr. Turner, MLA
Mr. Evans, MLO
Mr. Harkleroad, MLO
Mr. DeGraaf, MLS
Mr. Corey, MLS
Mr. Storm, MLR
Mr. Smith, MLT
Mr. W. Armstrong, MTX
Mr. C. Donlan, MD-T
Mr. W. Green, MLA
Mr. E. Hall, MTG
Mr. Hubbard, MT-1

DISTRIBUTION (Continued)

NASA Headquarters (Cont'd)
Mr. L. Jaffe, SA
Mr. R. Lohman, MTY
Mr. D. Lord, MTD
Dr. J. Lundholm, MLA
Mr. D. Rogers, SCF
Mr. D. Schnyer, MTV
Mr. R. Sprince, MTA
Dr. Tepper, SRD
Mr. M. Waugh, MTP
Dr. J. Wild, MTE

Bellcomm
955 L'Enfant Plaza N, SW
Washington, DC 20024
Attn: G. R. Andersen
C. L. Davis
F. E. Baz
W. A. Helm
N. W. Hinners
D. B. James
A. N. Kontaratos
H. S. London
K. E. Martersteck
L. D. Nelson
G. T. Orrok
S. Shapiro
J. L. Strand
W. B. Thompson
V. Thuraisamy
E. Radany
D. Belz

Martin Marietta
Huntsville, Ala.
Attn: Mr. Andreoni (2)

Langley Research Center
Attn: W. N. Bardner
W. C. Hayes, Jr.
W. R. Hook
C. Llewellyn

Ames Research Center
Attn: L. Roberts/M
N. Farlon (3)

Northrop
6025 Technology Drive
Huntsville, Alabama
Attn: W. Pease
J. Brown
L. Fox
T. Lyons
R. Chunn

Martin Marietta
Denver Division
Denver, Colorado 80201
Attn: B. Brown
A. Braunworth
C. Reichwein
J. O'Kelly

General Dynamics
Convair Division
Box 1128
San Diego, CA 92112
Attn: R. C. Ring
A. Ryan

North American - Huntsville
Attn: F. Garcia (3)

MDAC - Huntsville - Bldg 4481
Attn: V. Roth

McDonnell-Douglas Corp
Western Division
5301 Bolsa Avenue
Huntington Beach, California
Attn: B. Garlich
F. Riel
D. Davin
R. Holmen
P. Dixon

MSFC—RSA, Ala